SOUTHAMPTON OCEANOGRAPHY CENTRE

INTERNAL DOCUMENT No. 75

Airflow distortion at instrument sites on the *RRS James Clark Ross*

D I Berry, B I Moat & M J Yelland

2001

James Rennell Division for Ocean Circulation and Climate
Southampton Oceanography Centre
University of Southampton
Waterfront Campus
European Way
Southampton
Hants SO14 3ZH
UK

Tel: +44 (0)23 8059 6406
Fax: +44 (0)23 8059 6204
Email: bim@soc.soton.ac.uk

DOCUMENT DATA SHEET

AUTHOR

BERRY, D I, MOAT, B I & YELLAND, M J

PUBLICATION DATE

2001

TITLE

Airflow distortion at instrument sites on the *R.R.S. James Clark Ross*

REFERENCE

Southampton Oceanography Centre Internal Document, No. 75, 83 pp. (Unpublished manuscript)

ABSTRACT

Wind speed measurements obtained from anemometers mounted on ships are prone to systematic errors caused by the distortion of the air flow around the ship's hull and superstructure. This report describes the results of simulations of the air flow around the *R.R.S. James Clark Ross* made using the Computational Fluid Dynamics (CFD) software VECTIS. The airflow distortion at a number of anemometer sites has been quantified for wind speeds of 5 ms^{-1} and 15 ms^{-1} blowing a) directly over the bows of the ship, and b) directly over the port beam (90° to port of the bow). The anemometers in this study were located in the bows of the ship and also on the port bridge wing.

For bow-on flows the instrument sites in the bows of the ship experienced relatively small flow distortion. At these sites the flow was accelerated by between -1% to 1% and displaced vertically by between 1.7 m and 2.2 m. In contrast, the instrument sites on the port bridge wing experienced a severely distorted flow. The wind speed error varied rapidly from -40 % to 20 % depending on the exact location of the instrument, and the vertical displacement varied between 5.3 m and 6.3 m.

For flows over the port beam the instrument sites in the bows of the ship experienced moderate flow distortion with wind speed errors of 9 % to 13 % and vertical displacements of between 4.8 m and 5.4 m. The instruments sites located on the port bridge wing experienced wind speed errors of -7.1 % to 2.6 %, and vertical displacements of 9.4 m to 10.4 m.

KEYWORDS

AIRFLOW DISTORTION, COMPUTATIONAL FLUID DYNAMICS, CFD, *JAMES CLARK ROSS*, AMT 11, JCR 44, ARCICE, WIND SPEED MEASUREMENT

ISSUING ORGANISATION

Southampton Oceanography Centre
University of Southampton
Waterfront Campus
European Way
Southampton SO14 3ZH
UK

AIRFLOW DISTORTION AT INSTRUMENT SITES ON THE *R.R.S. JAMES CLARK ROSS*

1. INTRODUCTION **3**

2. DESCRIPTION OF THE *R.R.S. JAMES CLARK ROSS* MODELS **3**

3. THE AIRFLOW AT THE INSTRUMENT SITES FOR BOW-ON FLOWS **4**

3.1 The instrument locations 4

3.1.a JCR 44 4

3.1.b JCR 52 5

3.2 Results for a bow-on flow of 5 ms^{-1} 5

3.2.a The instrument sites on JCR cruise 44. 5

3.2.b The instrument sites on JCR cruise 52 7

3.3 Results for a bow-on flow of 15 ms^{-1}. 7

3.3.a The JCR 44 cruise 8

3.3.b The JCR 52 cruise 8

4. THE AIRFLOW AT THE INSTRUMENT SITES FOR FLOWS 90º OFF THE PORT BOW **9**

4.1 The instrument locations 9

4.1.a JCR 44 9

4.1.b JCR 52 9

4.2 Results for a beam-on flow of 5 ms^{-1} 9

4.2.a JCR 44 9

4.2.b JCR 52 10

4.3 Results for a beam-on flow of 15 ms^{-1} 10

4.3.a JCR 44 10

4.3.b JCR 52 11

5. SUMMARY **12**

6. ACKNOWLEDGEMENTS. **14**

7. REFERENCES **14**

8. TABLES 15

8.1 Bow-on flow of 5 ms^{-1} 15

8.1.a JCR 44 15

8.1.b JCR 52 17

8.2 Bow-on flow of 15 ms^{-1} 20

8.2.a JCR 44 20

8.2.b JCR 52 22

8.3 Beam-on flow of 5 ms^{-1} 25

8.3.a JCR 44 25

8.3.b JCR 52 27

8.4 Beam-on flow of 15 ms^{-1} 30

8.4.a JCR 44 30

8.4.b JCR 52 32

8.5 Summary 35

9. FIGURES 41

10. Appendix 71

AIRFLOW DISTORTION AT INSTRUMENT SITES ON THE *R.R.S. JAMES CLARK ROSS*

Berry, D. I., B. I. Moat and M. J. Yelland

August 2001

1. INTRODUCTION

This report describes an investigation of the airflow around the *R.R.S. James Clark Ross* (JCR). The study used Computational Fluid Dynamics (CFD) models to simulate the airflow over the ship in order to quantify the effects of airflow distortion (due to the hull and superstructure of the ship) on wind speed measurements made at various instrument sites. Corrections are derived for instrument sites on two cruises: the ARCICE cruise JCR 44 and the AMT11 cruise JCR52.

From examination of the cruise data it was decided to create four CFD models. These models represented a flow over the ship at two relative wind directions and two wind speeds. A brief description of these models is given in Section 2. The flow directly over the bow of the ship was modelled at wind speeds of 5 ms^{-1} and 15 ms^{-1}. The results from these models are detailed in Section 3. Separate models were used to represent airflows of 5 ms^{-1} and 15 ms^{-1} at 90° off the port bow (Section 4). The results from all four models are summarised and discussed in Section 5.

2. DESCRIPTION OF THE *R.R.S. JAMES CLARK ROSS* MODELS

The distortion of the airflow at the anemometer sites on the *R.R.S. James Clark Ross* has been determined for air flows directly over the bow of the ship and from 90 degrees to port. Figure 1 shows the modelled geometry of the *R.R.S. James Clark Ross*. As an example of the instrumentation positions, the instrument sites on the JCR 44 cruise are indicated by crosses and the co-ordinates are shown for the models with a flow directly over the bow. The origin of the co-ordinate system is located at the centre of the ship on the "sea surface".

The geometry was enclosed in the centre of a "wind tunnel", or computational volume. Two different sized computational volumes were used to model the airflows over the bow and at 90° to port. For flows directly over the bow the computational volume was 660 m long (-330 m < x < 330 m), 400 m wide (-200 m < y < 200 m) and 150 m high (0 m < z < 150 m). The centre line of the ship was parallel to the x-axis at z = 0 m. For flows from 90º to port a separate computational volume was used. The ship geometry was rotated 90º and consequently the computational volume was widened to 1600 m to prevent undue blockage of the flow. The inlet of both domains were defined as a fully logarithmic wind profile with a 10 m wind speed of 15 ms^{-1}, which was reduced to 5 ms^{-1} for the two subsequent models. All four models were solved using the CFD code VECTIS.

Whilst each model was being solved the flow was monitored to determine if the solution had converged. Eight locations were used in total; seven abeam of the ship in the free stream flow and one near an anemometer location. The locations are shown schematically for the bow-on models in Figure

2. Wind speed data from these monitoring locations showed the bow-on model run with a 5 ms^{-1} wind speed had converged after 14000 time steps. As an example, Figure 3 shows the convergence of the 5 ms^{-1} bow-on model for the last 300 time steps, by which point all the values were constant to the third significant figure. The model with a flow of 15 ms^{-1} over the bow had converged by 13000 time steps and the models with flows of 5 ms^{-1} and 15 ms^{-1} from 90º to port had converged by 12000 and 20000 time steps respectively. Once the models had converged post-processing files were written for the extraction of data throughout the computational volumes. Illustrations of the output can be found in the Appendix and a detailed description of the data extraction and analysis can be found in Moat *et. al.* (1996).

The flow in the computational volume was examined to check that free stream conditions existed at the sides and ends of the tunnel, i.e. that the presence of the ship did not cause a significant blockage of the flow to these regions. As an example, Figure 4a shows the variation in velocity along the tunnel for the model with a 5 ms^{-1} flow directly over the bow of the ship. The data were extracted on a plane at y = 150 m, i.e. towards one side of the tunnel, between –300 m < x < 300 m and at heights z of 10 m, 20 m, 30 m and 50 m. Equivalent data were extracted from the other side of the tunnel, at y = -150 m, and identical results were found. Figure 4b shows the velocity data abeam of the ship for the central section of the tunnel in more detail. This shows a change in the free stream velocity of about 0.05 ms^{-1} at a height of 10 m and –0.01 ms^{-1} at a height of 20 m. These small changes indicate the ship caused a minimal blockage of the flow at the sides of the tunnel. However, since the changes are not zero, the free stream velocity for a particular instrument site is estimated from the vertical profile of the velocity about 150 m directly abeam of the instrument site, rather than at the inlet or outlet of the tunnel. Examination of the free stream velocity close to the sides of the tunnel in the other models showed that the geometry likewise caused a minimal blockage of the flow.

3. THE AIRFLOW AT THE INSTRUMENT SITES FOR BOW-ON FLOWS.

3.1 The instrument locations

3.1.a JCR 44

The JCR 44 cruise had six meteorological instruments on board: the ship's sonic anemometer and an R2 sonic anemometer, both mounted on the bird table at the top of the foremast; an HS sonic anemometer forward of the foremast platform; and a dew point sensor, fast humidity sensor and an R2 sonic anemometer, all mounted on the port bridge wing. The instrument locations relative to the foremast and the port bridge wing are shown schematically in Figure 5.

In the VECTIS co-ordinates system, the instrument positions ("P" in Tables 1 to 6) for the bow-on models are;

R2 sonic x = 43.80 m y = -0.61 m z = 21.51 m

Ship's sonic	x = 43.80 m	y = 0.61 m	z = 21.51 m
HS sonic (JCR 44)	x = 45.19 m	y = 1.40 m	z = 15.94 m
Bridge R2 sonic	x = 9.62 m	y = 9.39 m	z = 16.20 m
Dew point	x = 10.79 m	y = 9.52 m	z = 14.85 m
Fast humidity	x = 11.49 m	y = 9.52 m	z = 14.85 m

3.1.b JCR 52

The JCR 52 cruise had three meteorological instruments mounted on the foremast platform: an HS sonic anemometer, a sonic temperature sensor and an IFM H2O/CO2 sensor. Both the IFM sensor and sonic temperature sensor were moved during the cruise. The first sites have #1 appended to their name and the second sites #2. The instrument locations relative to the foremast are shown schematically in Figure 6.

In the VECTIS co-ordinates system, the instrument positions ("P" in Tables 9 to 13) for the bow-on models are;

HS sonic (JCR 52)	x = 44.99 m	y = 1.40 m	z = 15.75 m
IFM #1	x = 44.39 m	y = 1.22 m	z = 15.55 m
IFM #2	x = 44.39 m	y = 2.10 m	z = 15.30 m
Sonic temperature #1	x = 44.09 m	y = 0.97 m	z = 15.75 m
Sonic temperature #2	x = 44.09 m	y = -1.70 m	z = 15.75 m

3.2 Results for a bow-on flow of 5 ms^{-1}

3.2.a The instrument sites on JCR cruise 44.

3.2.a.1 The vertical displacement of the flow

The vertical displacement of the flow reaching an instrument site is calculated by tracing a streamline from the inlet of the tunnel to the approximate position of the instrument site (see Figure A10 in the Appendix). Table 1 gives the co-ordinates of; "P" the position of the R2 sonic anemometer site, "P_{stream}" the point on the streamline closest to the anemometer and "P_{origin}" the origin of the streamline. It can be seen that the streamline has been displaced vertically by 1.71 m by the time it reaches the approximate position of the anemometer. Tables 2 to 6 give the equivalent information for the other instrument sites. In most cases the streamlines pass within a few centimetres of the instrument locations in the x and z directions. In the y (port-starboard) direction the difference between the streamline position and the instruments is generally larger, reaching a maximum of 0.28 m at the bridge R2 anemometer site. The streamlines miss in the y direction because they originate far upstream of the ship where the cell size is relatively large. A vertical section (constant y) of data is

viewed, and the x and z co-ordinates of the origin of the streamline are adjusted until the streamline passes through the anemometer site. Some adjustment in the y direction is also possible by changing the plane from which the streamline originates, but since the origin of the streamline is constrained to the centre of the plane only a coarse adjustment is possible. In most cases the effect on the resulting vertical displacement estimate is small, with differences of less than 0.10 m. However, in the case of the instruments mounted on the bridge wing the effect can be large, with differences in the calculated vertical displacement of up to 0.50 m between adjacent planes.

3.2.a.2 The free stream velocity

The estimates of the vertical displacement (Δz) are used to obtain the free stream velocities for the instrument sites. The air parcel reaching an instrument will have originated at a height of ($z - \Delta z$), where z is the instrument height, and the free stream velocity is obtained at that height on the free stream profile. The velocity of the flow at the instrument site is then compared to this free stream velocity, and the wind speed error is expressed in terms of a percentage of the free stream speed.

Figure 7 shows part of the free stream profile near the wind tunnel wall, directly abeam of the R2 sonic anemometer ($x = 43.80$ m, $y = 150$ m, $0 \text{ m} < z < 150$ m). This indicates a free stream velocity of 5.28 ms^{-1} at a height of 19.80 m. Free stream velocities were obtained in a similar fashion for the other instrument sites and the results are included in Table 7.

3.2.a.3 The effect of flow distortion on wind speed

The free stream velocity has small, predictable gradients and can be estimated accurately at any given point on the vertical profile. In contrast, the flow at an instrument site can suffer from severe flow distortion and from large gradients in the velocity field. In addition, it is not always possible to define the mesh so that the instruments are at the exact centres of the computational cells (see Moat *et. al.*, 1996). Therefore the velocity at an instrument site is estimated from lines of data extracted in all three directions. Figures 8 to 13 show the lines of data through the instrument sites, and the results are summarised in Table 7. The wind speed error at an instrument site (of height z) is expressed as a percentage of the free stream speed (at height $z - \Delta z$) with a positive error indicating an acceleration of the flow.

An indication of the accuracy of the error estimate and the severity of the flow distortion is given by estimates of the gradient of the flow. Estimates of the gradient of the flow are made from Figures 8 to 13 and the rates of change, per metre and per cell, are given in Table 8. The results for the ship's sonic, R2 sonic and HS sonic anemometer sites show small rates of change. In general the airflow distortion at these sites is fairly small, with a deceleration of the flow of 1.1 % at the sites on the bird table (the R2 sonic and ship's sonic anemometers) and a deceleration of the flow of 0.8 % at the HS sonic (JCR 44) anemometer site. The displacement of the flow reaching the sites on the bird table is 1.71 m and the flow reaching the HS sonic (JCR 44) anemometer has been lifted by 2.05 m. The angle of the air flow to the horizontal is also quite small; the wind speed components suggest an

angle of flow of about 3.5º for the instruments on the bird table and 5.9º for the HS sonic (JCR 44) anemometer.

In contrast, the instrument sites on the port bridge wing are near a region of re-circulation (see Figure A12 in the Appendix) and experience severe flow distortion and very large velocity gradients. For example, the flow reaching the bridge R2 sonic anemometer experiences a deceleration of 41.4 % whilst the flow to the fast humidity sensor (roughly 2.5 m distant from the R2) is accelerated by 17.66 %. This severe flow distortion is confirmed by the large rates of change in the velocity, both per cell and per meter, with a maximum of about 2 ms^{-1}/m along the tunnel at the bridge R2 site. In between these two sensors, at the dew point sensor site, the flow experiences an acceleration of only 0.95 %. However, the rates of change at this site are also large, which confirms that the flow distortion is severe. The angle of the flow to the horizontal ranges from –7.2º at the fast humidity sensor to 4.5º at the bridge R2 site. The severe flow distortion can be seen in Figures 11 to 13 with the influence of the bridge wing clearly visible.

3.2.b The instrument sites on JCR cruise 52.

This section summarises the results for the instrument sites on the JCR 52 cruise for a bow-on flow of 5 ms^{-1}. The instrument locations were given in Section 3.1.b and the methods used are those described in Sections 3.2.a. The vertical displacement of the flow to the instrument sites is given in Tables 9 to 13, and Figures 14 to 18 show the velocity data extracted at the instrument sites. The resulting velocity errors are given in Table 14 and Table 15 gives the rates of change at the instrument sites.

The distortion of the flow to all the instrument sites on the JCR 52 cruise is fairly small, with a maximum wind speed error of 0.90 %. This maximum occurs at the sonic temperature #1 site and the vertical displacement of the flow (2.2 m) is also at a maximum at this site. In general, the flow to the instrument sites directly above the foremast platform experiences an acceleration of between 0.2% and 0.9% whilst the flow to the HS sonic (JCR 52) anemometer, forward of the platform, is decelerated by 0.6%. The flow to the HS sonic (JCR52) anemometer is lifted by approximately 2.1 m and that to the instruments on the foremast platform by 2.2 m. The relatively slight distortion of the flow is confirmed by the small rates of change, which can be found in Table 15.

3.3 Results for a bow-on flow of 15 ms^{-1}.

This section summarises the results for a flow of 15 ms^{-1} directly over the bow. The instrument locations are those described in Section 3.1 and the methods used are described in Section 3.2.

3.3.a The JCR 44 cruise

The vertical displacement of the flow is given in Tables 16 to 21 and the extracted velocity data are shown in Figures 19 to 24. Tables 22 and 23 give the error estimates and rates of change at the instrument sites respectively.

In general, compared to a flow of 5 ms^{-1} over the bow, the vertical displacement of the 15 ms^{-1} flow and the velocity error estimates have both decreased only slightly for the instrument sites on the foremast. The flow to the R2 sonic anemometer has been decelerated by 1.08 % and the flow reaching the ship's sonic anemometer is decelerated by 1.07 %. Both experience a flow which has been displaced vertically by 1.5 m. The flow to the HS sonic (JCR 44) anemometer has been lifted by 1.84 m and decelerated by 0.50 %. The rates of change at all the sites on the foremast are small.

The instruments on the port bridge wing are again near a region of re-circulation and the flow to the bridge wing is severely distorted. The flow reaching the bridge R2 sonic anemometer has been raised by 6.17 m and decelerated by 32.66 % by the time it reaches the site. The flow to the dew point sensor has also been decelerated, with a deceleration of 25.66 % whilst that to the fast humidity sensor site has been accelerated by 4.82 %. The vertical displacement of the flow to these two sites is 5.22 m and 5.29 m respectively. The rates of change of velocity at all three sites on the port bridge wing are large, with a maximum of 3.1 ms^{-1} per cell at the bridge R2 sonic anemometer site. The influence of the bridge wing and the severe distortion of the flow can been seen in Figures 22 to 24.

3.3.b The JCR 52 cruise

The displacement of the flow to the instrument sites on the JCR 52 cruise is given in Tables 24 to 28 and the extracted velocity data are shown in Figures 25 to 29. The percentage wind speed errors are given in Table 29 and the rates of change at each instrument site are given in Table 30.

In general, compared to a flow of 5 ms^{-1} over the bow, the displacement of the flow to all the sites has decreased slightly. The wind speed errors have increased slightly at the sites directly above the foremast platform and decreased slightly for the HS site forward of the platform. The deceleration of the flow at the HS sonic (JCR 52) anemometer site has decreased to 0.21 % whilst the acceleration of the flow to the sites on the foremast platform has increased to between 0.66 % and 1.18 %. The flow to the sites on the foremast platform has been raised by 2.0 m and the flow to the HS sonic (JCR 52) anemometer lifted by 1.9 m. The rates of change are small at all the sites.

4. THE AIRFLOW AT THE INSTRUMENT SITES FOR FLOWS 90º OFF THE PORT BOW

4.1 The instrument locations

4.1.a JCR 44

A description of the locations of the instruments on board the JCR 44 cruise can be found in Section 3.1.a. This section gives the co-ordinates of the instruments for a flow from 90º to port.

In the VECTIS co-ordinates system, the instrument positions ("P" in Tables 31 to 36) for the beam-on models are;

R2 sonic	x = -0.61 m	y = -43.80 m	z = 21.51 m
Ship's sonic	x = 0.61 m	y = -43.80 m	z = 21.51 m
HS sonic (JCR 44)	x = 1.40 m	y = -45.19 m	z = 15.94 m
Bridge R2	x = 9.39 m	y = -9.62 m	z = 16.20 m
Dew point	x = 9.52 m	y = -10.79 m	z = 14.85 m
Fast humidity	x = 9.52 m	y = -11.49 m	z = 14.85 m

4.1.b JCR 52

A description of the locations of the instruments on board the JCR 52 cruise can be found in Section 3.1.b. This section gives the co-ordinates of the instruments for a flow from 90º to port.

In the VECTIS co-ordinates system, the instrument positions ("P" in Tables 39 to 43) for the beam-on models are;

HS sonic (JCR 52)	x = 1.40 m	y = -44.99 m	z = 15.75 m
IFM #1	x = 1.22 m	y = -44.39 m	z = 15.55 m
IFM #2	x = 2.10 m	y = -44.39 m	z = 15.30 m
Sonic temperature #1	x = 0.97 m	y = -44.09 m	z = 15.75 m
Sonic temperature #2	x = -1.70 m	y = -44.09 m	z = 15.75 m

4.2 Results for a beam-on flow of 5 ms^{-1}

4.2.a JCR 44

The vertical displacement of the flow is given in Tables 31 to 36, the velocity errors are given in Table 37 and the rates of change of velocity at the instrument sites are given in Table 38. Figures 30 to 35 show the velocity data extracted at the instrument sites.

The vertical displacement of the flow to all the sites is larger than for a bow-on flow (Section 3.2.a). This is to be expected since the ship presents a larger obstacle when beam-on to the flow than when bow-on. The vertical displacement of the flow reaching the sites on the bird table, the ship's sonic and R2 sonic anemometers, has increased to 4.74 m and 4.86 m respectively. The vertical displacement of the flow reaching the HS sonic (JCR 44) anemometer site has increased to 5.45 m. The velocity error estimates at these sites have also increased with the greater flow distortion. The flow reaching the ship's sonic and R2 sonic anemometers has been accelerated by 8.73 % and 9.66 % respectively. The flow reaching the HS sonic (JCR 44) anemometer has been accelerated by 12.44 % by the time it reaches the instrument position.

In contrast, the velocity errors at the instrument sites on the port bridge wing have decreased compared to those found for bow-on flows, but these sites are still severely affected by flow distortion. The flow reaching the bridge R2 sonic anemometer has been raised by 9.83 m and decelerated by 0.19 %. The flow reaching the dew point and fast humidity sensors has been lifted by 9.39 m and 9.40 m and accelerated by –4.50 % and 2.57 % respectively. This decrease in the velocity error estimates is confirmed by a decrease in the rates of change of velocity. However, the angle of the flow to the horizontal at these sites is extremely large (roughly 40º), confirming the severity of the flow distortion.

4.2.b JCR 52

The vertical displacement of the flow is given in Tables 39 to 43, the velocity errors in Table 44 and the rates of change of velocity at the instrument sites in Table 45. The velocity data extracted at the instrument sites are shown in Figures 36 to 40.

The flow reaching the instruments on the foremast platform has been raised by between 5.38 m and 5.86 m depending on their exact location. The maximum displacement of the flow is found at the sonic temperature #2 site. The displacement of the flow reaching the HS sonic (JCR 52) anemometer has increased to 5.45 m. The velocity errors also reach a maximum of 16.54 % at the sonic temperature #2 site. The minimum velocity error, which occurs at the IFM #2 site, has increased to 11.41 %. The rates of change of velocity have also increased compared to those for a flow directly over the bow, but in general they are still small. The angle of the flow to the horizontal has increased to between 4.4º and 9.3º.

4.3 Results for a beam-on flow of 15 ms^{-1}

4.3.a JCR 44

The vertical displacement of the flow is given in Tables 46 to 51 and the velocity error estimates are given in Table 52. The velocity data extracted at the instrument sites are shown in Figures 41 to 46 and the rates of change of velocity are given in Table 53.

In general, the vertical displacement of the flow and the velocity errors have both increased slightly at the instrument sites compared with a flow of 5 ms^{-1} from 90 degrees to port. The vertical

displacement of the flow reaching the R2 sonic anemometer has increased to 5.05 m and the displacement of the flow reaching the ship's sonic anemometer increased to 4.91 m. The maximum displacement of the flow occurs on the downwind (starboard) side of the foremast at the R2 sonic anemometer site. The vertical displacement of the flow to the HS sonic (JCR 44) anemometer has decreased to 5.41 m. The velocity error estimates at the R2 sonic and ship's sonic anemometers have increased to 9.98 % and 9.24 % respectively. The acceleration of the flow to the HS sonic (JCR 44) anemometer site has increased to 12.96 %. These increased errors are again matched by an increase in the rates of change of velocity, which can be found in Table 53, confirming the slightly increased flow distortion.

The velocity error estimates at the sites on the port bridge wing have decreased compared with a flow of 15 ms^{-1} directly over the bow. They have, however, increased slightly compared to a flow of 5 ms^{-1} from 90 degrees to port. The flow reaching the bridge R2 anemometer has been decelerated by 2.47 % by the time it reaches the instrument site and has been lifted by 10.48 m. The flow to both the dew point sensor and the fast humidity sensor has been raised by 9.96 m by the time it reaches the instrument sites. However, the velocity error estimates are significantly different, with the flow reaching the dew point sensor decelerated by 7.06 % and that reaching the fast humidity sensor decelerated by 0.57 %. The rates of change are again smaller at these sites compared with a flow directly over the bow. The large angle of the flow to the horizontal at the instrument sites on the bridge wing combined with the large vertical displacements indicate a significant flow distortion is still occurring. The angle of the flow to the horizontal ranges from 38.8º at the fast humidity sensor to 44.6º at the dew point sensor site.

4.3.b JCR 52

The vertical displacement of the flow is given in Tables 54 to 58 and the velocity data extracted at the instrument sites are shown in Figures 47 to 51. The velocity error estimates and the rates of change of the velocity at the instrument sites are given in Tables 59 and 60 respectively.

Again, the vertical displacement of the flow and the velocity error estimates have increased when compared to a flow directly over the bow of the ship. They have also increased slightly compared to a flow of 5 ms^{-1} from 90 degrees to port. The flow reaching the HS sonic (JCR 52) anemometer has been lifted by 5.44 m by the time it reaches the anemometer site and has been accelerated by 13.18 %. The displacement of the flow reaching the foremast platform ranges from 5.38 m on the upwind side of the platform (at the IFM #2 site) to 6.22m on the downwind side of the platform (at the sonic temperature #2 site). The acceleration of the flow to the instrument sites on the platform ranges from 11.97 % to 16.21 %, with the maximum acceleration on the downwind side of the platform. The angle of the flow to the horizontal at the instrument sites ranges from 4.2º at the sonic temperature #2 site to 9.6º at the IFM #2 site.

5. SUMMARY

The distortion of the air flow over the *R.R.S. James Clark Ross* has been quantified for the instrument sites used during the two cruises JCR 44 and JCR 52. Two wind speeds and two relative wind directions were used in a total of four separate models: a) a bow-on flow of 5 ms^{-1}, b) a bow-on flow of 15 ms^{-1}, c) a 5 ms^{-1} flow on to the port beam, d) a 15 ms^{-1} flow on to the port beam. The results of the four models are shown in Tables 61a to 61d respectively, where the effects of flow distortion at all the instruments sites on both cruises are summarised. In these tables, as in the previous Sections, the wind speed error is defined as the acceleration of the flow at the instrument site expressed as a percentage of the freestream speed. A negative error indicates that the flow has been decelerated. The freestream speed is calculated at a height ($z-\Delta z$) where z is the height of the instrument and Δz is the vertical displacement of the flow from its original height. This method is required if the wind speed measurements are used to calculate the wind stress using the inertial dissipation technique (Yelland *et al.*, 1998). The wind speed error may also be calculated using a free stream speed obtained at the instrument height (without allowing for the vertical displacement of the flow). Since this may be the preferred method for some purposes the results have also been re-calculated in this fashion and are displayed in Tables 62a to 62d, but they will not be discussed further.

We will consider the results for **bow-on flow**s first (Tables 61a and 61b);

The anemometers (R2 sonic and the ship's sonic) mounted on the "**bird table**" at the top of the foremast extension experience a flow which has been decelerated by about 1.1 % and raised by 1.7 m for a flow of 5 ms^{-1}. For a flow of 15 ms^{-1} the deceleration is not significantly different and the vertical displacement is similar at 1.5 m. Given the uncertainties in the results, a vertical displacement of 1.6 m could be used for any bow-on flow with a speed of between 5 and 20 ms^{-1}.

The instruments mounted directly above the foremast platform (the **IFM** and the **sonic temperature** sensors) experience a flow which has been accelerated by between 0.2 % and 0.9 % and raised by 2.2 m for a flow of 5 ms^{-1}. For a 15 ms^{-1} flow the acceleration increases slightly to between 0.6 and 1.2 %, and the vertical displacement decreases slightly to 2.0 m. Again, given the uncertainty in the results it could be acceptable to use mean values, i.e. a wind speed error of 0.7 % and a displacement of 2.1 m for both instrument sites for any bow-on flow with a speed of between 5 and 20 ms^{-1}.

The **HS sonic** was mounted forwards of the foremast platform and experienced a flow which was decelerated by between 0.2% and 0.8% and raised by about 1.9 m, depending on its exact location and the mean speed of the flow. Again, these decelerations are very small and the difference between models is even smaller in comparison to the uncertainties in the results. A mean wind speed error of -0.5 % could be used for any bow-on flow with a speed of between 5 and 20 ms^{-1}.

The summary above shows that all the instrument sites on the foremast experience small (but significant) flow distortion for bow-on flows, with wind speed errors in the range of -1 % to + 1% and vertical displacements of between 1.7 and 2.2 m. In contrast, the instruments located on the **port bridge wing** of the ship (a second R2 sonic, a dew point sensor and a fast response humidity sensor) all experience a severely distorted flow, with large vertical displacements of between 5.3 m and 6.3 m. Although all three instruments were mounted fairly close together (within 2.5 m) the flow to the sites

varied greatly, with accelerations of -40 % (R2 sonic site) to + 20 % (fast humidity site) for a 5 ms^{-1} flow, and -30 % to + 5 % for a 15 ms^{-1} flow. This rapid rate of change and the correspondingly large uncertainty in the results leads to the conclusion that data from these instruments should not be relied on. In addition, although the CFD model has been verified for flows where the distortion is slight or moderate (Moat *et al.*, 2001), it has not yet been verified for the severely distorted flow seen in the region of the port bridge wing for bow-on flows. The *in-situ* data from the JCR cruises will be used in a future study to test the model results in this region.

We now consider the results for the two models with a **flow on to the port beam** (Tables 61c and 61d). It must be noted that the models did not include representations of the actual instruments, or of other small structures such as the bird table or the instrument supports. It can also be seen (Figures 5 and 6) that, in reality, a number of instrument sites will be down wind of a small structure for a flow on to the port beam. Data from these instruments would be discarded. The affected instrument sites are: the R2 sonic on the bird table, the sonic temperature sensor (both sites) and the IFM (first site). The model results for these instruments will not be discussed further. The results for the other sites are summarised below;

The ship's sonic mounted on the "**bird table**" at the top of the foremast extension experiences a flow which has been accelerated by about 8.7 % and raised by 4.7 m for a beam-on flow of 5 ms^{-1}. For a flow of 15 ms^{-1} the acceleration increases slightly to 9.2 % and the vertical displacement also increases slightly to 4.9 m. Given the uncertainties in the results it would be reasonable to use a wind speed error of 9 % and a vertical displacement of 4.8 m for any beam-on flow with a speed of between 5 and 20 ms^{-1}.

The **IFM sensor** (second site) mounted directly above the foremast platform experiences a flow which has been accelerated by 11.4 % and raised by 5.4 m for a flow of 5 ms^{-1}. For a 15 ms^{-1} flow the acceleration increases slightly to 12.0 %, but the vertical displacement remains unchanged. The uncertainty in the results at this site is relatively large (1.2% per cell) hence a wind speed error of 11.7 % could be used for any beam-on flow with a speed of between 5 and 20 ms^{-1}.

The **HS sonic** was mounted forwards of the platform and experienced a flow which was accelerated by 12.8 % (± 0.5 % depending on exact location and the speed of the flow) and raised by 5.4 m.

The summary above shows that the instrument sites on the foremast experienced moderate flow distortion for flows on the port beam. The effects of flow distortion at these sites are greater for a beam-on flow than for a bow-on flow since the ship presents a much larger obstacle to the flow when beam-on. In contrast, the instruments located on the **port bridge wing** of the ship may have experienced a decrease in the severity of the flow distortion when the ship was beam-on rather than bow-on to the flow. For the beam-on flow, the range of accelerations was smaller, varying from -4.6 % (dew point sensor site) to + 2.6 % (fast humidity site) for a 5 ms^{-1} flow, and -7.1 % to -0.6 % for a 15 ms^{-1} flow. However, the instruments on the bridge wing experienced very large vertical displacements of between 9.4 m and 10.4 m (c.f. instrument heights of about 15 m), and the angle of the flow to the horizontal was similarly large (up to 45º). The model results for the flow in the region of the bridge wing must be validated before data from these instruments can be used.

6. ACKNOWLEDGEMENTS.

This work was supported by funds from the NERC Thematic Project "ARCICE" and by the MAST project "AutoFlux" (MAS3-CT97-0108).

7. REFERENCES

Moat, B. I., M. J. Yelland, and J. Hutchings, 1996: Airflow over the R.R.S. Discovery using the Computational Fluid Dynamics package VECTIS, Southampton Oceanography Centre, Southampton, UK. SOC Internal Report No. 2, 41 pp.

Moat, B. I., M. J. Yelland and R. W. Pascal, 2001: The accuracy of CFD in predicting the air flow distortion at anemometer sites on research ships. Southampton Oceanography Centre, Southampton, UK. SOC Internal Report

Yelland, M. J., B. I. Moat, P. K. Taylor, R. W. Pascal, J. Hutchings and V. C. Cornell, 1998: Wind stress measurements from the open ocean corrected for air flow distortion by the ship. *Journal of Physical Oceanography,* 28 (7), 1511 - 1526

8. TABLES

8.1 Bow-on flow of 5 ms^{-1}

8.1.a JCR 44

Location	x (m)	y (m)	z (m)
P (R2 sonic)	43.80	-0.61	21.51
P_{stream}	43.81	-0.52	21.51
$P-P_{stream}$	-0.01	0.09	0.00
P_{origin}	283.97	-0.48	19.80
$P_{stream}-P_{origin}$			$\Delta z= 1.71$

Table 1 The vertical displacement, Δ **z**, of the flow to the **R2 sonic** anemometer

Location	x (m)	y (m)	z (m)
P (Ship's sonic)	43.80	0.61	21.51
P_{stream}	43.81	0.49	21.49
$P-P_{stream}$	-0.01	0.12	0.02
P_{origin}	285.24	0.46	19.78
$P_{stream}-P_{origin}$			$\Delta z= 1.71$

Table 2 The vertical displacement, Δ **z,** of the flow to the **ship's sonic** anemometer

Location	x (m)	y (m)	z (m)
P (HS sonic)	45.19	1.40	15.94
P_{stream}	45.17	1.54	15.93
$P-P_{stream}$	0.02	-0.14	0.01
P_{origin}	285.49	1.39	13.88
$P_{stream}-P_{origin}$			$\Delta z= 2.05$

Table 3 The vertical displacement, Δ **z**, of the flow to the **HS Sonic (JCR 44)** anemometer

Location	x (m)	y (m)	z (m)
P (Bridge R2)	9.62	9.39	16.20
P_{stream}	9.63	9.67	16.28
$P-P_{stream}$	-0.01	-0.28	-0.08
P_{origin}	284.28	4.59	9.93
$P_{stream}-P_{origin}$			$\Delta z= 6.35$

Table 4 The vertical displacement, Δ **z**, of the flow to the **Bridge R2** anemometer

Location	x (m)	y (m)	z (m)
P (Dew point)	10.79	9.52	14.85
P_{stream}	10.79	9.66	14.79
$P-P_{stream}$	0	- 0.14	- 0.06
P_{origin}	289.00	4.59	9.51
$P_{stream}-P_{origin}$			$\Delta z = 5.28$

Table 5 The vertical displacement, $\Delta \mathbf{z}$, of the flow to the **dew point** sensor

Location	x (m)	y (m)	z (m)
P (Humidity)	11.49	9.52	14.85
P_{stream}	11.49	9.39	14.89
$P-P_{stream}$	0	0.13	-0.04
P_{origin}	283.97	4.59	9.51
$P_{stream}-P_{origin}$			$\Delta z = 5.38$

Table 6 The vertical displacement, $\Delta \mathbf{z}$, of the flow to the **fast humidity** sensor

Instrument site	Velocity from each direction	Average velocity (ms^{-1})	Free stream velocity (ms^{-1})	% Error
R2 sonic	5.223(x)	5.223	5.281	-1.10
	5.223(y)			
	5.223(z)			
Ship's sonic	5.223(x)	5.223	5.281	-1.10
	5.223(y)			
	5.223(z)			
HS sonic	5.095(x)	5.096	5.138	-0.82
	5.094(y)			
	5.100(z)			
Bridge R2	2.893(x)	2.915	4.974	-41.40
	2.875(y)			
	2.976(z)			
Dew point	5.548(x)	4.995	4.948	0.95
	3.917(y)			
	5.520(z)			
Fast humidity	5.818(x)	5.810	4.938	17.66
	5.765(y)			
	5.846(z)			

Table 7 **Wind speed errors** at the instrument sites on the JCR44 cruise (for a 5 ms^{-1} bow-on flow)

Instrument site	Velocity data line	Rate of change of velocity per metre (ms^{-1}/m)	Rate of change of velocity per cell (ms^{-1}/cell)
R2 sonic	Along (x)	-0.006	-0.002
	Across (y)	0	0.001
	Up (z)	0.021	0.005
Ship's sonic	Along (x)	-0.006	-0.001
	Across (y)	-0.001	-0.001
	Up (z)	0.021	0.005
HS sonic	Along (x)	-0.044	-0.005
	Across (y)	0.004	0.001
	Up (z)	0.044	0.007
Bridge R2	Along (x)	1.888	1.330
	Across (y)	2.197	0.307
	Up (z)	1.985	0.743
Dew point	Along (x)	0.412	0.386
	Across (y)	2.316	1.093
	Up (z)	0.383	0.053
Fast humidity	Along (x)	0.250	0.213
	Across (y)	1.615	0.188
	Up (z)	0.293	0.125

Table 8 Rate of change of velocity close to the instrument sites on the JCR 44 cruise (for a 5 ms^{-1} bow-on flow)

8.1.b JCR 52

Location	x (m)	y (m)	z (m)
P (HS sonic)	44.99	1.40	15.75
P_{stream}	44.98	1.54	15.73
$P-P_{stream}$	0.01	-0.14	-0.02
P_{origin}	281.59	1.39	13.64
$P_{stream}-P_{origin}$			$\Delta z = 2.09$

Table 9 The vertical displacement, Δ **z,** of the flow to the **HS Sonic (JCR 52)** anemometer

Location	x (m)	y (m)	z (m)
P (IFM #1)	44.39	1.22	15.55
P_{stream}	44.39	1.68	15.55
$P-P_{stream}$	0.00	-0.46	0.00
P_{origin}	284.62	1.39	13.37
$P_{stream}-P_{origin}$			$\Delta z = 2.18$

Table 10 The vertical displacement, Δ **z**, of the flow to the **IFM #1** sensor

Location	x (m)	y (m)	z (m)
P (IFM #2)	44.39	2.10	15.30
P_{stream}	44.39	2.25	15.30
$P-P_{stream}$	0.00	-0.15	0.00
P_{origin}	284.69	2.32	13.11
$P_{stream}-P_{origin}$			$\Delta z = 2.19$

Table 11 The vertical displacement, Δ **z**, of the flow to the **IFM #2** sensor

Location	x (m)	y (m)	z (m)
P (Sonic temp. #1)	44.09	0.97	15.75
P_{stream}	44.08	0.50	15.76
$P-P_{stream}$	0.01	0.47	-0.01
P_{origin}	283.41	0.46	13.55
$P_{stream}-P_{origin}$			$\Delta z = 2.21$

Table 12 The vertical displacement, Δ **z**, of the flow to the **sonic temperature #1** sensor

Location	x (m)	y (m)	z (m)
P (Sonic temp. #2)	44.09	-1.70	15.75
P_{stream}	44.08	-1.63	15.75
$P-P_{stream}$	0.01	0.07	0.00
P_{origin}	283.67	-1.41	13.57
$P_{stream}-P_{origin}$			$\Delta z = 2.18$

Table 13 The vertical displacement, Δ **z**, of the flow to the **sonic temperature #2** sensor

Instrument site	Velocity from each direction	Average velocity (ms^{-1})	Free stream velocity (ms^{-1})	% Error
HS sonic	5.102(x)	5.100	5.129	-0.57
	5.100(y)			
	5.099(z)			
IFM #1	5.145(x)	5.145	5.118	0.53
	5.146(y)			
	5.143(z)			
IFM #2	5.118(x)	5.119	5.108	0.22
	5.120(y)			
	5.119(z)			
Sonic temperature #1	5.168(x)	5.170	5.124	0.90
	5.170(y)			
	5.173(z)			
Sonic temperature #2	5.157(x)	5.159	5.126	0.64
	5.160(y)			
	5.160(z)			

Table 14 Wind speed errors at the instrument sites on the JCR52 cruise (for a 5 ms^{-1} bow-on flow).

Instrument site	Velocity data line	Rate of change of velocity per metre (ms^{-1}/m)	Rate of change of velocity per cell (ms^{-1}/cell)
HS sonic	Along (x)	-0.048	-0.012
	Across (y)	0.002	0
	Up (z)	0.055	0.006
IFM #1	Along (x)	-0.070	-0.024
	Across (y)	-0.010	-0.002
	Up (z)	0.037	0.009
IFM #2	Along (x)	-0.061	-0.021
	Across (y)	-0.012	-0.003
	Up (z)	0.021	0.006
Sonic temperature #1	Along (x)	-0.059	-0.020
	Across (y)	-0.013	-0.003
	Up (z)	-0.035	-0.009
Sonic temperature #2	Along (x)	-0.047	-0.015
	Across (y)	0.017	0.005
	Up (z)	-0.009	-0.005

Table 15 Rate of change of velocity close to the instrument sites on the JCR 52 cruise (for a 5 ms^{-1} bow-on flow).

8.2 Bow-on flow of 15 ms^{-1}

8.2.a JCR 44

Location	x (m)	y (m)	z (m)
P (R2 sonic)	43.80	-0.61	21.51
P_{stream}	43.79	-0.52	21.53
$P-P_{stream}$	0.01	0.09	-0.02
P_{origin}	283.25	-0.48	20.01
$P_{stream}-P_{origin}$			$\Delta z = 1.52$

Table 16 The vertical displacement, $\Delta \mathbf{z}$, of the flow to the **R2 sonic** anemometer

Location	x (m)	y (m)	z (m)
P (Ship's sonic)	43.80	0.61	21.51
P_{stream}	43.79	0.48	21.51
$P-P_{stream}$	0.01	0.13	0.00
P_{origin}	283.65	0.46	19.98
$P_{stream}-P_{origin}$			$\Delta z = 1.53$

Table 17 The vertical displacement, $\Delta \mathbf{z}$, of the flow to the **ship's sonic** anemometer

Location	x (m)	y (m)	z (m)
P (HS sonic)	45.19	1.40	15.94
P_{stream}	45.21	1.52	15.95
$P-P_{stream}$	-0.02	-0.12	-0.01
P_{origin}	284.15	1.39	14.11
$P_{stream}-P_{origin}$			$\Delta z = 1.84$

Table 18 The vertical displacement, $\Delta \mathbf{z}$, of the flow to the **HS sonic (JCR 44)** anemometer

Location	x (m)	y (m)	z (m)
P (Bridge R2)	9.62	9.39	16.20
P_{stream}	9.61	9.65	16.16
$P-P_{stream}$	0.01	-0.26	0.04
P_{origin}	284.00	4.59	9.99
$P_{stream}-P_{origin}$			$\Delta z = 6.17$

Table 19 The vertical displacement, $\Delta \mathbf{z}$, of the flow to the **bridge R2** anemometer

Location	x (m)	y (m)	z (m)
P (Dew point)	10.79	9.52	14.85
P_{stream}	10.81	9.70	14.76
$P-P_{stream}$	-0.02	-0.18	0.09
P_{origin}	283.71	4.59	9.54
$P_{stream}-P_{origin}$			$\Delta z = 5.22$

Table 20 The vertical displacement, $\Delta \mathbf{z}$, of the flow to the **dew point** sensor

Location	x (m)	y (m)	z (m)
P (Humidity)	11.49	9.52	14.85
P_{stream}	11.48	9.46	14.83
$P-P_{stream}$	0.01	0.06	0.02
P_{origin}	283.71	4.59	9.54
$P_{stream}-P_{origin}$			$\Delta z = 5.29$

Table 21 The vertical displacement, $\Delta \mathbf{z}$, of the flow to the **fast humidity** sensor

Instrument site	Velocity from each direction	Average velocity (ms^{-1})	Free stream velocity (ms^{-1})	% Error
R2 sonic	14.324(x)	14.324	14.480	-1.08
	14.324(y)			
	14.324(z)			
Ship's sonic	14.324(x)	14.324	14.479	-1.07
	14.324(y)			
	14.323(z)			
HS sonic	14.051(x)	14.053	14.123	-0.50
	14.048(y)			
	14.060(z)			
Bridge R2	9.119(x)	9.281	13.782	-32.66
	9.280(y)			
	9.444(z)			
Dew point	10.066(x)	10.211	13.736	-25.66
	10.579(y)			
	9.989(z)			
Fast humidity	14.218(x)	14.388	13.727	4.82
	14.505(y)			
	14.441(z)			

Table 22 **Wind speed errors** at the instrument sites on the JCR44 cruise (for a 15 ms^{-1} bow-on flow).

Instrument site	Velocity data line	Rate of change of velocity per metre (ms^{-1}/m)	Rate of change of velocity per cell (ms^{-1}/cell)
R2 sonic	Along (x)	-0.017	-0.004
	Across (y)	0.001	0.001
	Up (z)	0.042	0.010
Ship's sonic	Along (x)	-0.017	-0.004
	Across (y)	-0.003	-0.001
	Up (z)	0.042	0.010
HS sonic	Along (x)	-0.125	-0.027
	Across (y)	0.009	0.003
	Up (z)	0.109	0.027
Bridge R2	Along (x)	4.119	2.998
	Across (y)	5.619	0.607
	Up (z)	5.606	1.624
Dew point	Along (x)	5.395	2.533
	Across (y)	6.536	2.705
	Up (z)	3.193	-0.115
Fast humidity	Along (x)	3.808	2.070
	Across (y)	4.071	0.724
	Up (z)	1.800	0.159

Table 23 Rate of change of velocity close to the instrument sites on the JCR 44 cruise (for a 15 ms^{-1} bow-on flow).

8.2.b JCR 52

Location	x (m)	y (m)	z (m)
P (HS sonic)	44.99	1.40	15.75
P_{stream}	44.99	1.53	15.76
$P-P_{stream}$	0.00	-0.13	-0.01
P_{origin}	287.63	1.39	13.88
$P_{stream}-P_{origin}$			$\Delta z = 1.88$

Table 24 The vertical displacement, $\Delta \mathbf{z}$, of the flow to the **HS sonic (JCR 52)** anemometer

Location	x (m)	y (m)	z (m)
P (IFM #1)	44.39	1.22	15.55
P_{stream}	44.39	1.54	15.57
$P-P_{stream}$	0.00	-0.32	-0.02
P_{origin}	284.24	1.39	13.59
$P_{stream}-P_{origin}$			$\Delta z = 1.98$

Table 25 The vertical displacement, Δ **z**, of the flow to the **IFM #1** sensor

Location	x (m)	y (m)	z (m)
P (IFM #2)	44.39	2.10	15.30
P_{stream}	44.39	2.58	15.32
$P-P_{stream}$	0.00	-0.48	-0.02
P_{origin}	282.23	2.32	13.36
$P_{stream}-P_{origin}$			$\Delta z = 1.96$

Table 26 The vertical displacement, Δ **z**, of the flow to the **IFM #2** sensor

Location	x (m)	y (m)	z (m)
P (Sonic temp. #1)	44.09	0.97	15.75
P_{stream}	44.09	0.49	15.77
$P-P_{stream}$	0.00	0.48	-0.02
P_{origin}	283.28	0.46	13.79
$P_{stream}-P_{origin}$			$\Delta z = 1.98$

Table 27 The vertical displacement, Δ **z**, of the flow to th**e sonic temperature #1** sensor

Location	x (m)	y (m)	z (m)
P (Sonic temp. #2)	44.09	-1.70	15.75
P_{stream}	44.09	-1.71	15.73
$P-P_{stream}$	0.00	-0.01	0.02
P_{origin}	283.18	-1.41	13.76
$P_{stream}-P_{origin}$			$\Delta z = 1.97$

Table 28 The vertical displacement, Δ **z,** of the flow to the **sonic temperature #2** sensor

Instrument site	Velocity from each direction	Average velocity (ms^{-1})	Free stream velocity (ms^{-1})	% Error
HS sonic	14.078(x)	14.073	14.102	-0.21
	14.076(y)			
	14.065(z)			
IFM #1	14.185(x)	14.185	14.074	0.79
	14.187(y)			
	14.183(z)			
IFM #2	14.148(x)	14.150	14.057	0.66
	14.153(y)			
	14.149(z)			
Sonic temperature #1	14.254(x)	14.258	14.092	1.18
	14.260(y)			
	14.260(z)			
Sonic temperature #2	14.225(x)	14.229	14.094	0.96
	14.232(y)			
	14.231(z)			

Table 29 Wind speed errors at the instrument sites on the JCR52 cruise (for a 15 ms^{-1} bow-on flow).

Instrument site	Velocity data line	Rate of change of velocity per metre (ms^{-1}/m)	Rate of change of velocity per cell (ms^{-1}/cell)
HS sonic	Along (x)	-0.133	-0.039
	Across (y)	0.001	0.001
	Up (z)	0.129	0.023
IFM #1	Along (x)	-0.162	-0.059
	Across (y)	-0.025	-0.006
	Up (z)	0.160	0.012
IFM #2	Along (x)	-0.146	-0.049
	Across (y)	-0.033	-0.008
	Up (z)	0.045	0.0063
Sonic temperature #1	Along (x)	-0.122	-0.043
	Across (y)	-0.034	-0.009
	Up (z)	-0.055	-0.013
Sonic temperature #2	Along (x)	-0.103	-0.035
	Across (y)	-0.048	0.012
	Up (z)	-0.023	-0.010

Table 30 Rate of change of velocity close to the instrument sites on the JCR 52 cruise (for a 15 ms^{-1} bow-on flow).

8.3 Beam-on flow of 5 ms^{-1}

8.3.a JCR 44

Location	x (m)	y (m)	z (m)
P (R2 sonic)	-0.61	-43.80	21.51
P_{stream}	-0.61	-44.77	21.54
$P-P_{stream}$	0.00	0.97	-0.03
P_{origin}	287.84	-39.06	16.68
$P_{stream}-P_{origin}$			$\Delta z = 4.86$

Table 31 The vertical displacement, Δ **z**, of the flow to the **R2 sonic** anemometer

Location	x (m)	y (m)	z (m)
P (Ship's sonic)	0.61	-43.80	21.51
P_{stream}	0.61	-44.67	21.51
$P-P_{stream}$	0.00	0.87	0.00
P_{origin}	287.57	-39.06	16.77
$P_{stream}-P_{origin}$			$\Delta z = 4.74$

Table 32 The vertical displacement, Δ **z**, of the flow to the **ship's sonic** anemometer

Location	x (m)	y (m)	z (m)
P (HS sonic)	1.40	-45.19	15.94
P_{stream}	1.39	-44.39	15.94
$P-P_{stream}$	0.01	-0.80	0.00
P_{origin}	287.49	-37.39	10.49
$P_{stream}-P_{origin}$			$\Delta z = 5.45$

Table 33 The vertical displacement, Δ z, of the flow to the **HS sonic (JCR 44)** anemometer

Location	x (m)	y (m)	z (m)
P (Bridge R2)	9.39	-9.62	16.20
P_{stream}	9.37	-9.58	16.24
$P-P_{stream}$	-0.02	-0.04	-0.04
P_{origin}	295.00	-4.25	6.41
$P_{stream}-P_{origin}$			$\Delta z = 9.83$

Table 34 The vertical displacement, Δ **z,** of the flow to the **bridge R2** anemometer

Location	x (m)	y (m)	z (m)
P (Dew point)	9.52	-10.79	14.85
P_{stream}	9.52	-11.09	14.84
$P-P_{stream}$	0.00	0.30	0.01
P_{origin}	287.00	-4.25	5.45
$P_{stream}-P_{origin}$			$\Delta z = 9.39$

Table 35 The vertical displacement, $\Delta \mathbf{z}$, of the flow to the **dew point** sensor

Location	x (m)	y (m)	z (m)
P (Humidity)	9.52	-11.49	14.85
P_{stream}	9.52	-11.09	14.85
$P-P_{stream}$	0.00	-0.40	0.00
P_{origin}	287.50	-4.25	5.45
$P_{stream}-P_{origin}$			$\Delta z = 9.40$

Table 36 The vertical displacement, $\Delta \mathbf{z}$, of the flow to the **fast humidity** sensor

Instrument site	Velocity from each direction	Average velocity (ms^{-1})	Free stream velocity (ms^{-1})	% Error
R2 sonic	5.722(x)	5.724	5.220	9.66
	5.724(y)			
	5.725(z)			
Ship's sonic	5.676(x)	5.677	5.221	8.73
	5.678(y)			
	5.677(z)			
HS sonic	5.658(x)	5.658	5.032	12.44
	5.657(y)			
	5.658(z)			
Bridge R2	4.716(x)	4.712	4.721	-0.19
	4.717(y)			
	4.704(z)			
Dew point	4.354(x)	4.372	4.583	-4.60
	4.356(y)			
	4.407(z)			
Fast humidity	4.692(x)	4.702	4.584	2.57
	4.673(y)			
	4.742(z)			

Table 37 Wind speed errors at the instrument sites on the JCR44 cruise (for a 5 ms^{-1} beam-on flow).

Instrument site	Velocity data line	Rate of change of velocity per metre (ms^{-1}/m)	Rate of change of velocity per cell (ms^{-1}/cell)
R2 sonic	Along (x)	-0.027	-0.011
	Across (y)	0.015	0.095
	Up (z)	-0.037	-0.011
Ship's sonic	Along (x)	-0.037	-0.014
	Across (y)	0.011	0.003
	Up (z)	-0.011	-0.004
HS sonic	Along (x)	-0.081	-0.050
	Across (y)	-0.005	0.002
	Up (z)	-0.012	-0.005
Bridge R2	Along (x)	0.273	0.012
	Across (y)	-0.089	-0.030
	Up (z)	0.255	0.053
Dew point	Along (x)	0.223	0.051
	Across (y)	-0.245	-0.041
	Up (z)	0.300	0.091
Fast humidity	Along (x)	0.070	0.036
	Across (y)	-0.505	-0.204
	Up (z)	0.206	0.057

Table 38 Rate of change of velocity close to the instrument sites on the JCR 44 cruise (for a 5 ms^{-1} beam-on flow).

8.3.b JCR 52

Location	x (m)	y (m)	z (m)
P (HS sonic)	1.40	-44.99	15.75
P_{stream}	1.40	-44.46	15.76
$P-P_{stream}$	0.00	-0.53	-0.01
P_{origin}	287.40	-37.39	10.31
$P_{stream}-P_{origin}$			$\Delta z = 5.45$

Table 39 The vertical displacement, $\Delta \mathbf{z}$, of the flow to the **HS sonic (JCR 52)** anemometer

Location	x (m)	y (m)	z (m)
P (IFM #1)	1.22	-44.39	15.55
P_{stream}	1.23	-44.57	15.55
$P-P_{stream}$	-0.01	0.18	0.00
P_{origin}	285.60	-37.39	10.06
$P_{stream}-P_{origin}$			$\Delta z = 5.49$

Table 40 The vertical displacement, Δ **z**, of the flow to the **IFM #1** sensor

Location	x (m)	y (m)	z (m)
P (IFM #2)	2.10	-44.39	15.30
P_{stream}	2.11	-44.52	15.31
$P-P_{stream}$	-0.01	0.13	-0.01
P_{origin}	287.17	-37.39	9.93
$P_{stream}-P_{origin}$			$\Delta z = 5.38$

Table 41 The vertical displacement, Δ **z**, of the flow to the **IFM #2** sensor

Location	x (m)	y (m)	z (m)
P (Sonic temp. #1)	0.97	-44.09	15.75
P_{stream}	0.97	-44.54	15.75
$P-P_{stream}$	0.00	0.45	0.00
P_{origin}	287.54	-37.39	10.22
$P_{stream}-P_{origin}$			$\Delta z = 5.53$

Table 42 The vertical displacement, Δ **z**, of the flow to the **sonic temperature #1** sensor

Location	x (m)	y (m)	z (m)
P (Sonic temp. #2)	-1.70	-44.09	15.75
P_{stream}	-1.71	-44.92	15.75
$P-P_{stream}$	0.01	0.83	0.00
P_{origin}	287.56	-37.39	9.89
$P_{stream}-P_{origin}$			$\Delta z = 5.86$

Table 43 The vertical displacement, Δ **z**, of the flow to the **sonic temperature #2** sensor

Instrument site	Velocity from each direction	Average velocity (ms^{-1})	Free stream velocity (ms^{-1})	% Error
HS sonic	5.660(x)	5.659	5.023	12.66
	5.656(y)			
	5.661			
IFM #1	5.686(x)	5.684	5.012	13.41
	5.686(y)			
	5.680(z)			
IFM #2	5.579(x)	5.577	5.006	11.41
	5.576(y)			
	5.575(z)			
Sonic temperature #1	5.682(x)	5.681	5.029	12.96
	5.674(y)			
	5.686(z)			
Sonic temperature #2	5.875(x)	5.863	5.031	16.54
	5.839(y)			
	5.874(z)			

Table 44 Wind speed errors at the instrument sites on the JCR52 cruise (for a 5 ms^{-1} beam-on flow).

Instrument site	Velocity data line	Rate of change of velocity per metre (ms^{-1}/m)	Rate of change of velocity per cell (ms^{-1}/cell)
HS sonic	Along (x)	-0.081	-0.050
	Across (y)	-0.011	-0.005
	Up (z)	-0.015	-0.005
IFM #1	Along (x)	-0.136	-0.075
	Across (y)	-0.034	0.005
	Up (z)	-0.095	-0.034
IFM #2	Along (x)	-0.095	-0.064
	Across (y)	-0.023	-0.007
	Up (z)	0.024	0.008
Sonic temperature #1	Along (x)	-0.152	-0.051
	Across (y)	-0.085	-0.016
	Up (z)	-0.132	-0.039
Sonic temperature #2	Along (x)	0.090	0.072
	Across (y)	-0.550	-0.272
	Up (z)	0.167	-0.004

Table 45 Rate of change of velocity close to the instrument sites on the JCR 52 cruise (for a 5 ms^{-1} beam-on flow).

8.4 Beam-on flow of 15 ms^{-1}

8.4.a JCR 44

Location	x (m)	y (m)	z (m)
P (R2 sonic)	-0.61	-43.80	21.51
P_{stream}	-0.61	-43.24	21.51
$P-P_{stream}$	0.00	-0.56	0.00
P_{origin}	287.74	-37.39	16.46
$P_{stream}-P_{origin}$			$\Delta z = 5.05$

Table 46 The vertical displacement, Δ **z,** of the flow to the **R2 sonic** anemometer

Location	x (m)	y (m)	z (m)
P (Ship's sonic)	0.61	-43.80	21.51
P_{stream}	0.62	-43.24	21.51
$P-P_{stream}$	-0.01	-0.56	0.00
P_{origin}	287.78	-37.39	16.60
$P_{stream}-P_{origin}$			$\Delta z = 4.91$

Table 47 The vertical displacement, Δ **z**, of the flow to the **ship's sonic** anemometer

Location	x (m)	y (m)	z (m)
P (HS sonic)	1.40	-45.19	15.94
P_{stream}	1.40	-44.60	15.94
$P-P_{stream}$	0.00	-0.59	0.00
P_{origin}	287.61	-37.39	10.53
$P_{stream}-P_{origin}$			$\Delta z = 5.41$

Table 48 The vertical displacement, Δ **z**, of the flow to the **HS sonic (JCR 44)** anemometer

Location	x (m)	y (m)	z (m)
P (Bridge R2)	9.39	-9.62	16.20
P_{stream}	9.37	-9.80	16.21
$P-P_{stream}$	0.02	0.18	-0.01
P_{origin}	288.87	-4.25	5.73
$P_{stream}-P_{origin}$			$\Delta z = 10.48$

Table 49 The vertical displacement, Δ **z**, of the flow to the **bridge R2** anemometer

Location	x (m)	y (m)	z (m)
P (Dew point)	9.52	-10.79	14.85
P_{stream}	9.52	-11.45	14.89
$P-P_{stream}$	0.00	0.66	-0.04
P_{origin}	288.39	-4.25	4.93
$P_{stream}-P_{origin}$			$\Delta z = 9.96$

Table 50 The vertical displacement, Δ **z**, of the flow to the **dew point** sensor

Location	x (m)	y (m)	z (m)
P (Humidity)	9.52	-11.49	14.85
P_{stream}	9.52	-11.45	14.89
$P-P_{stream}$	0.00	-0.04	-0.04
P_{origin}	288.39	-4.25	4.93
$P_{stream}-P_{origin}$			$\Delta z = 9.96$

Table 51 The vertical displacement, Δ **z**, of the flow to the **fast humidity** sensor

Instrument site	Velocity from each direction	Average velocity (ms^{-1})	Free stream velocity (ms^{-1})	% Error
R2 sonic	15.733(x)	15.735	14.307	9.98
	15.737(y)			
	15.734(z)			
Ship's sonic	15.633(x)	15.634	14.311	9.24
	15.638(y)			
	15.632(z)			
HS sonic	15.661(x)	15.660	13.863	12.96
	15.660(y)			
	15.659(z)			
Bridge R2	12.964(x)	12.951	13.279	-2.47
	12.962(y)			
	12.928(z)			
Dew point	12.123(x)	12.169	13.094	-7.06
	12.126(y)			
	12.258(z)			
Fast humidity	12.998(x)	13.020	13.094	-0.57
	12.940(y)			
	13.122(z)			

Table 52 **Wind speed errors** at the instrument sites on the JCR44 cruise (for a 15 ms^{-1} beam-on flow).

Instrument site	Velocity data line	Rate of change of velocity per metre (ms^{-1}/m)	Rate of change of velocity per cell (ms^{-1}/cell)
R2 sonic	Along (x)	-0.052	-0.018
	Across (y)	0.029	0.007
	Up (z)	-0.015	-0.003
Ship's sonic	Along (x)	-0.089	-0.036
	Across (y)	0.026	0.007
	Up (z)	0.019	0.001
HS sonic	Along (x)	-0.203	-0.129
	Across (y)	-0.011	0.010
	Up (z)	-0.066	-0.022
Bridge R2	Along (x)	0.951	0.050
	Across (y)	-0.224	-0.075
	Up (z)	0.592	0.111
Dew point	Along (x)	0.958	0.128
	Across (y)	-0.511	-0.106
	Up (z)	0.655	0.245
Fast humidity	Along (x)	0.756	0.123
	Across (y)	-1.239	-0.515
	Up (z)	0.477	0.149

Table 53 Rate of change of velocity close to the instrument sites on the JCR 44 cruise (for a 15 ms^{-1} beam-on flow).

8.4.b JCR 52

Location	x (m)	y (m)	z (m)
P (HS sonic)	1.40	-44.99	15.75
P_{stream}	1.40	-44.69	15.75
$P-P_{stream}$	0.00	-0.30	0.00
P_{origin}	287.73	-37.39	10.31
$P_{stream}-P_{origin}$			$\Delta z = 5.44$

Table 54 The vertical displacement, $\Delta \mathbf{z}$, of the flow to the **HS sonic (JCR 52)** anemometer

Location	x (m)	y (m)	z (m)
P (IFM #1)	1.22	-44.39	15.55
P_{stream}	1.23	-44.78	15.55
$P-P_{stream}$	-0.01	0.39	0.00
P_{origin}	287.70	-37.39	10.06
$P_{stream}-P_{origin}$			$\Delta z = 5.49$

Table 55 The vertical displacement, Δ **z**, of the flow to the **IFM #1** sensor

Location	x (m)	y (m)	z (m)
P (IFM #2)	2.10	-44.39	15.30
P_{stream}	2.10	-44.74	15.31
$P-P_{stream}$	0.00	0.35	-0.01
P_{origin}	287.75	-37.39	9.95
$P_{stream}-P_{origin}$			$\Delta z = 5.36$

Table 56 The vertical displacement, Δ **z**, of the flow to the **IFM #2** sensor

Location	x (m)	y (m)	z (m)
P (Sonic temp. #1)	0.97	-44.09	15.75
P_{stream}	0.98	-44.73	15.78
$P-P_{stream}$	-0.01	0.64	-0.03
P_{origin}	288.87	-37.39	10.28
$P_{stream}-P_{origin}$			$\Delta z = 5.50$

Table 57 The vertical displacement, Δ **z**, of the flow to the **sonic temperature #1** sensor

Location	x (m)	y (m)	z (m)
P (Sonic temp. #2)	-1.70	-44.09	15.75
P_{stream}	-1.70	-43.40	15.76
$P-P_{stream}$	0.00	-0.69	-0.01
P_{origin}	288.70	-35.72	9.54
$P_{stream}-P_{origin}$			$\Delta z = 6.22$

Table 58 The vertical displacement, Δ **z**, of the flow to the **sonic temperature #2** sensor

Instrument site	Velocity from each direction	Average velocity (ms^{-1})	Free stream velocity (ms^{-1})	% Error
HS sonic	15.667(x)	15.666	13.842	13.18
	15.660(y)			
	15.672(z)			
IFM #1	15.747(x)	15.747	13.821	13.94
	15.761(y)			
	15.734(z)			
IFM #2	15.472(x)	15.464	13.811	11.97
	15.462(y)			
	15.459(z)			
Sonic temperature #1	15.707(x)	15.701	13.855	13.32
	15.678(y)			
	15.719(z)			
Sonic temperature #2	16.098(x)	16.053	13.814	16.21
	15.964(y)			
	16.097(z)			

Table 59 Wind speed errors at the instrument sites on the JCR52 cruise.

Instrument site	Velocity data line	Rate of change of velocity per metre (ms^{-1}/m)	Rate of change of velocity per cell (ms^{-1}/cell)
HS sonic	Along (x)	-0.204	-0.129
	Across (y)	-0.032	0.016
	Up (z)	-0.073	-0.024
IFM #1	Along (x)	-0.347	-0.197
	Across (y)	-0.195	0.008
	Up (z)	-0.280	-0.117
IFM #2	Along (x)	-0.254	-0.167
	Across (y)	-0.062	-0.021
	Up (z)	0.044	0.012
Sonic temperature #1	Along (x)	-0.383	-0.118
	Across (y)	-0.248	-0.111
	Up (z)	-0.393	-0.122
Sonic temperature #2	Along (x)	0.304	0.234
	Across (y)	-1.431	-0.910
	Up (z)	0.357	-0.057

Table 60 Rate of change of velocity close to the instrument sites on the JCR 52 cruise (for a 15 ms^{-1} beam-on flow).

8.5 Summary

Instrument	Instrument height z (m)	Velocity at instrument site (ms^{-1})	Free stream velocity (at $z - \Delta z$) (ms^{-1})	% velocity error at instrument site	Vertical displacement Δz (m)	Angle of flow to the horizontal (degrees)
JCR 44						
R2 sonic	21.51	5.223	5.281	**-1.10 (0.09)**	**1.71 ± 0.1**	**3.5**
Ship's sonic	21.51	5.223	5.281	**-1.10 (0.09)**	**1.71 ± 0.1**	**3.6**
HS sonic (JCR 44)	15.94	5.096	5.138	**-0.82 (0.14)**	**2.05 ± 0.1**	**5.9**
Bridge R2	16.20	2.915	4.974	**-41.40 (26.74)**	**6.35 ± 0.5**	**4.5**
Dew point	14.85	4.995	4.948	**0.95 (22.09)**	**5.28 ± 0.5**	**-7.2**
Fast humidity	14.85	5.810	4.938	**17.66 (4.31)**	**5.38 ± 0.5**	**-4.0**
JCR 52						
HS Sonic (JCR 52)	15.75	5.100	5.129	**-0.57 (0.23)**	**2.09 ± 0.1**	**6.1**
IFM #1	15.55	5.145	5.118	**0.53 (0.47)**	**2.18 ± 0.1**	**6.5**
IFM #2	15.30	5.119	5.108	**0.22 (0.41)**	**2.19 ± 0.1**	**6.1**
Sonic temp. #1	15.75	5.170	5.124	**0.90 (0.39)**	**2.21 ± 0.1**	**6.2**
Sonic temp. #2	15.75	5.159	5.126	**0.64 (0.29)**	**2.18 ± 0.1**	**5.9**

Table 61a. Summary of the effects of flow distortion for a **bow-on flow of 5 ms^{-1}.** The figures in brackets indicate the maximum rate of change of velocity per cell.

Instrument	Instrument height z (m)	Velocity at instrument site (ms^{-1})	Free stream velocity (at $z - \Delta z$) (ms^{-1})	% velocity error at instrument site	Vertical displacement Δz (m)	Angle of flow to the horizontal (degrees)
JCR 44						
R2 sonic	21.51	14.324	14.480	**-1.08 (0.03)**	**1.52 ± 0.1**	**3.4**
Ship's sonic	21.51	14.324	14.479	**-1.07 (0.03)**	**1.53 ± 0.1**	**3.4**
HS sonic (JCR 44)	15.94	14.053	14.123	**-0.50 (0.19)**	**1.84 ± 0.1**	**5.4**
Bridge R2	16.20	9.281	13.782	**-32.66 (21.75)**	**6.17 ± 0.5**	**3.7**
Dew point	14.85	10.211	13.736	**-25.66 (19.69)**	**5.22 ± 0.5**	**-18.4**
Fast humidity	14.85	14.388	13.727	**4.82 (15.08)**	**5.29 ± 0.5**	**-13.1**
JCR 52						
HS Sonic (JCR 52)	15.75	14.073	14.102	**-0.21 (0.28)**	**1.88 ± 0.1**	**5.6**
IFM #1	15.55	14.185	14.074	**0.79 (0.42)**	**1.98 ± 0.1**	**5.9**
IFM #2	15.30	14.150	14.057	**0.66 (0.35)**	**1.96 ± 0.1**	**5.5**
Sonic temp. #1	15.75	14.258	14.092	**1.18 (0.31)**	**1.98 ± 0.1**	**5.5**
Sonic temp. #2	15.75	14.229	14.094	**0.96 (0.25)**	**1.97 ± 0.1**	**5.2**

Table 61b. Summary of the effects of flow distortion for a **bow-on flow of 15 ms^{-1}.** The figures in brackets indicate the maximum rate of change of velocity per cell.

Instrument	Instrument height z (m)	Velocity at instrument site (ms^{-1})	Free stream velocity (at $z - \Delta z$) (ms^{-1})	% velocity error at instrument site	Vertical displacement Δz (m)	Angle of flow to the horizontal (degrees)
JCR 44						
R2 sonic	21.51	5.724	5.220	**9.66 (1.82)**	**4.86 ± 0.1**	**5.0**
Ship's sonic	21.51	5.677	5.221	**8.73 (0.27)**	**4.74 ± 0.1**	**5.6**
HS sonic (JCR 44)	15.94	5.658	5.032	**12.44 (0.99)**	**5.45 ± 0.1**	**7.6**
Bridge R2	16.20	4.712	4.721	**-0.19 (1.12)**	**9.83 ± 0.5**	**38.9**
Dew point	14.85	4.372	4.583	**-4.60 (1.99)**	**9.39 ± 0.5**	**41.8**
Fast humidity	14.85	4.702	4.584	**2.57 (4.45)**	**9.40 ± 0.5**	**36.1**
JCR 52						
HS Sonic (JCR 52)	15.75	5.659	5.023	**12.66 (1.00)**	**5.45 ± 0.1**	**7.8**
IFM #1	15.55	5.684	5.012	**13.41 (1.50)**	**5.49 ± 0.1**	**8.7**
IFM #2	15.30	5.577	5.006	**11.41 (1.28)**	**5.38 ± 0.1**	**9.3**
Sonic temp. #1	15.75	5.681	5.029	**12.96 (1.01)**	**5.53 ± 0.1**	**8.2**
Sonic temp. #2	15.75	5.863	5.031	**16.54 (5.41)**	**5.86 ± 0.1**	**4.4**

Table 61c. Summary of the effects of flow distortion for a **beam-on flow of 5 ms^{-1}.** The figures in brackets indicate the maximum rate of change of velocity per cell.

Instrument	Instrument height z (m)	Velocity at instrument site (ms^{-1})	Free stream velocity (at $z - \Delta z$) (ms^{-1})	% velocity error at instrument site	Vertical displacement Δz (m)	Angle of flow to the horizontal (degrees)
JCR 44						
R2 sonic	21.51	15.735	14.307	**9.98 (0.13)**	**5.05 ± 0.1**	**5.3**
Ship's sonic	21.51	15.634	14.311	**9.24 (0.25)**	**4.91 ± 0.1**	**5.9**
HS sonic (JCR 44)	15.94	15.660	13.863	**12.96 (0.93)**	**5.41 ± 0.1**	**8.0**
Bridge R2	16.20	12.951	13.279	**-2.47 (0.84)**	**10.48 ± 0.5**	**39.7**
Dew point	14.85	12.169	13.094	**-7.06 (1.87)**	**9.96 ± 0.5**	**44.6**
Fast humidity	14.85	13.020	13.094	**-0.57 (3.93)**	**9.96 ± 0.5**	**38.8**
JCR 52						
HS Sonic (JCR 52)	15.75	15.666	13.842	**13.18 (0.93)**	**5.44 ± 0.1**	**8.2**
IFM #1	15.55	15.747	13.821	**13.94 (1.43)**	**5.94 ± 0.1**	**9.0**
IFM #2	15.30	15.464	13.811	**11.97 (1.21)**	**5.36 ± 0.1**	**9.6**
Sonic temp. #1	15.75	15.701	13.855	**13.32 (0.88)**	**5.50 ± 0.1**	**8.3**
Sonic temp. #2	15.75	16.053	13.814	**16.21 (6.59)**	**6.22 ± 0.1**	**4.2**

Table 61d. Summary of the effects of flow distortion for a **beam-on flow of 15 ms^{-1}.** The figures in brackets indicate the maximum rate of change of velocity per cell.

Instrument	Instrument height, z (m)	Velocity at instrument (ms^{-1})	Free stream velocity at height z (ms^{-1})	% velocity error at instrument site
JCR 44				
R2 sonic	21.51	5.223	5.315	-1.73
Ship's sonic	21.51	5.223	5.315	-1.73
HS sonic	15.94	5.096	5.194	-1.89
Bridge R2	16.20	2.915	5.205	-44.00
Dew point	14.85	4.995	5.170	-3.39
Fast humidity	14.85	5.810	5.170	12.38
JCR 52				
HS sonic	15.75	5.100	5.190	-1.73
IFM #1	15.55	5.145	5.186	-0.79
IFM #2	15.30	5.119	5.181	-1.20
Sonic temp. #1	15.75	5.170	5.190	-0.39
Sonic temp. #2	15.75	5.159	5.190	-0.60

Table 62a. The wind speed errors calculated using a free stream velocity at the **actual instrument height, z,** for a **bow-on flow of 5 ms^{-1}.**

Instrument	Instrument height, z (m)	Velocity at instrument (ms^{-1})	Free stream velocity at height z (ms^{-1})	% velocity error at instrument site
JCR 44				
R2 sonic	21.51	14.324	14.554	-1.58
Ship's sonic	21.51	14.324	14.554	-1.58
HS sonic	15.94	14.053	14.244	-1.34
Bridge R2	16.20	9.281	14.271	-34.97
Dew point	14.85	10.211	14.183	-28.01
Fast humidity	14.85	14.388	14.183	1.45
JCR 52				
HS sonic	15.75	14.073	14.234	-1.13
IFM #1	15.55	14.185	14.223	-0.27
IFM #2	15.30	14.150	14.210	-0.42
Sonic temp. #1	15.75	14.258	14.234	0.17
Sonic temp. #2	15.75	14.229	14.234	-0.04

Table 62b. The wind speed errors calculated using a free stream velocity at the **actual instrument height, z,** for a **bow-on flow of 15 ms^{-1}.**

Instrument	Instrument height, z (m)	Velocity at instrument (ms^{-1})	Free stream velocity at height z (ms^{-1})	% velocity error at instrument site
JCR 44				
R2 sonic	21.51	5.724	5.324	7.51
Ship's sonic	21.51	5.677	5.323	6.65
HS sonic	15.94	5.658	5.211	8.58
Bridge R2	16.20	4.712	5.214	-9.63
Dew point	14.85	4.372	5.182	-15.63
Fast humidity	14.85	4.702	5.181	-9.25
JCR 52				
HS sonic	15.75	5.659	5.207	8.68
IFM #1	15.55	5.684	5.203	9.25
IFM #2	15.30	5.577	5.198	7.29
Sonic temp. #1	15.75	5.681	5.198	9.29
Sonic temp. #2	15.75	5.863	5.196	12.84

Table 62c. The wind speed errors calculated using a free stream velocity at the **actual instrument height, z,** for a **beam-on flow of 5 ms^{-1}.**

Instrument	Instrument height, z (m)	Velocity at instrument (ms^{-1})	Free stream velocity at height z (ms^{-1})	% velocity error at instrument site
JCR 44				
R2 sonic	21.51	15.735	14.582	7.91
Ship's sonic	21.51	15.634	14.580	7.23
HS sonic	15.94	15.660	14.292	9.57
Bridge R2	16.20	12.951	14.301	-9.44
Dew point	14.85	12.169	14.219	-14.42
Fast humidity	14.85	13.020	14.219	-8.43
JCR 52				
HS sonic	15.75	15.666	14.283	9.68
IFM #1	15.55	15.747	14.273	10.33
IFM #2	15.30	15.464	14.259	8.45
Sonic temp. #1	15.75	15.701	14.260	10.11
Sonic temp. #2	15.75	16.053	14.254	12.62

Table 62d. The wind speed errors calculated using a free stream velocity at the **actual instrument height, z,** for a **beam-on flow of 15 ms^{-1}.**

9. FIGURES

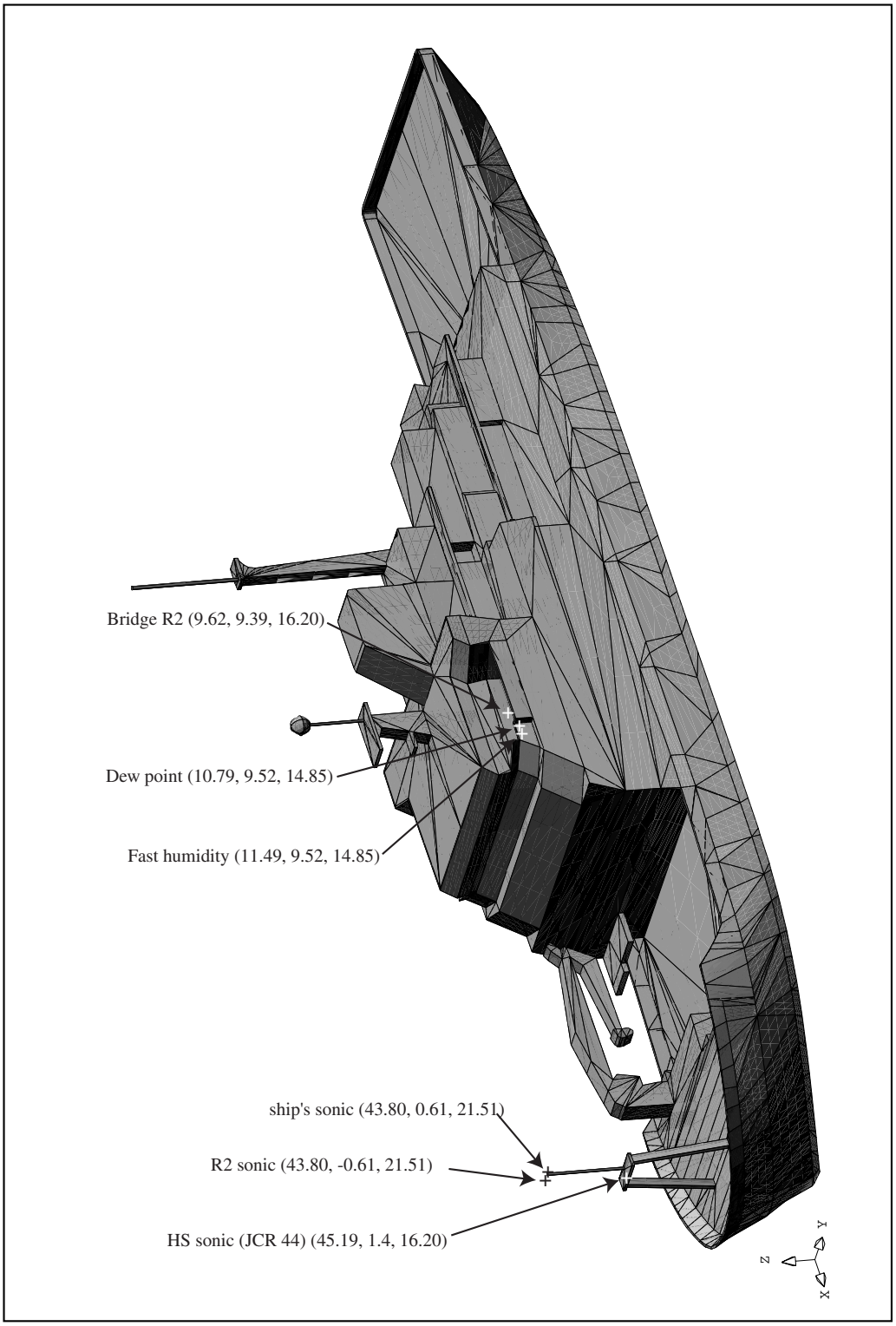

Figure 1. A 3-dimensional view of the *R.R.S. James Clark Ross*. The x, y and z co-ordinates of the instruments on the JCR 44 cruise are shown.

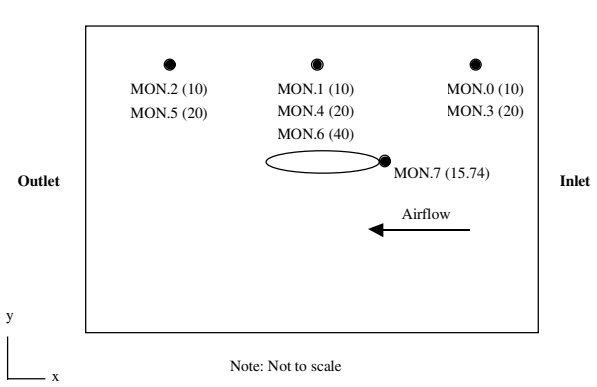

Figure 2. Schematic plan view of the wind tunnel used to simulate a flow of air over the bows of the *R.R.S. James Clark Ross*. The monitoring points are shown by the solid circles and their heights in metres are indicated in brackets.

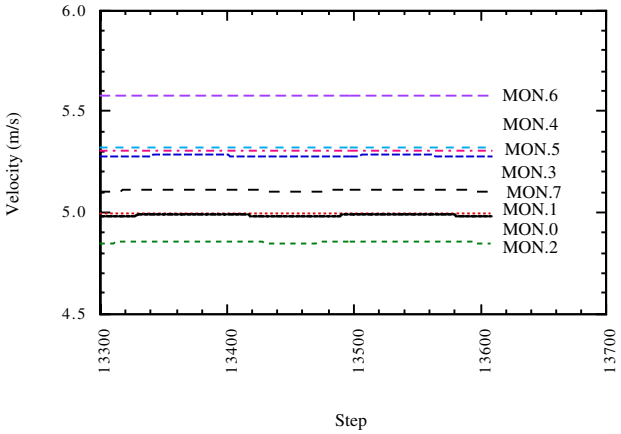

Figure 3. Velocity data for the last 300 time steps at the eight monitoring locations in the model with a flow of 5 ms^{-1} over the bow.

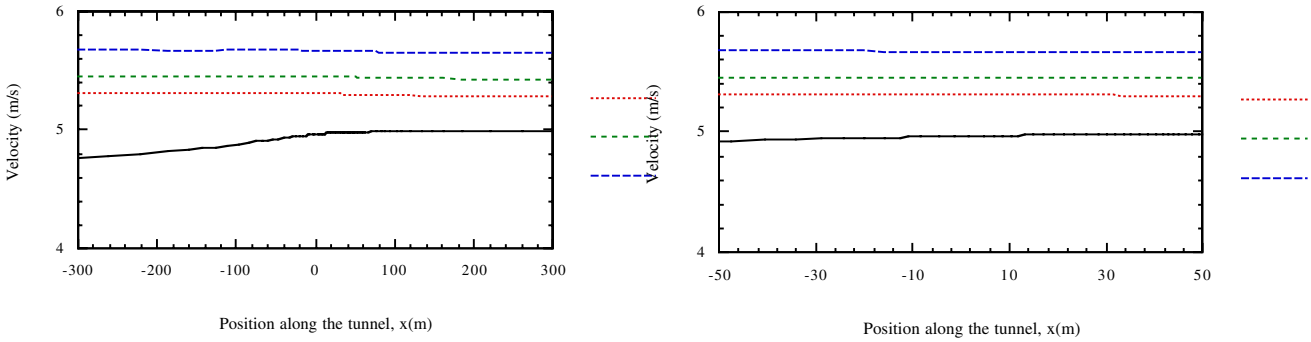

Figure 4. Lines of velocity data along the length of the tunnel for a flow directly over the bows. The data were obtained at heights (top to bottom) of 50, 30. 20 and 10 m, in the free stream region on the port side of the model at y = 150 m. a) left - the full length of the tunnel and b) right - only the central section of the tunnel.

.

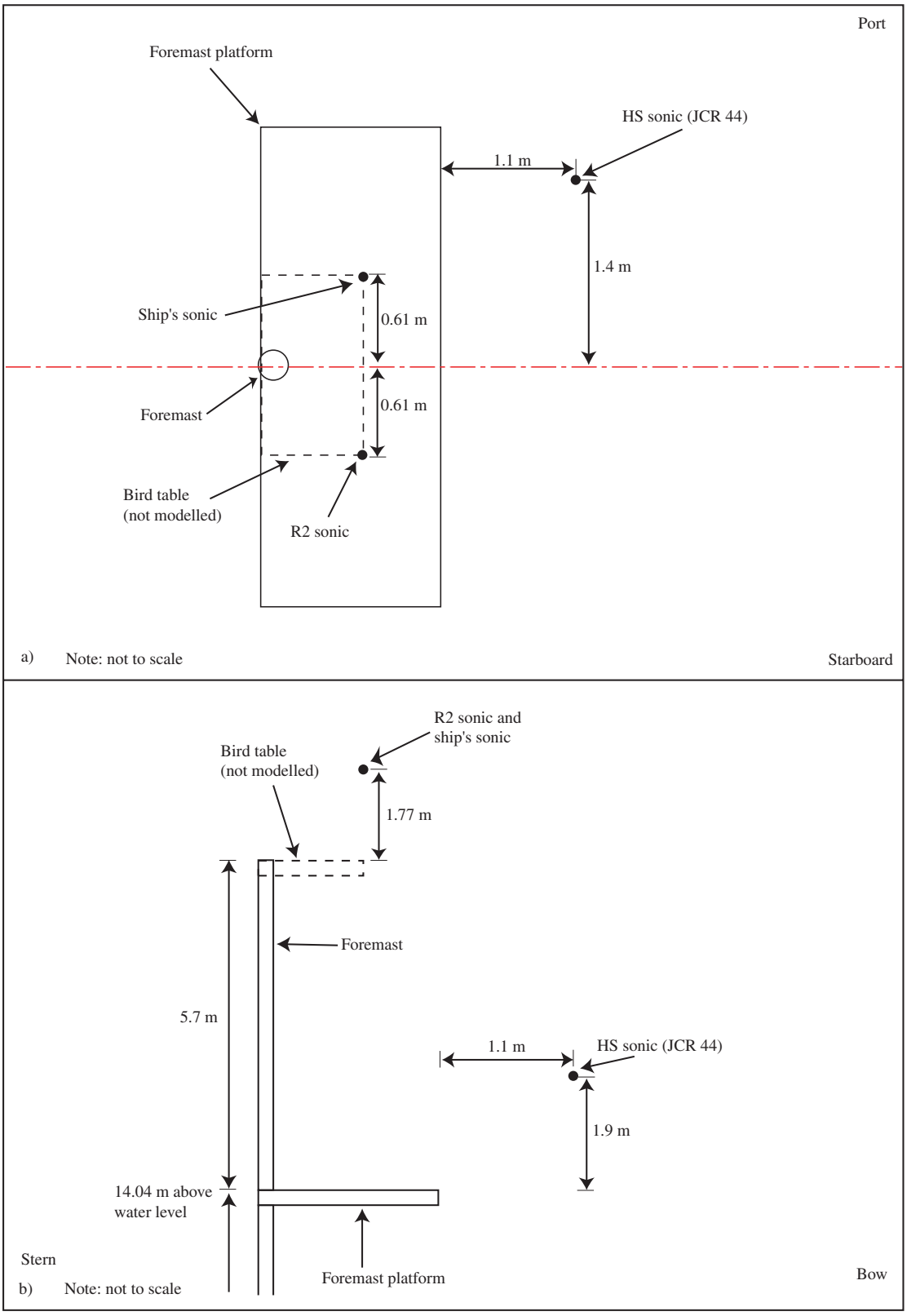

Figure 5. Schematic of the instrument positions on the foremast of the *R.R.S. James Clark Ross* relative to the foremast platform and bird table for the JCR 44 cruise; a) Plan view and b) side view.

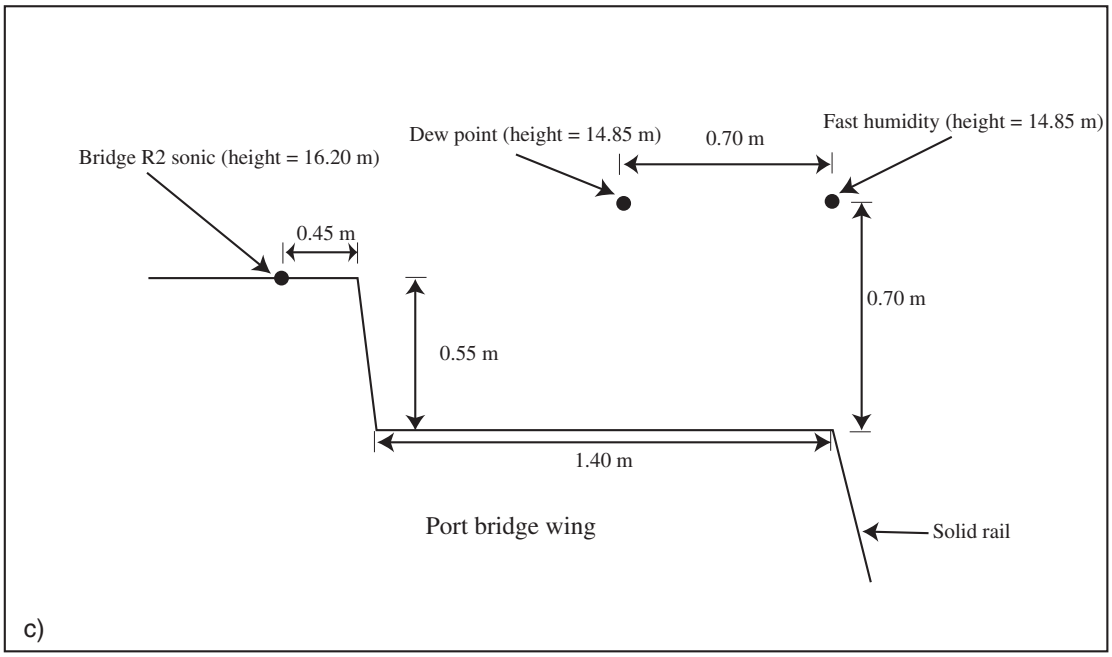

Figure 5c. Plan view of the instrument sites on the port bridge wing on the JCR 44 cruise.

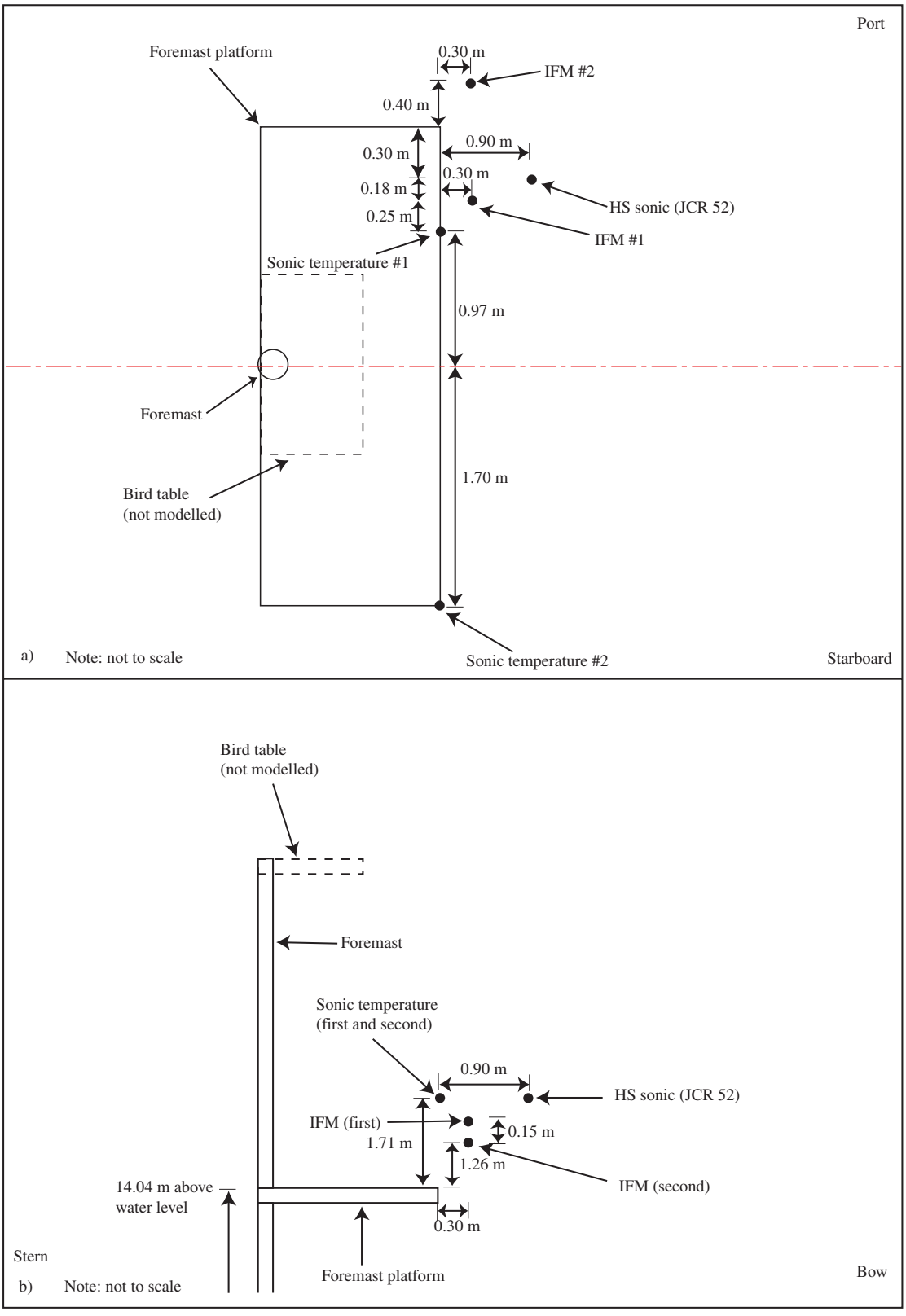

Figure 6. Schematic of the instrument positions on the foremast of the *R.R.S. James Clark Ross* relative to the foremast platform and bird table for the JCR 52 cruise; a) Plan view and b) side view.

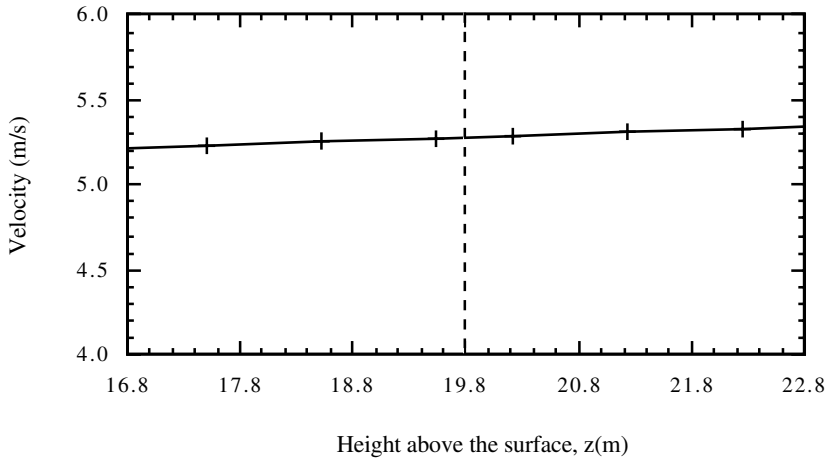

Figure 7. The vertical profile of velocity abeam of the R2 sonic anemometer site. The dashed line indicates the height at which the airflow originated.

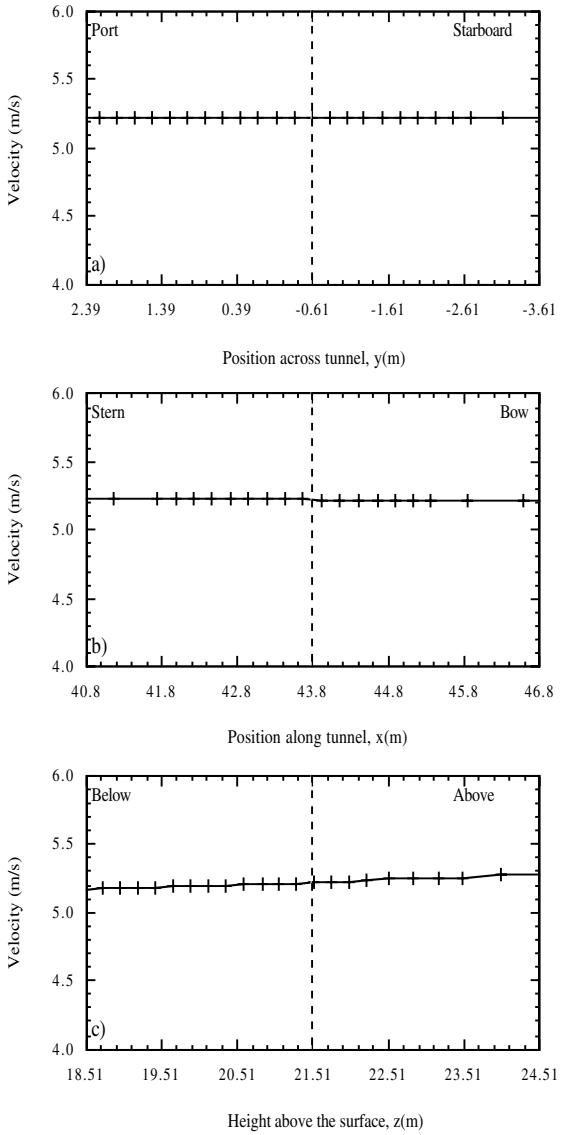

Figure 8. Lines of velocity data through the instrument position (indicated by the dashed line) in all three directions: top - across the tunnel; middle - along the tunnel, and bottom - vertically. The results are for a **bow-on flow of 5 ms^{-1}** to the **R2 sonic** anemometer site.

.

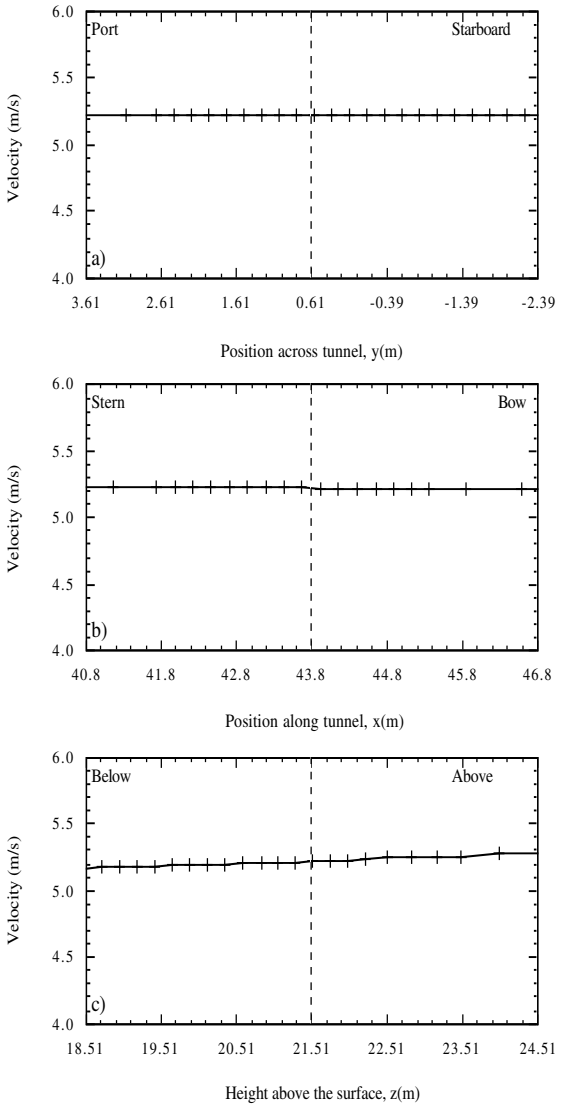

Figure 9. As Figure 8 but for the **ship's sonic** anemometer site.

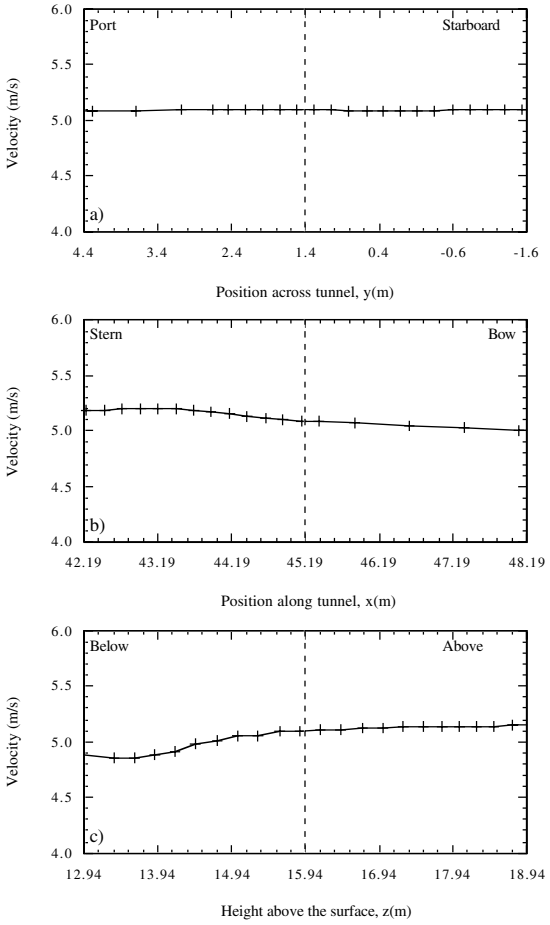

Figure 10. As for Figure 8, but for the **HS sonic (JCR 44)** site.

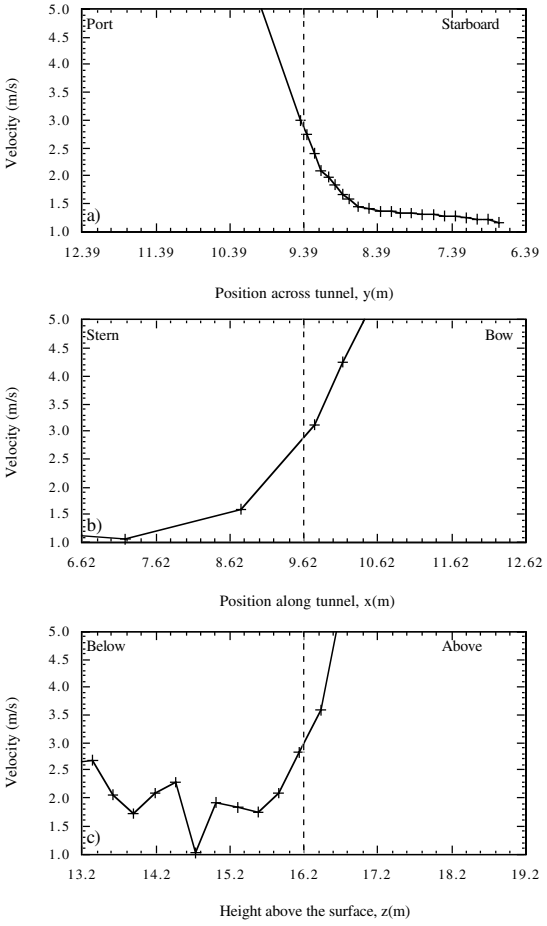

Figure 11 As Figure 8 but for the **bridge R2 sonic** site.

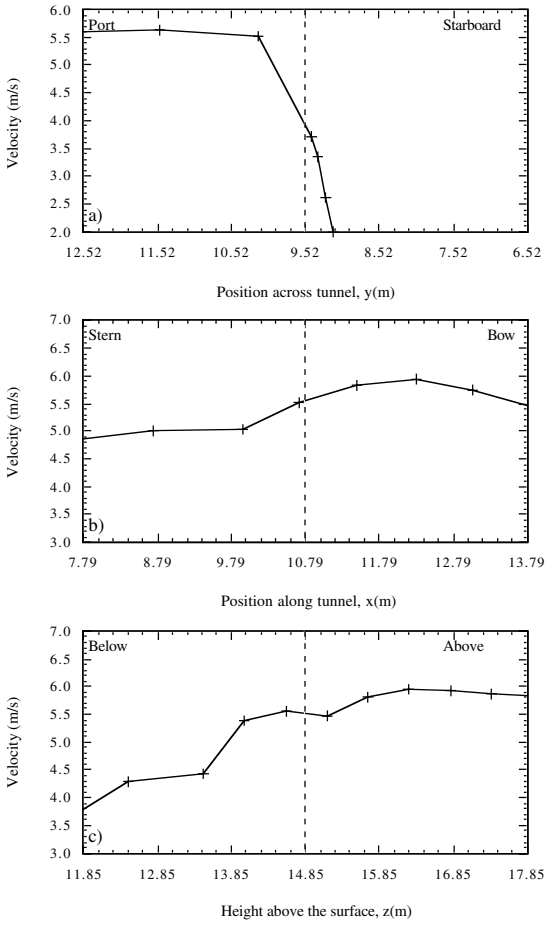

Figure 12. As for Figure 8, but for the **dew point** sensor site.

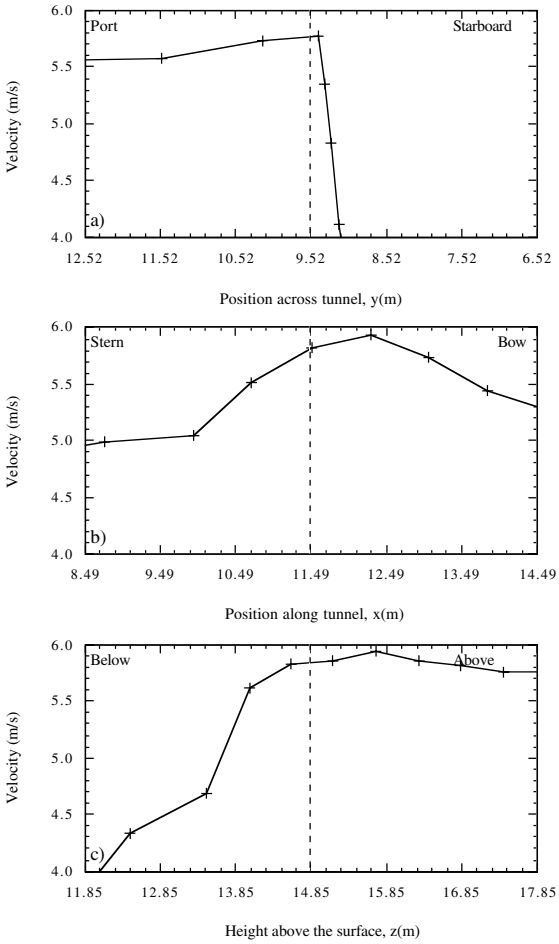

Figure 13. As for Figure 8, but for the **fast humidity** sensor site.

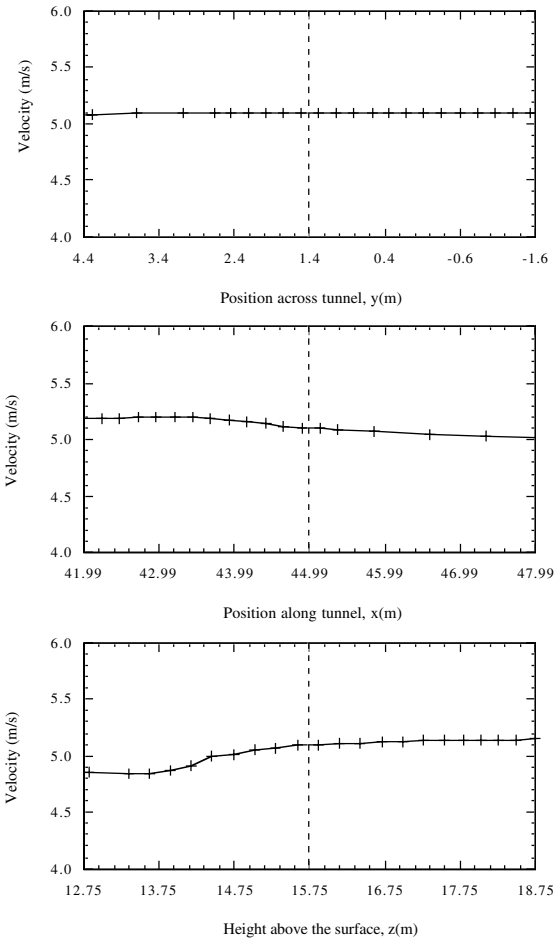

Figure 14. As for Figure 8, but for the **HS sonic (JCR 52)** anemometer site.

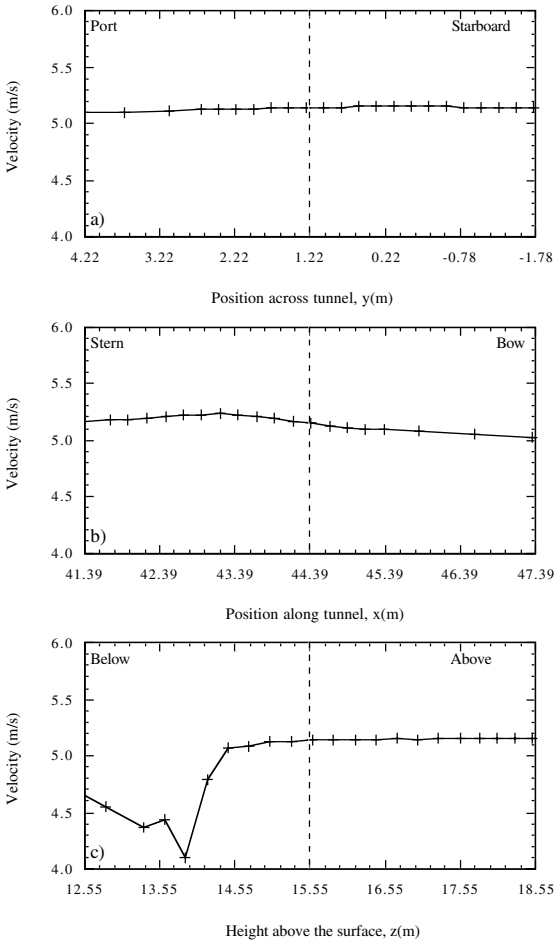

Figure 15. As for Figure 8, but for the **IFM #1** sensor site.

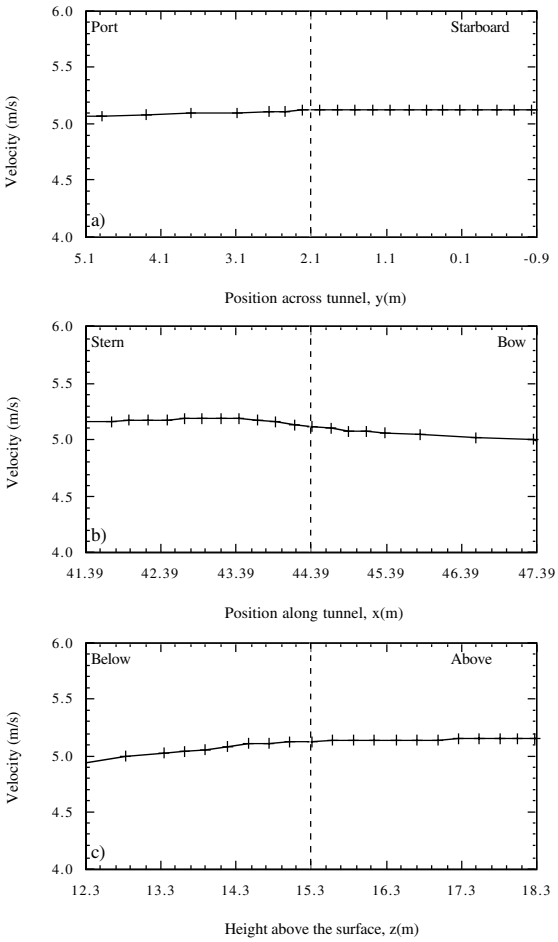

Figure 16. As for Figure 8, but for the **IFM #2** sensor site.

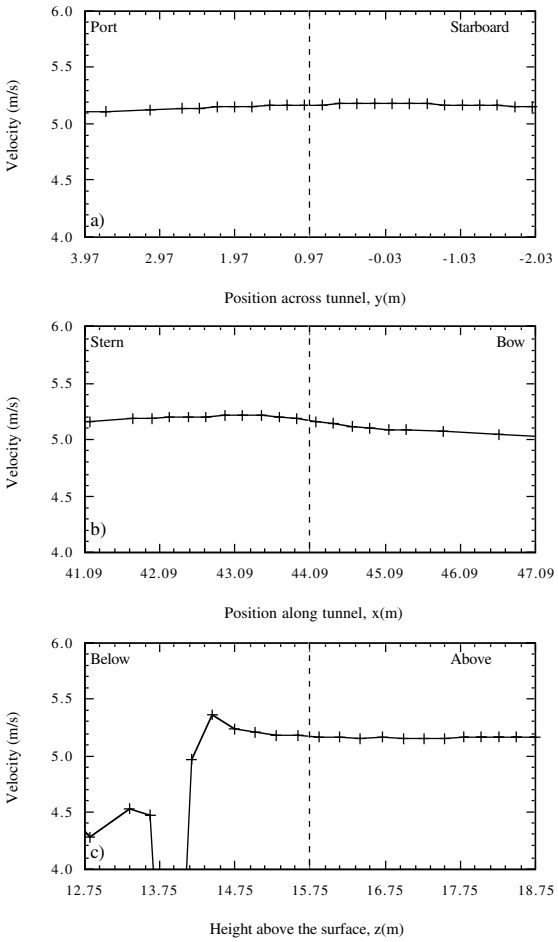

Figure 17. As for Figure 8, but for the **sonic temperature #1** sensor site.

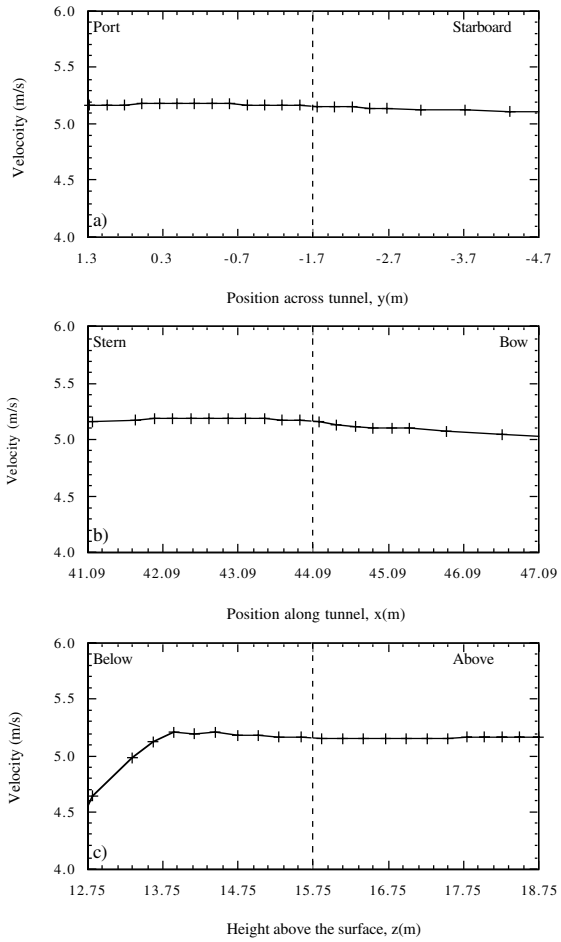

Figure 18. As for Figure 8, but for the **sonic temperature #2** site.

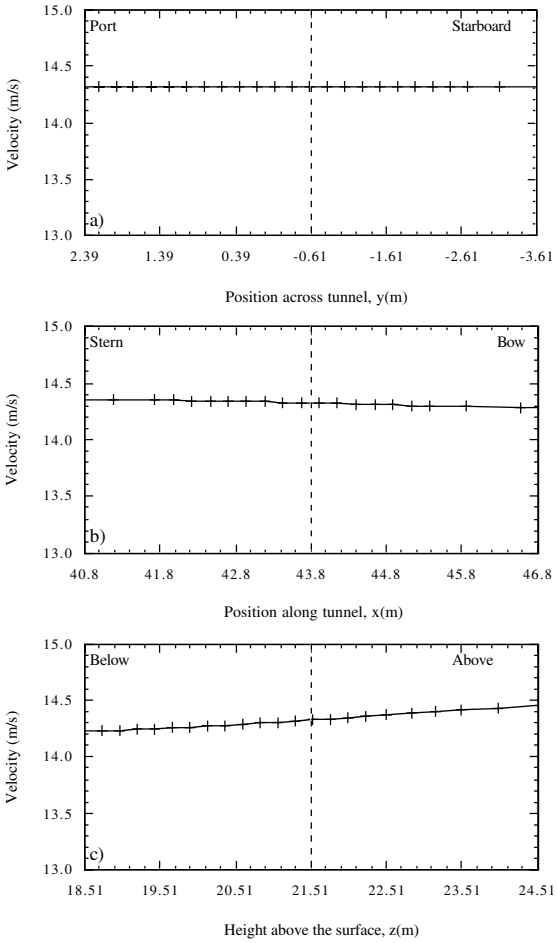

Figure 19. Lines of velocity data through the instrument position (indicated by the dashed line) in all three directions: top - across the tunnel; middle - along the tunnel, and bottom - vertically. The results are for a **bow-on flow of 15 ms^{-1}** to the **R2 sonic** anemometer site.

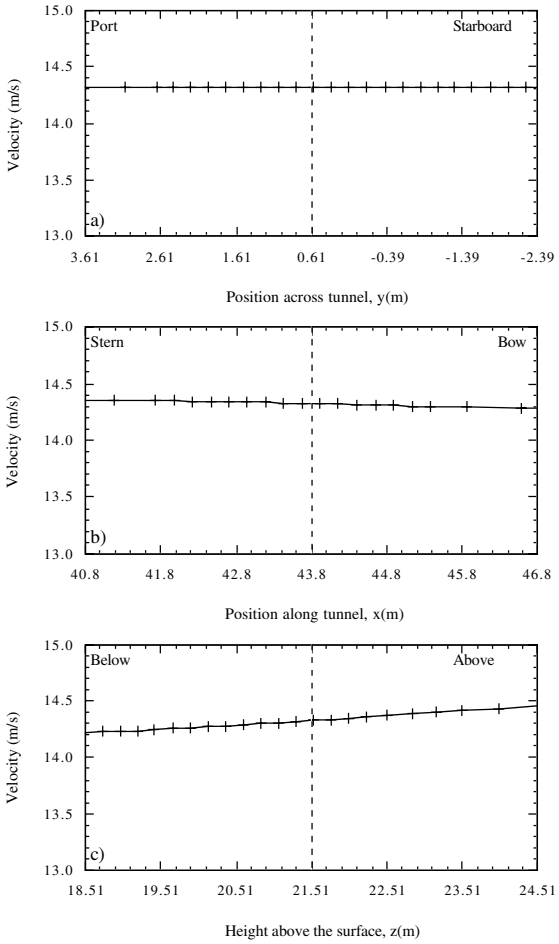

Figure 20 . As Figure 19 but for the **ship's sonic** site.

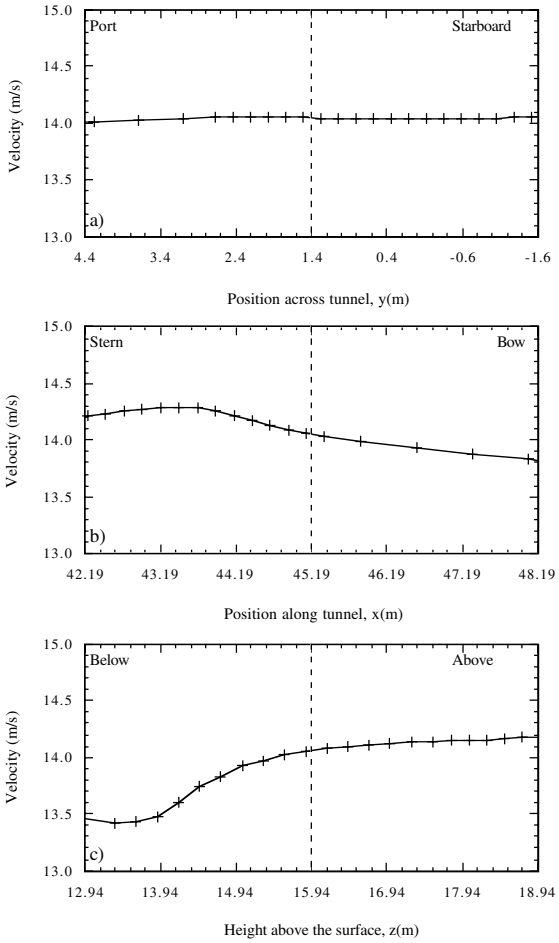

Figure 21. As for Figure 19, but for the **HS sonic (JCR 44)** anemometer site.

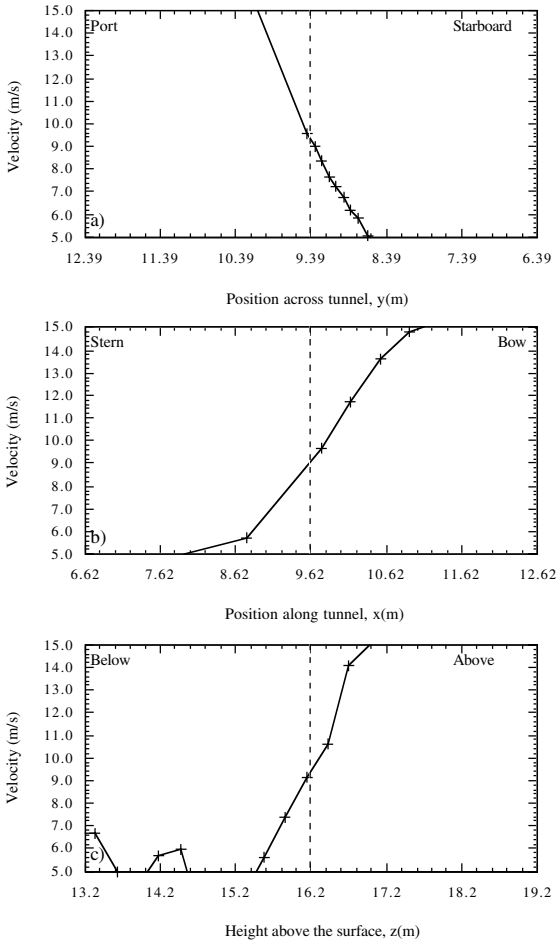

Figure 22. As for Figure 19, but for the **bridge R2 sonic** anemometer site.

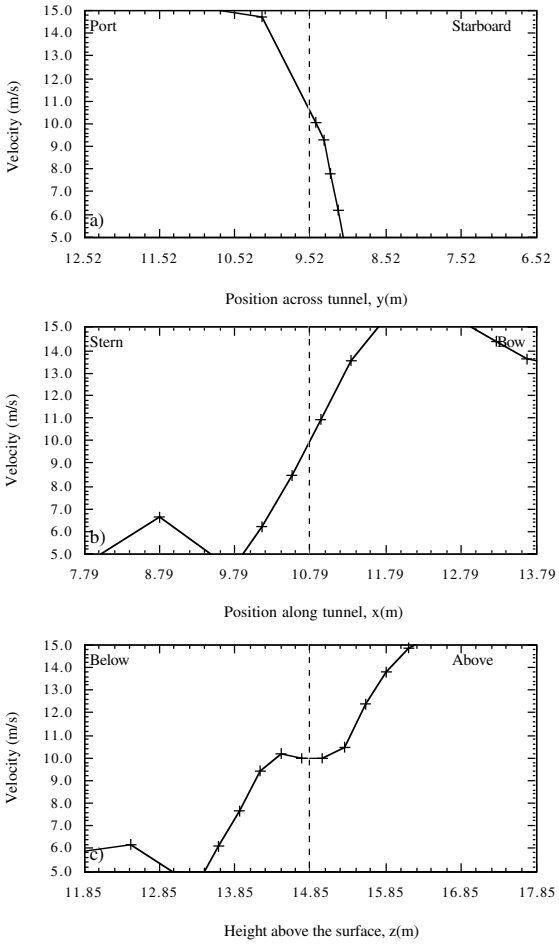

Figure 23. As for Figure 19, but for the **dew point** sensor site.

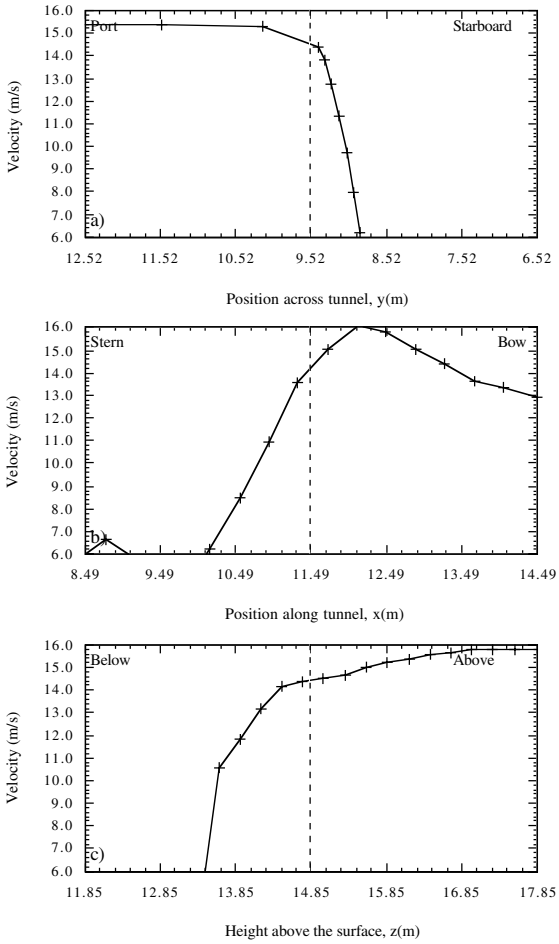

Figure 24. As for Figure 19, but for the **fast humidity** sensor site.

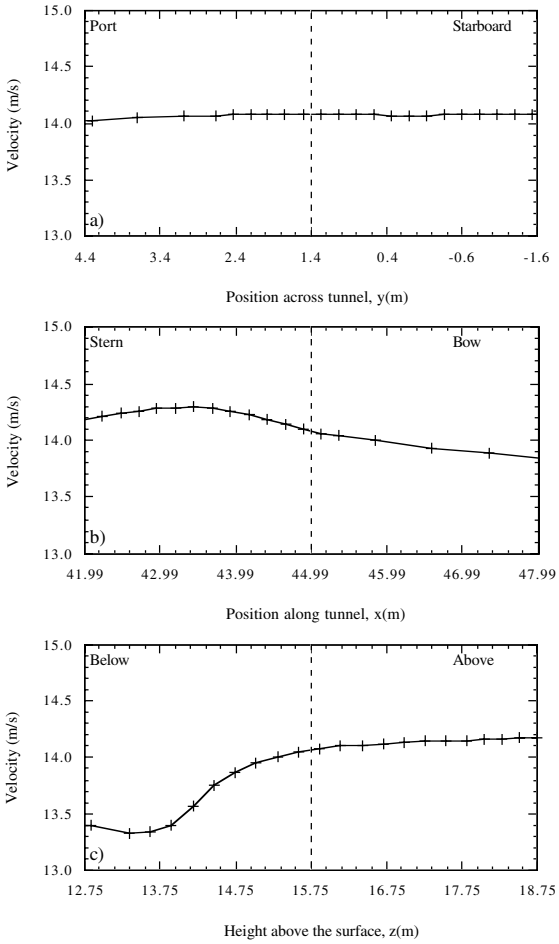

Figure 25. As for Figure 19, but for the **HS sonic (JCR 52)** anemometer site**.**

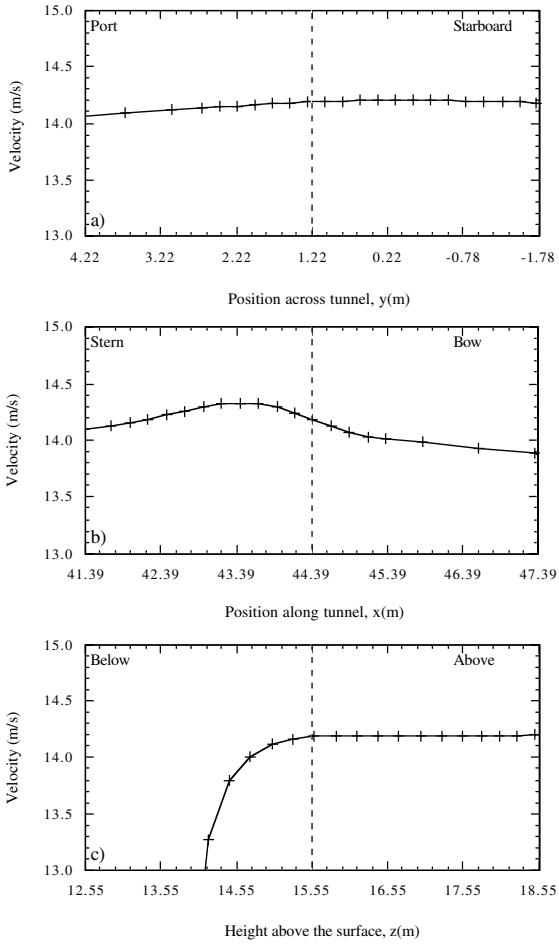

Figure 26. As for Figure 19, but for the **IFM #1** sensor site.

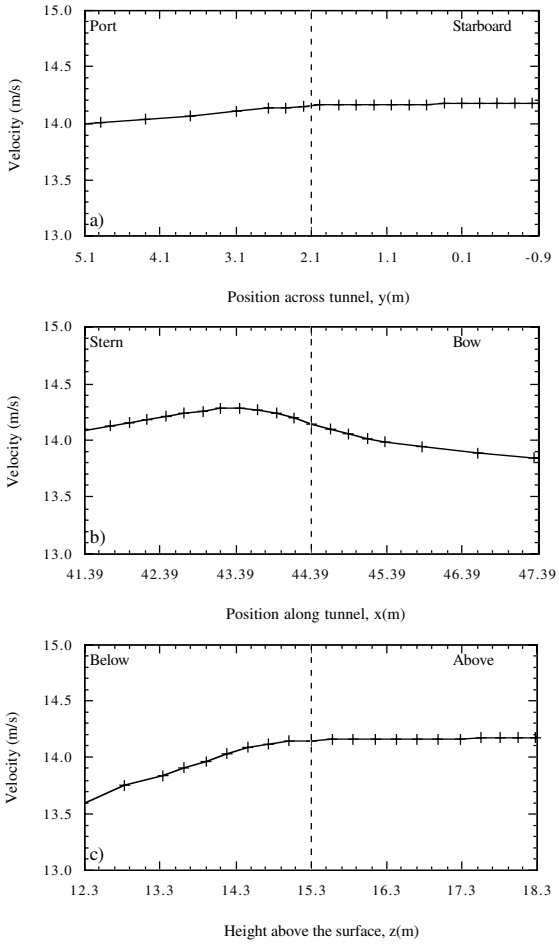

Figure 27. As for Figure 19, but for the **IFM #2** sensor site.

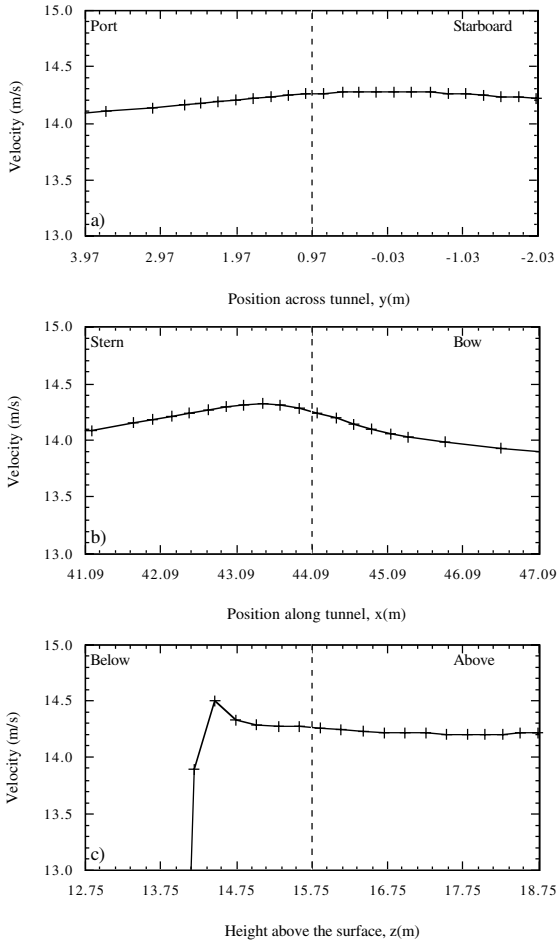

Figure 28. As for Figure 19, but for the **sonic temperature #1** sensor site.

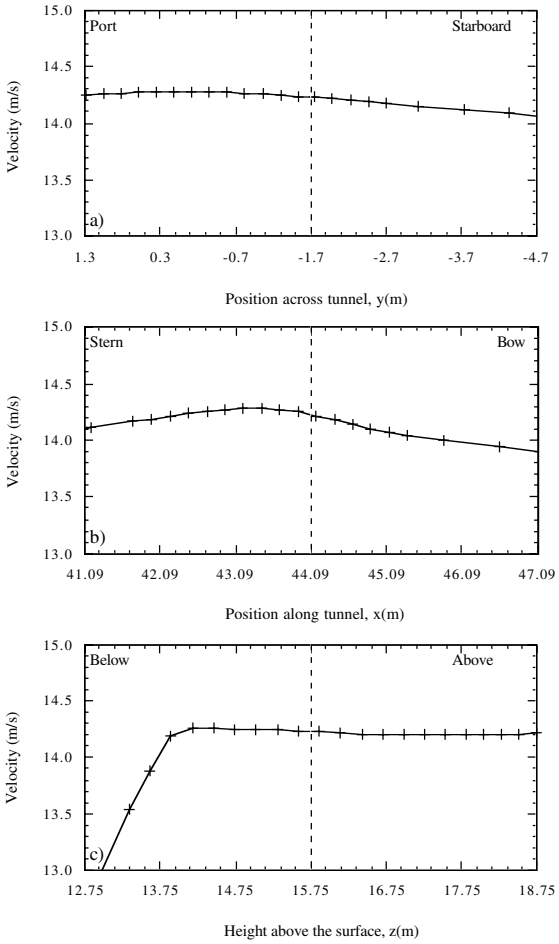

Figure 29. As for Figure 19, but for the **sonic temperature #2** sensor site.

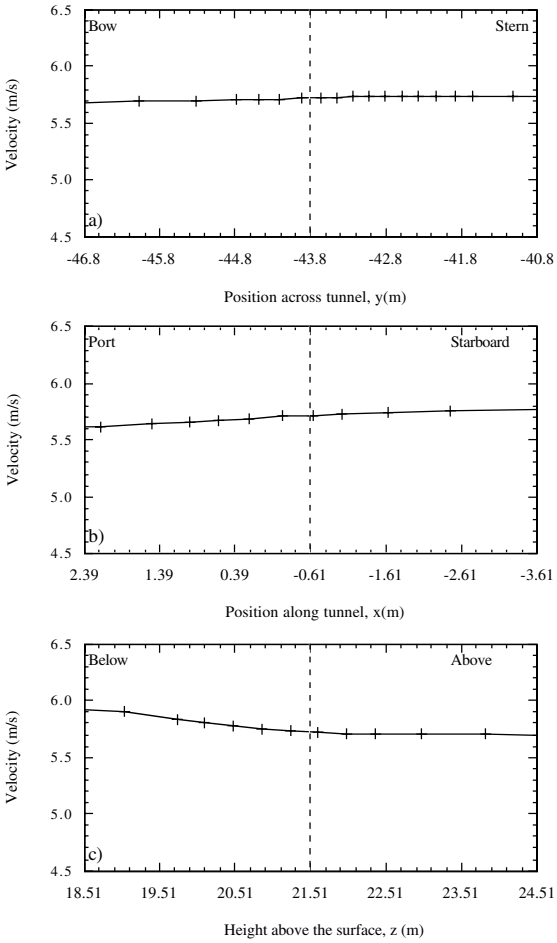

Figure 30. Lines of velocity data through the instrument position (indicated by the dashed line) in all three directions: top - across the tunnel; middle - along the tunnel, and bottom - vertically. The results are for a **5 ms^{-1}** flow from **90º to port** at the **R2 sonic** anemometer site.

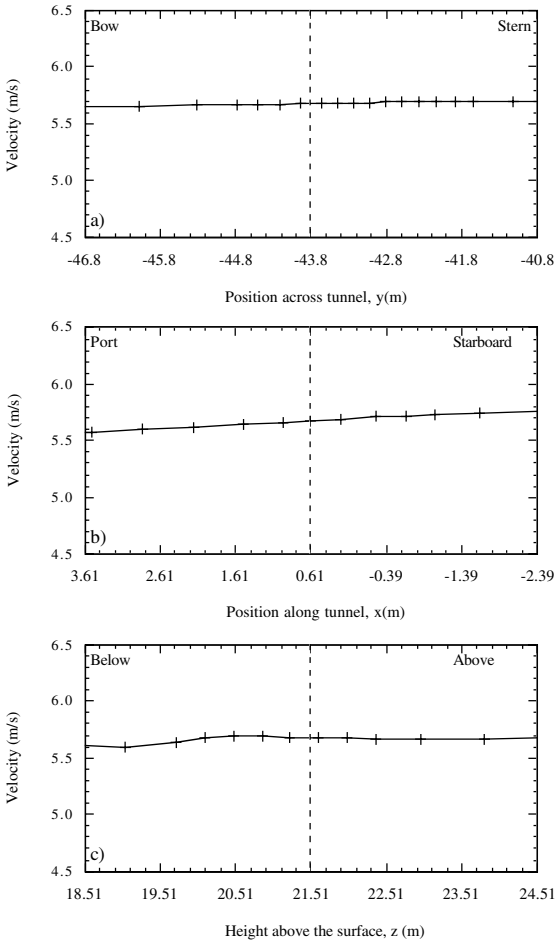

Figure 31. As for Figure 30, but for the **ship's sonic** anemometer site**.**

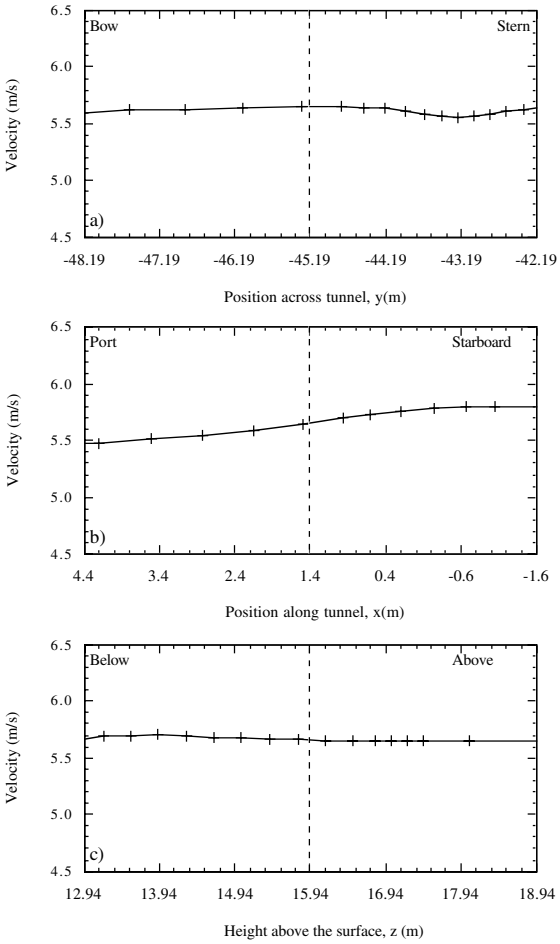

Figure 32. As for Figure 30, but for the **HS sonic (JCR 44)** anemometer site.

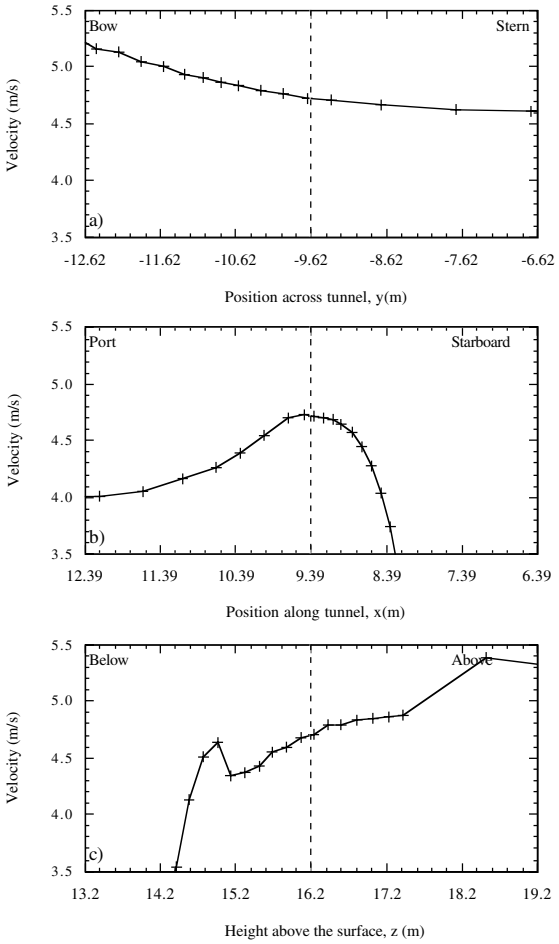

Figure 33. As for Figure 30, but for the **bridge R2 sonic** anemometer site.

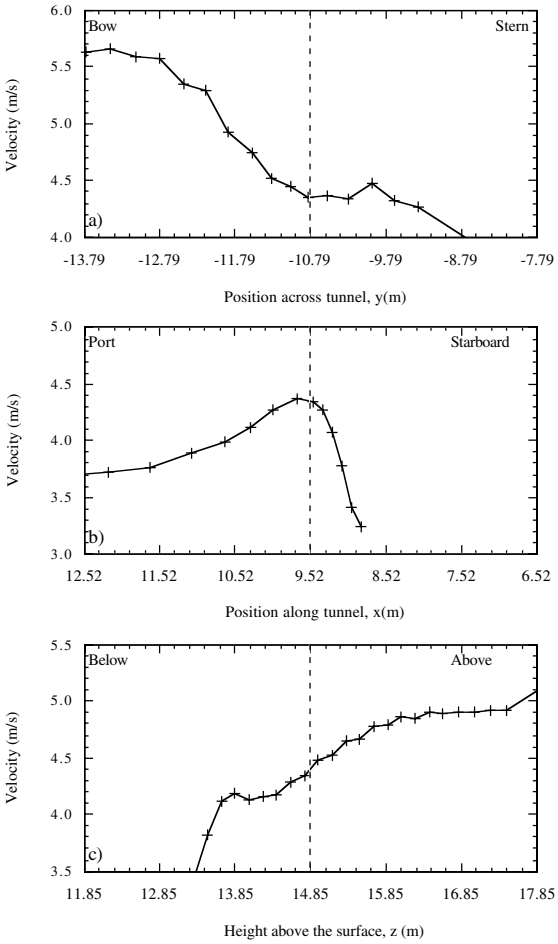

Figure 34. As for Figure 30, but for the **dew point** sensor site.

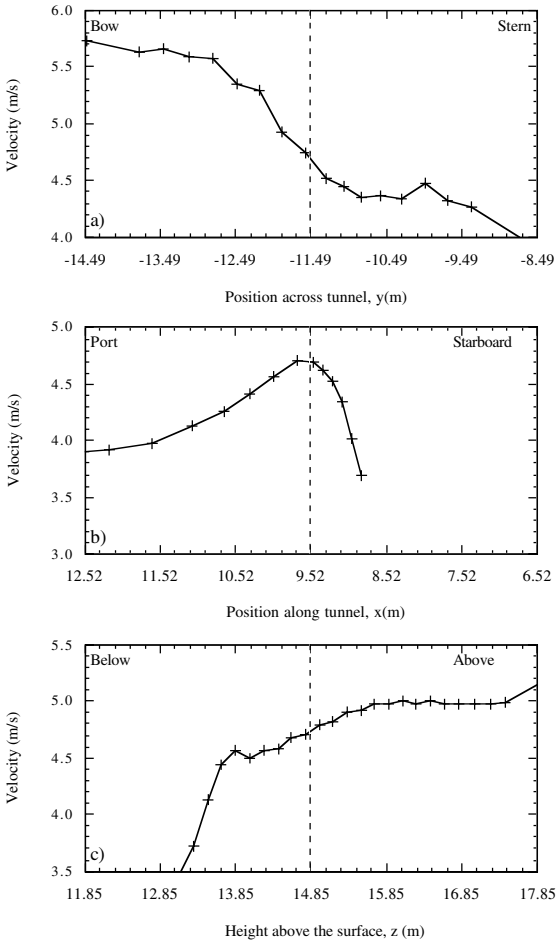

Figure 35. As for Figure 30, but for the **fast humidity** sensor site.

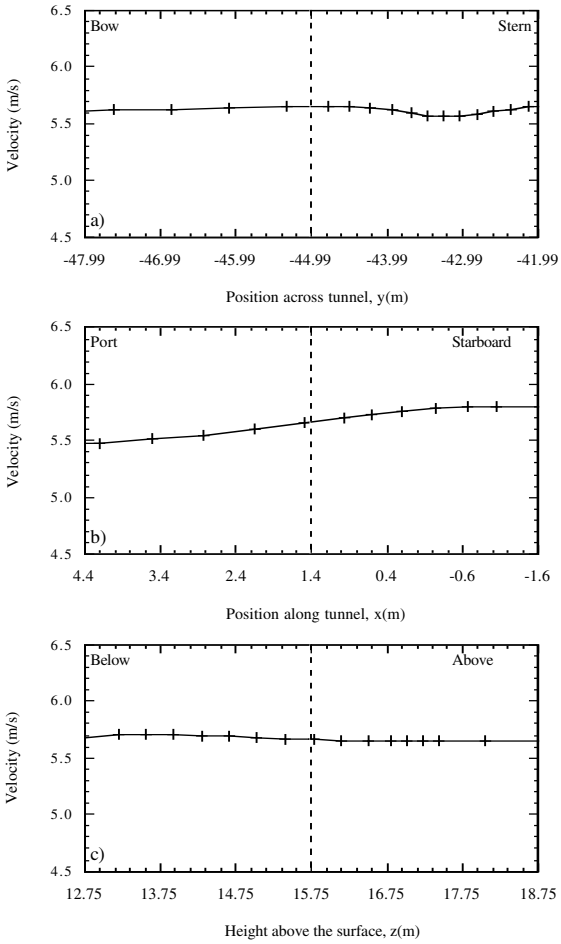

Figure 36. As for Figure 30, but for the **HS sonic (JCR 52)** anemometer site.

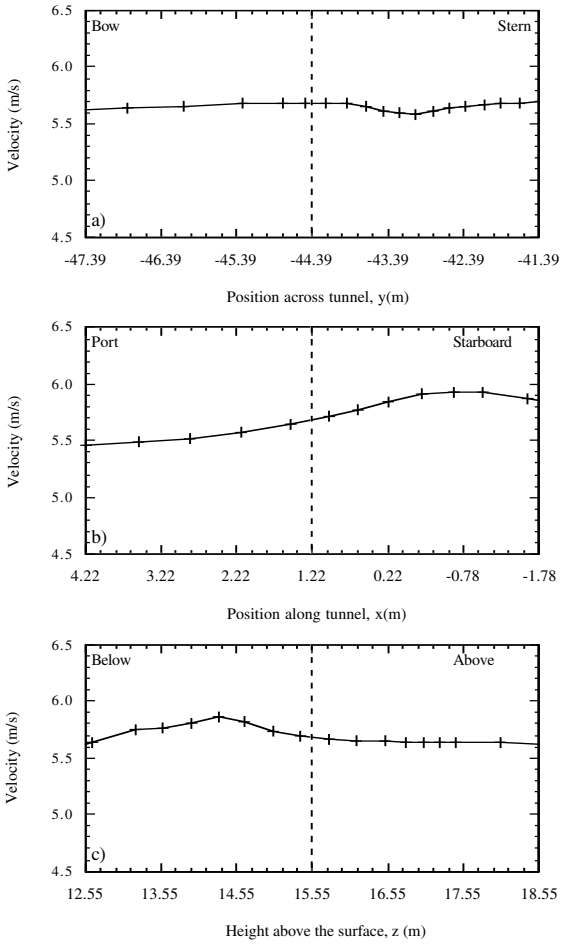

Figure 37. As for Figure 30, but for the **IFM #1** sensor site.

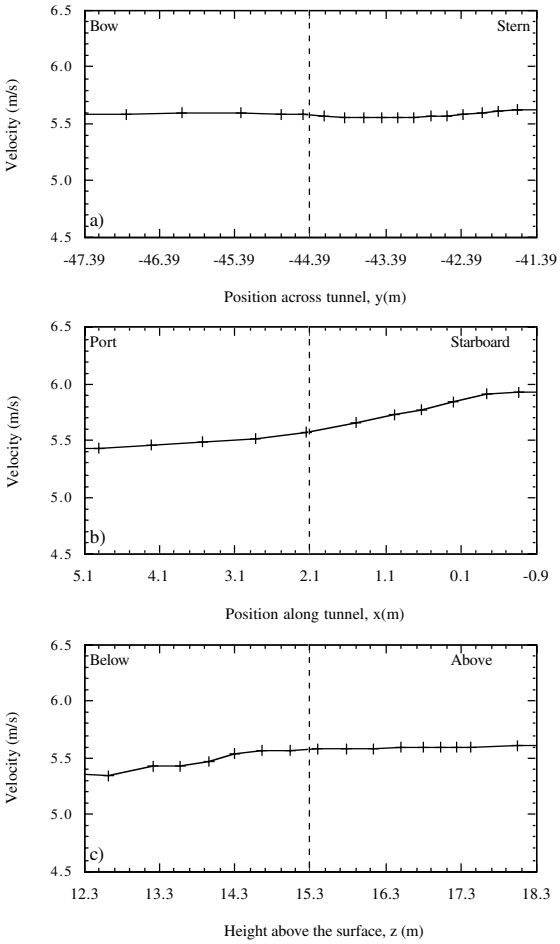

Figure 38. As for Figure 30, but for the **IFM #2** sensor site.

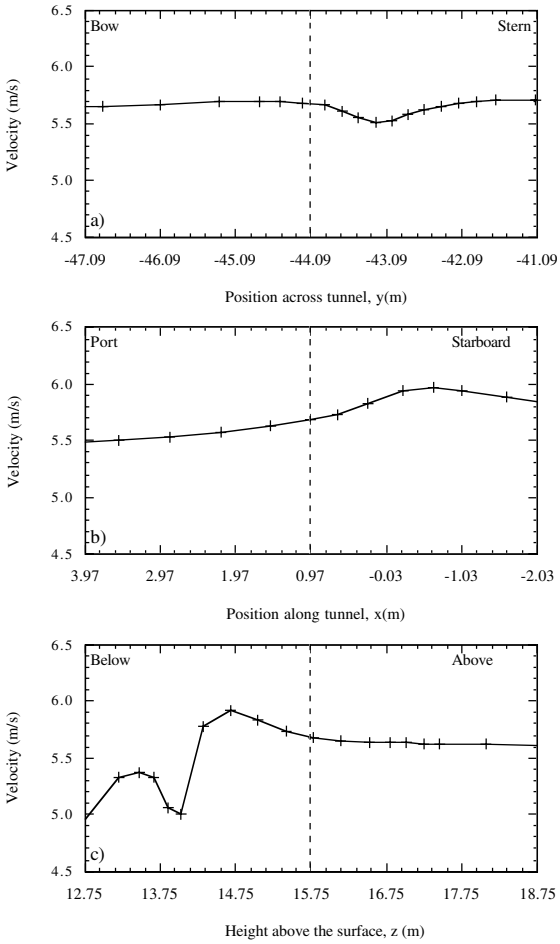

Figure 39. As for Figure 30, but for the **sonic temperature #1** sensor site.

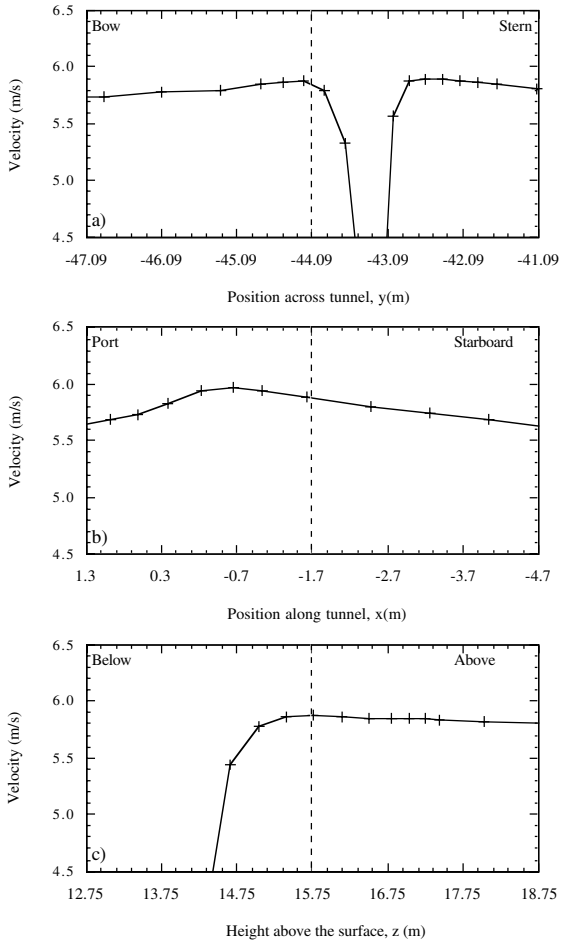

Figure 40. As for Figure 30, but for the **sonic temperature #2** site.

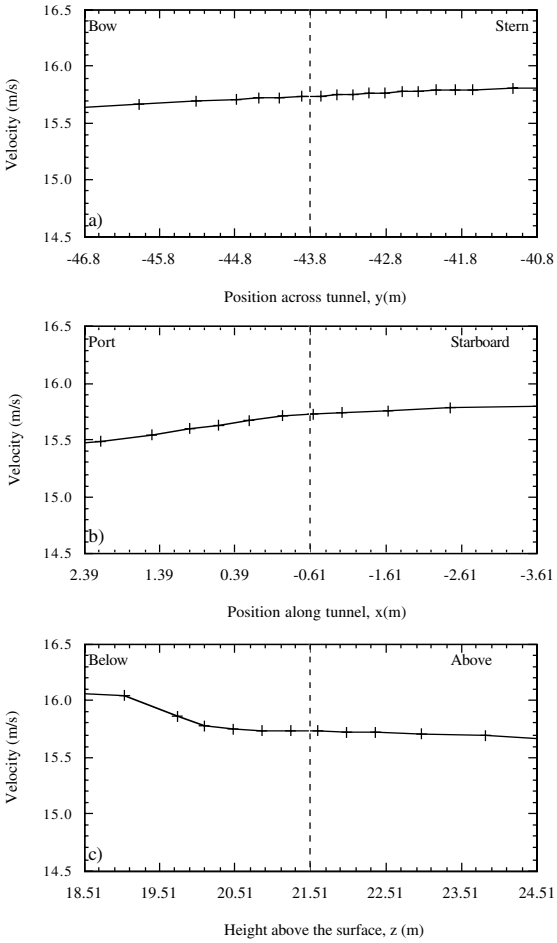

Figure 41. Lines of velocity data through the instrument position (indicated by the dashed line) in all three directions: top - across the tunnel; middle - along the tunnel, and bottom - vertically. The results are for a **15 ms^{-1}** flow from **90º to port** at the **R2 sonic** anemometer site.

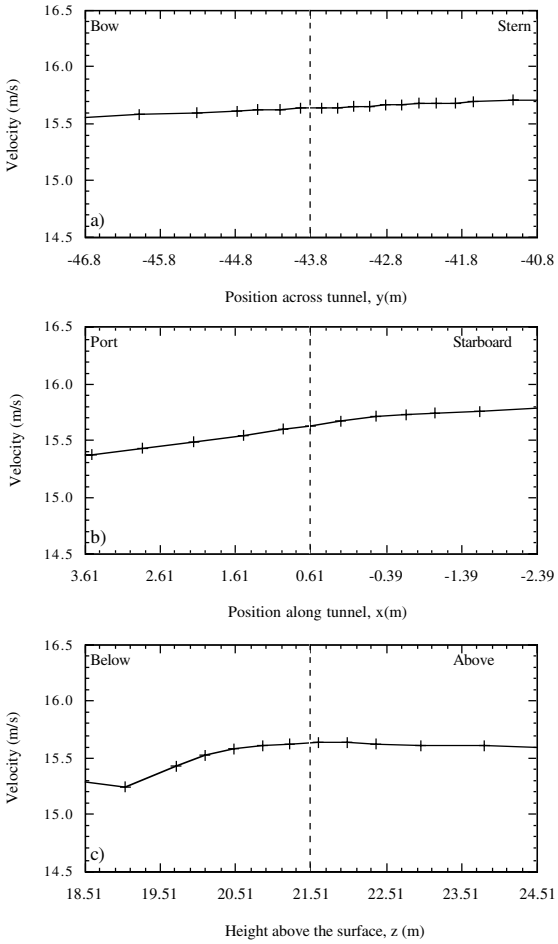

Figure 42. As for Figure 41 but for the **ship's sonic** anemometer site.

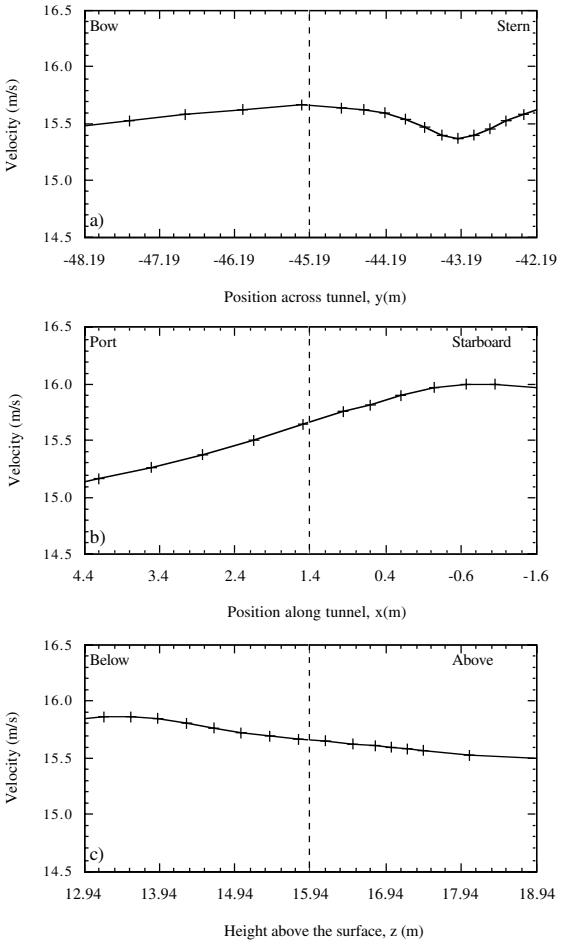

Figure 43. As for Figure 41, but for the **HS sonic (JCR 44)** anemometer site.

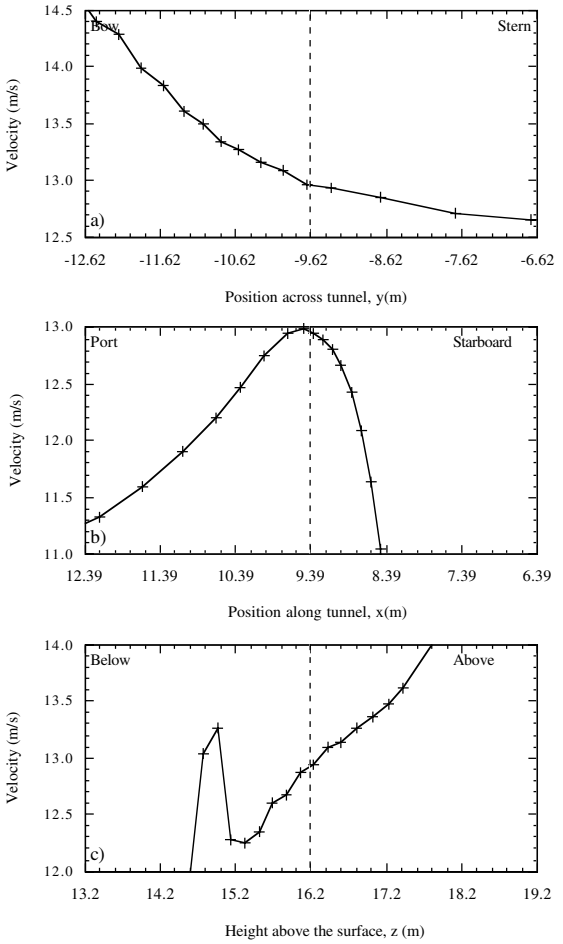

Figure 44. As for Figure 41, but for the **bridge R2 sonic** anemometer site.

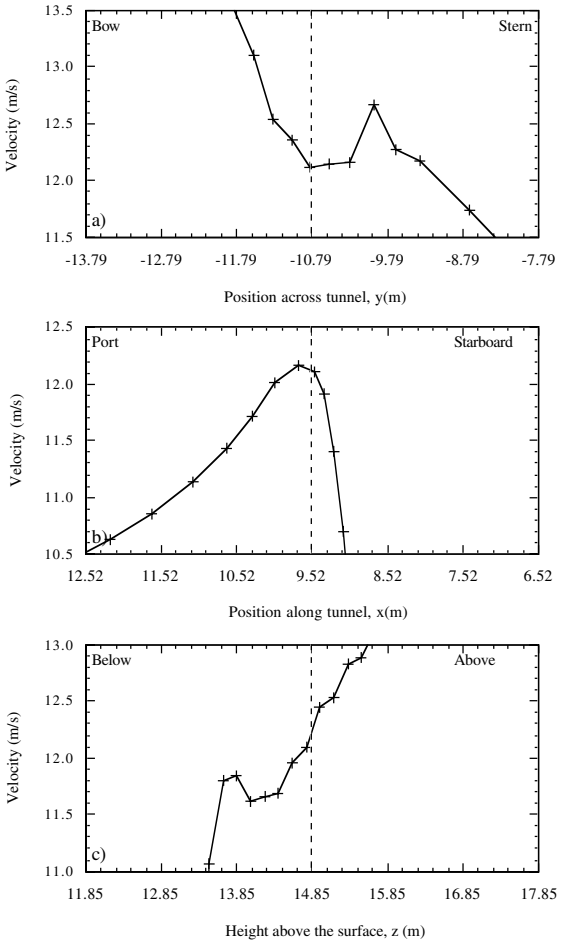

Figure 45. As for Figure 41, but for the **dew point** sensor site.

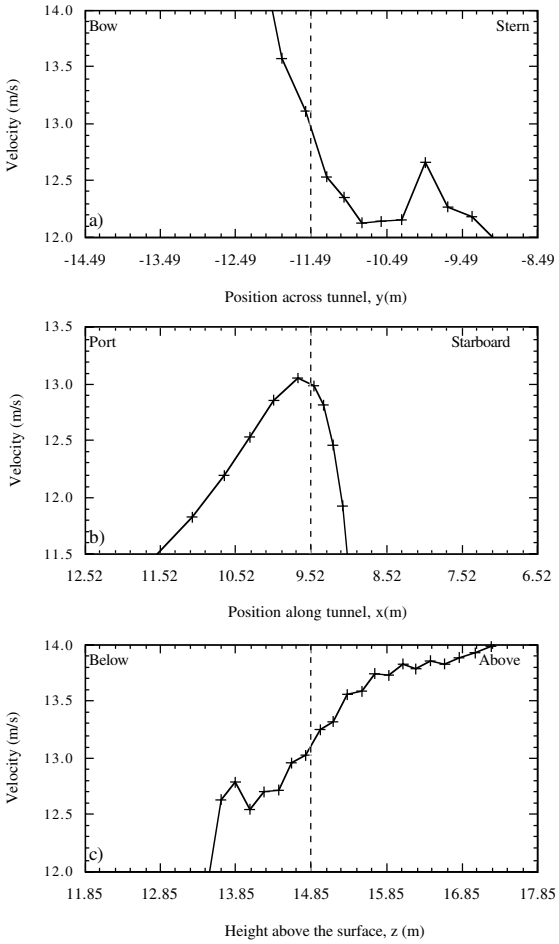

Figure 46. As for Figure 41, but for the **fast humidity** sensor site.

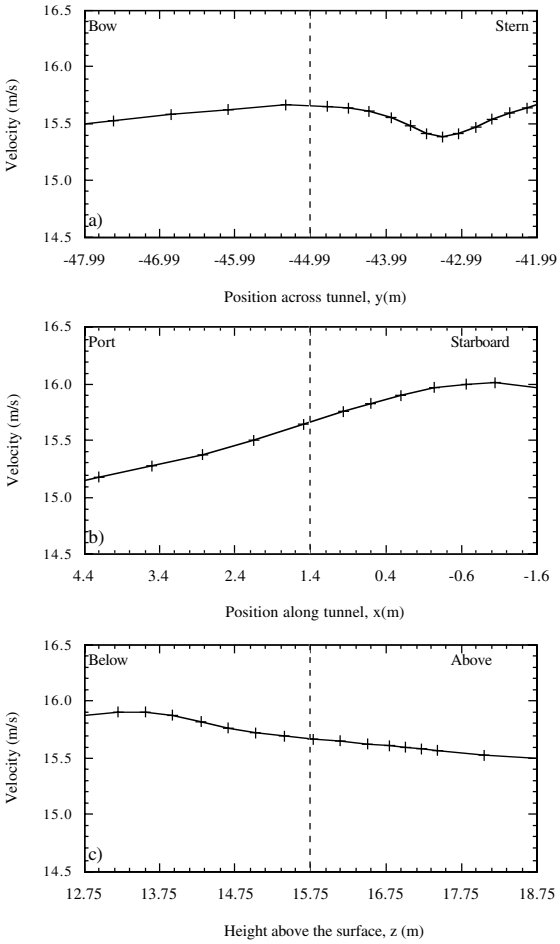

Figure 47. As for Figure 41, but for the **HS sonic (JCR 52)** anemometer site.

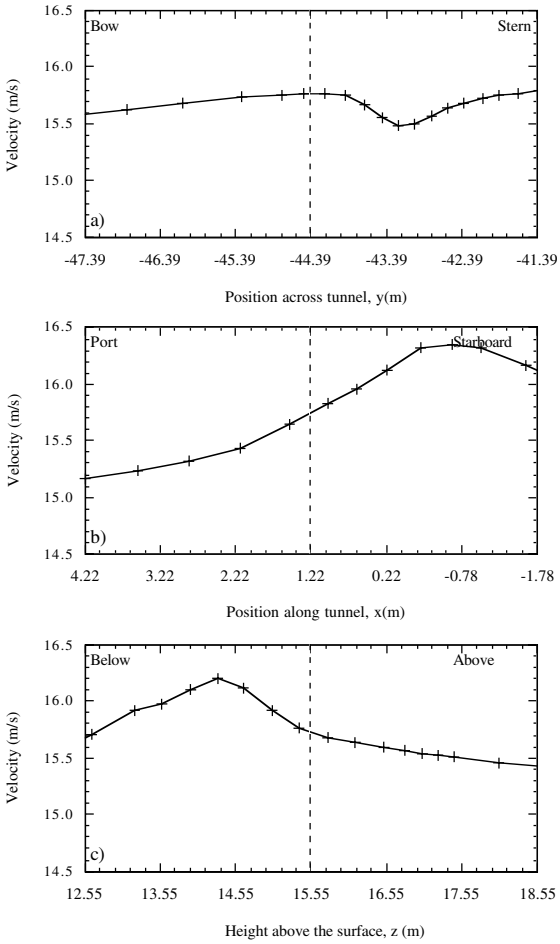

Figure 48. As for Figure 41, but for the **IFM #1** sensor site.

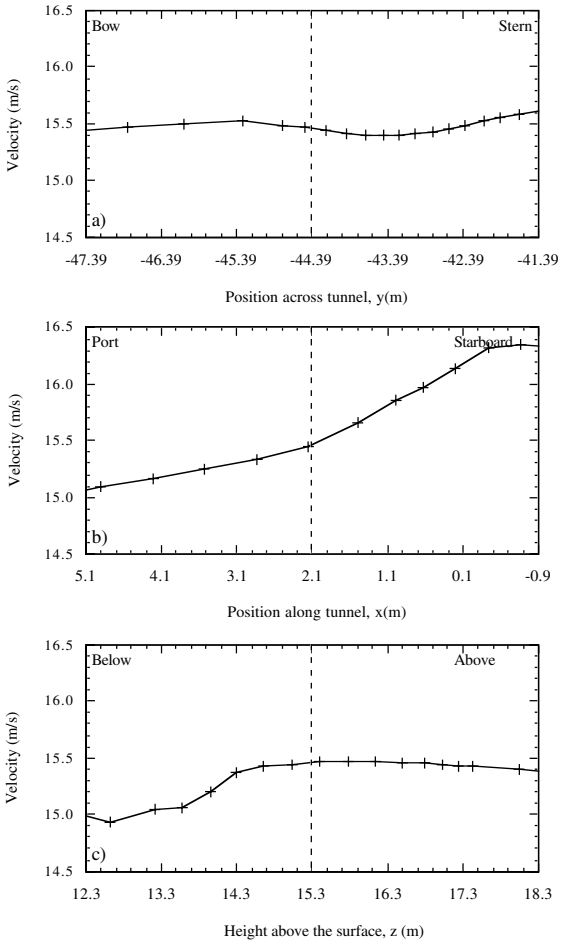

Figure 49. As for Figure 41, but for the **IFM #2** sensor site.

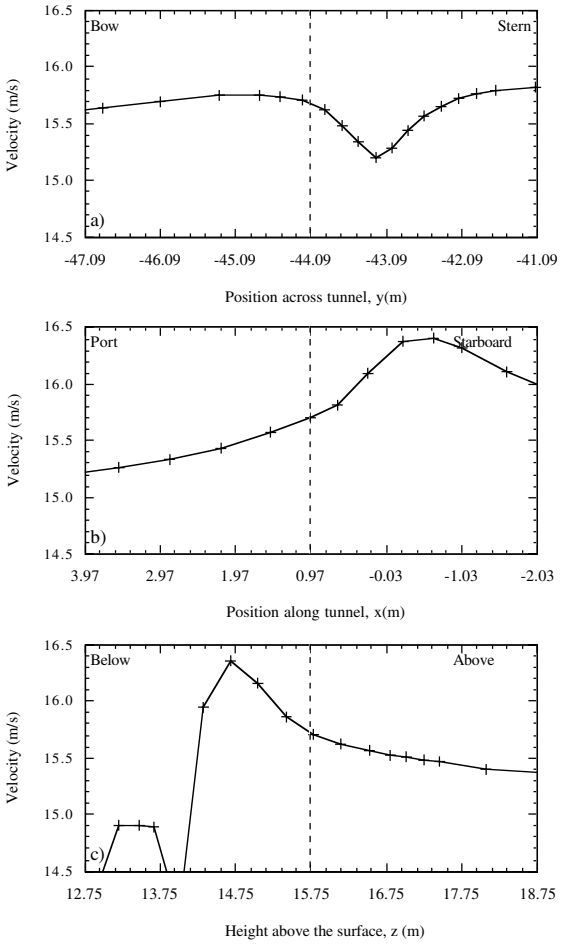

Figure 50. As for Figure 41, but for the **sonic temperature #1** sensor site.

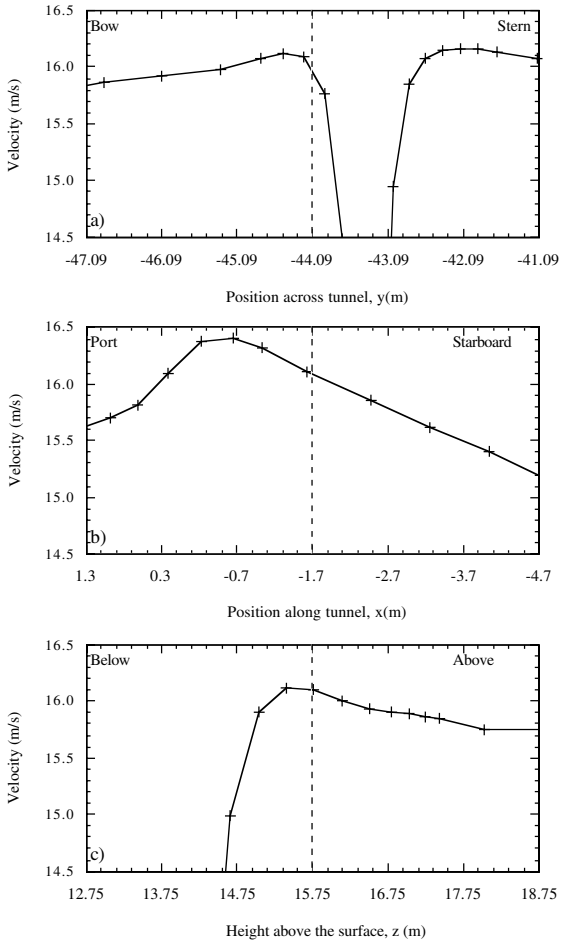

Figure 51. As for Figure 41, but for the **sonic temperature #2** site.

10. Appendix

The Figures in this Appendix were generated using the VECTIS post-processing software. Each Figure shows data on a major plane, and the orientation of the plane is indicated by a red line in the small box at the top left of each Figure. The variable size of the computational cells can been seen in each Figure. Figures A1 to A5 and A10 to A11 are for a flow of 5 ms^{-1} directly over the bow and Figures A6 to A9 are for a flow of 5 ms^{-1} from 90º to port.

FIGURE A1 Velocity vectors on a vertical plane through the HS sonic (JCR 52) anemometer site. The magnitude of the velocity is indicated by the colour of the arrows. The length and direction of the arrows represent the magnitude and component of the velocity in the plane of view. Each arrow represents the results from one computational cell. The position of the anemometer is indicated by a cross and the velocity scale corresponds to 0 ms^{-1} to 8 ms^{-1}.

FIGURE A2 As Figure A1 for a vertical section across the tunnel which intersects the HS sonic (JCR52) anemometer (indicated by a cross). The velocity scale corresponds to 2 ms^{-1} to 6 ms^{-1}.

FIGURE A3 As Figure A1 for a vertical section across the tunnel which intersects the bridge R2 anemometer (indicated by a cross). The velocity scale corresponds to 2 ms^{-1} to 6 ms^{-1}.

FIGURE A4 As Figure A1 for a horizontal section through the HS sonic (JCR 52) anemometer site (indicated by a cross). The velocity scale corresponds to 2 ms^{-1} to 6 ms^{-1}.

FIGURE A5 As Figure A1 for a horizontal section through the dew point and humidity sensor sites (indicated by crosses). The velocity scale corresponds to 2 ms^{-1} to 6 ms^{-1}.

FIGURE A6 As Figure A1 for a vertical section across the tunnel which intersects the HS sonic (JCR 52) anemometer site (indicated by a cross). The velocity scale corresponds to 2 ms^{-1} to 6 ms^{-1}.

FIGURE A7 As Figure A1 for a vertical section across the tunnel which intersects the bridge R2 anemometer site (indicated by a cross). The velocity scale corresponds to 2 ms^{-1} to 6 ms^{-1}.

FIGURE A8 As Figure A1 for a horizontal section through the HS sonic (JCR 52) anemometer site (indicated by a cross). The velocity scale corresponds to 2 ms^{-1} to 6 ms^{-1}.

FIGURE A9 As Figure A1 for a horizontal section through the dew point and humidity sensor sites (indicated by crosses). The velocity scale corresponds to 2 ms^{-1} to 6 ms^{-1}.

FIGURE A10 A streamline, or massless particle trace, which passes through the HS sonic (JCR 44) anemometer site (indicated by the cross).

FIGURE A11 A streamline, or massless particle trace, which passes through the bridge R2 anemometer site (indicated by the cross).

FIGURE A12 Vertical velocity vectors on a horizontal plane through the bridge R2 anemometer site (indicated by the cross) showing the re-circulation region.

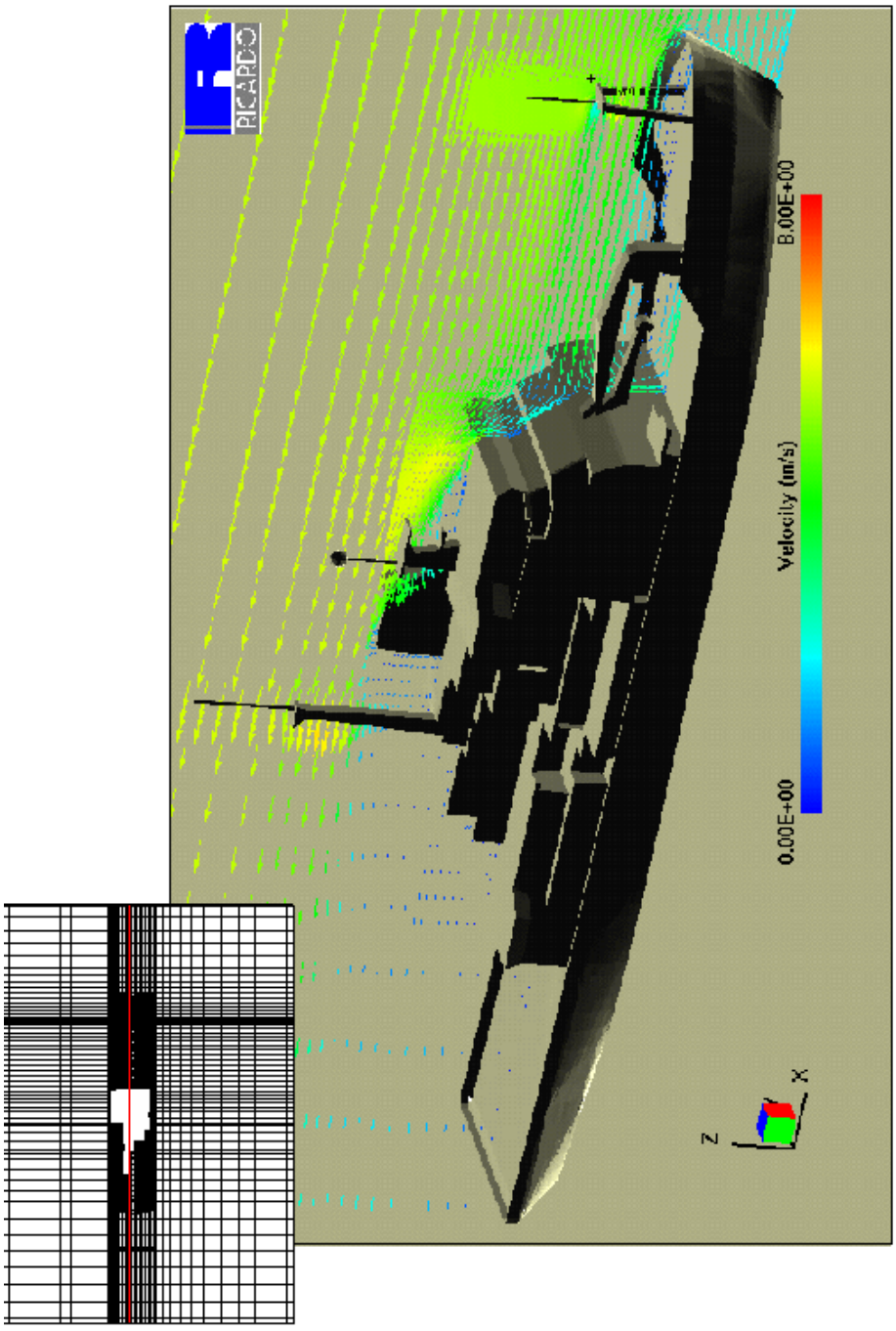

Figure A1

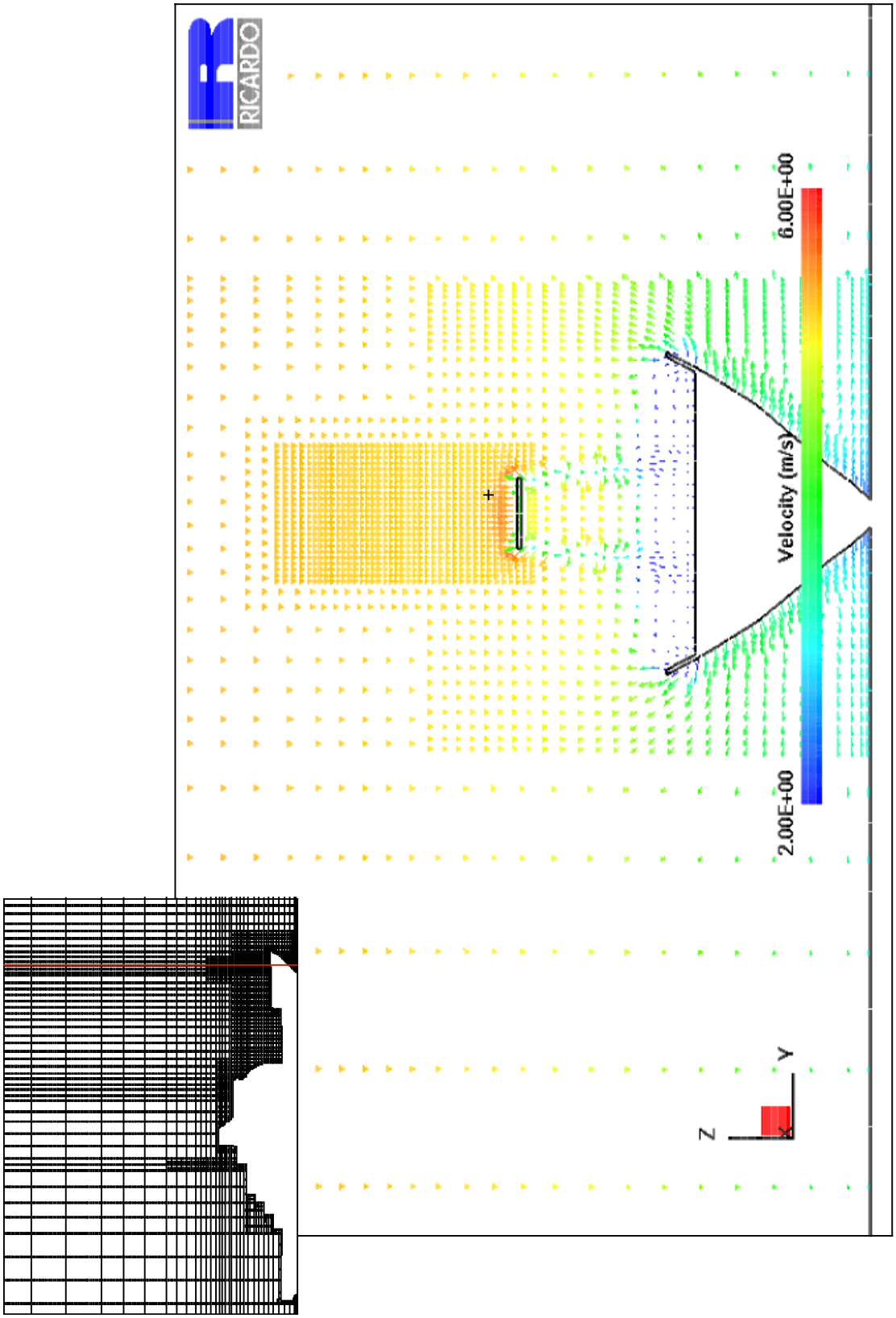

Figure A2

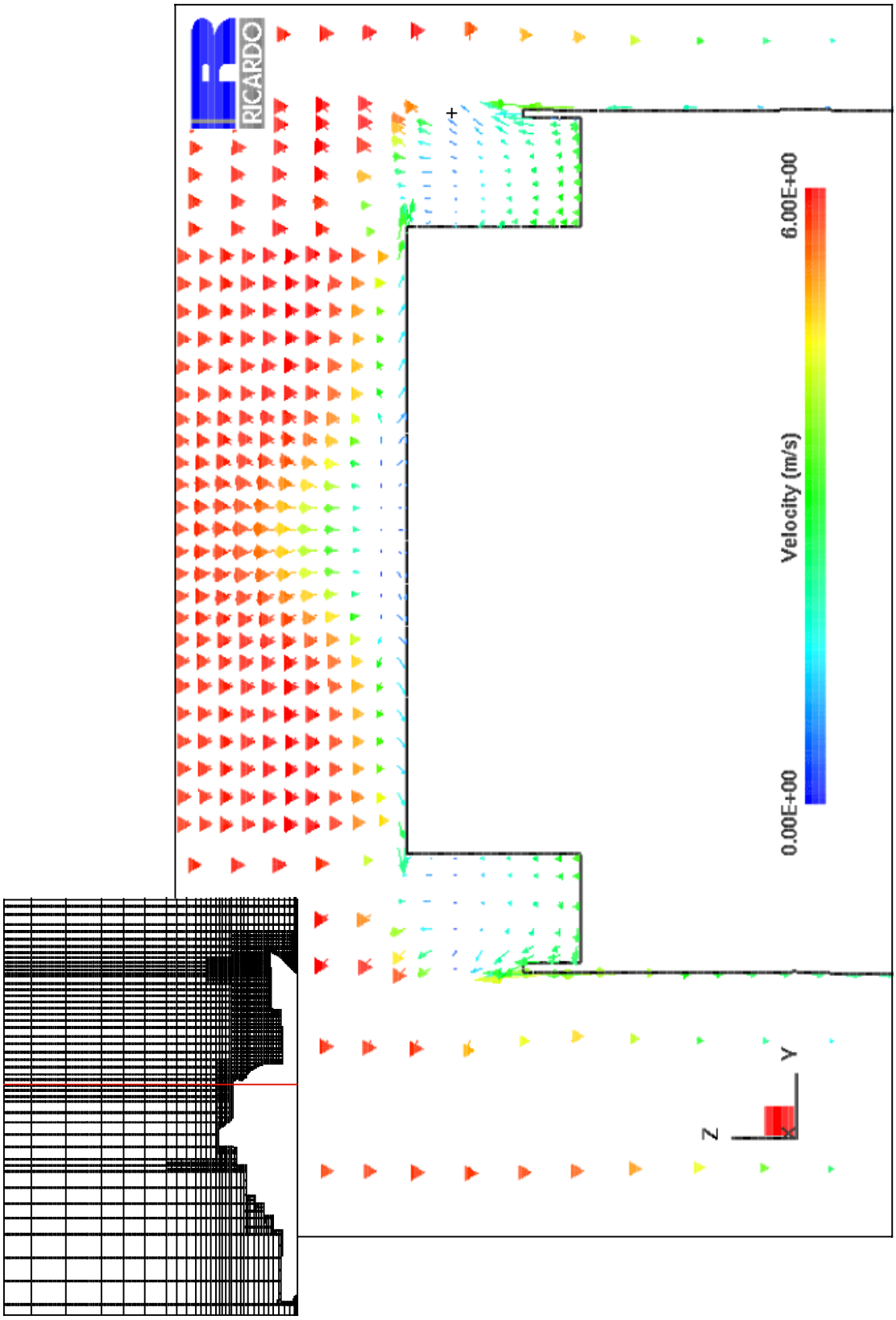

Figure A3

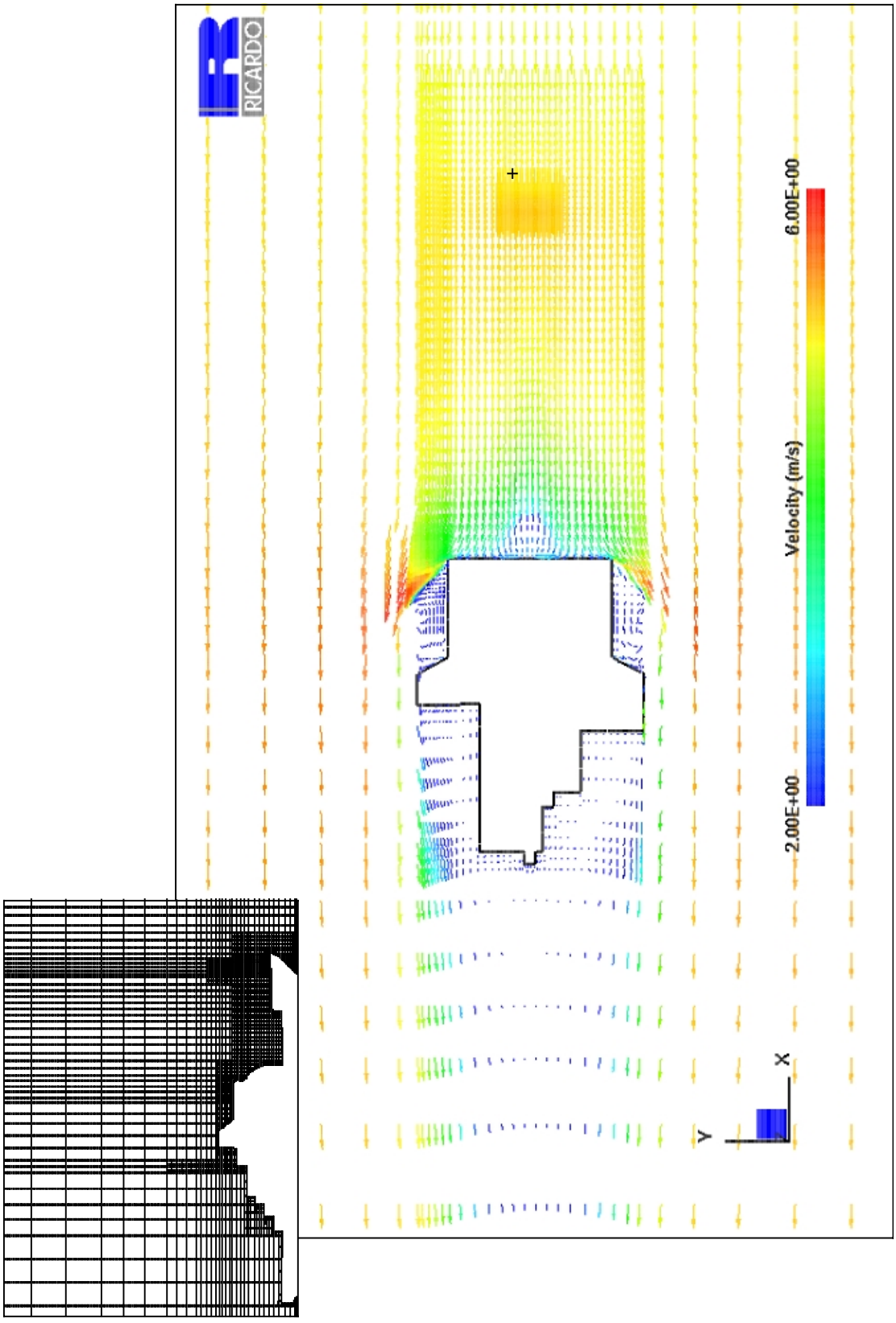

Figure A4

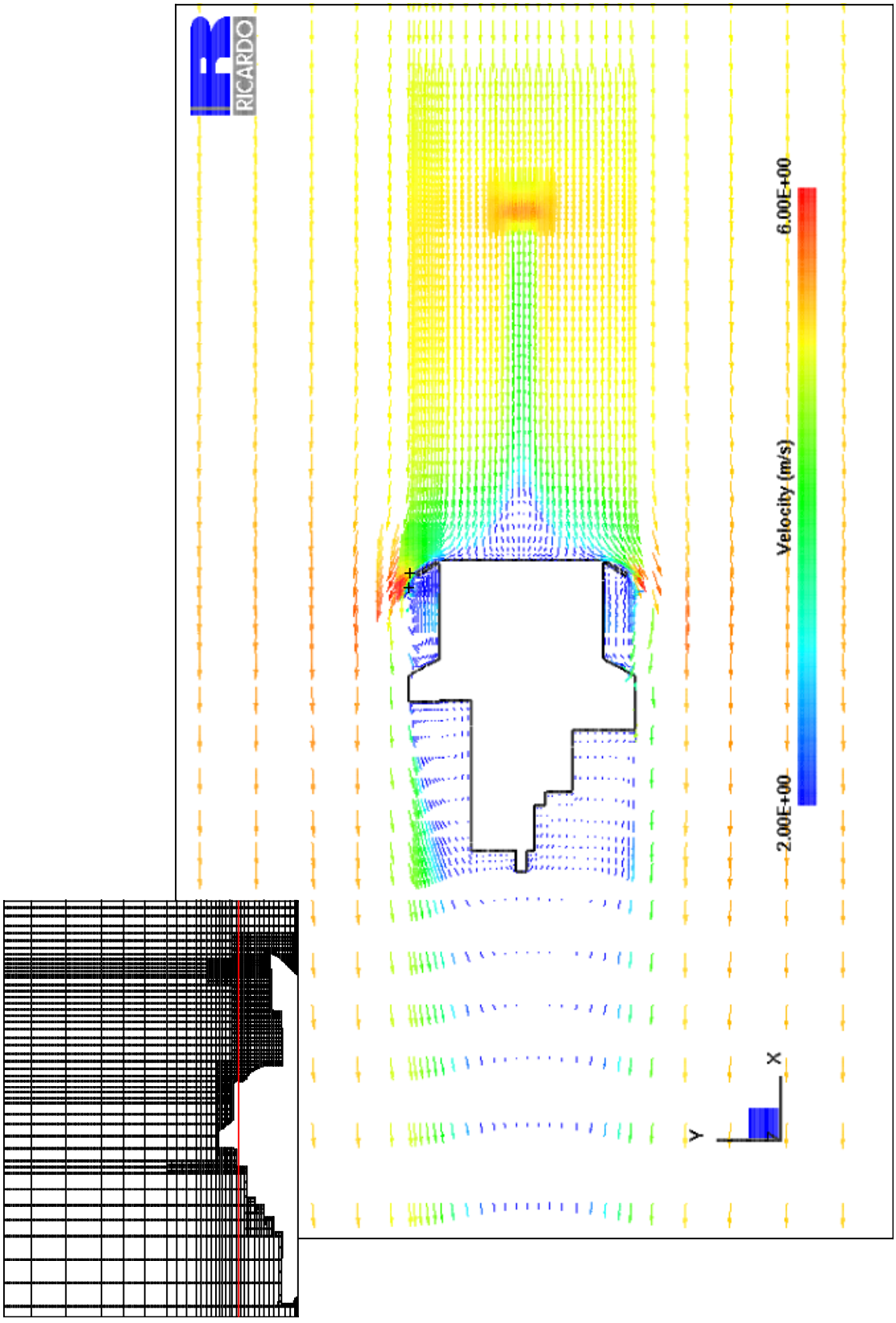

Figure A5

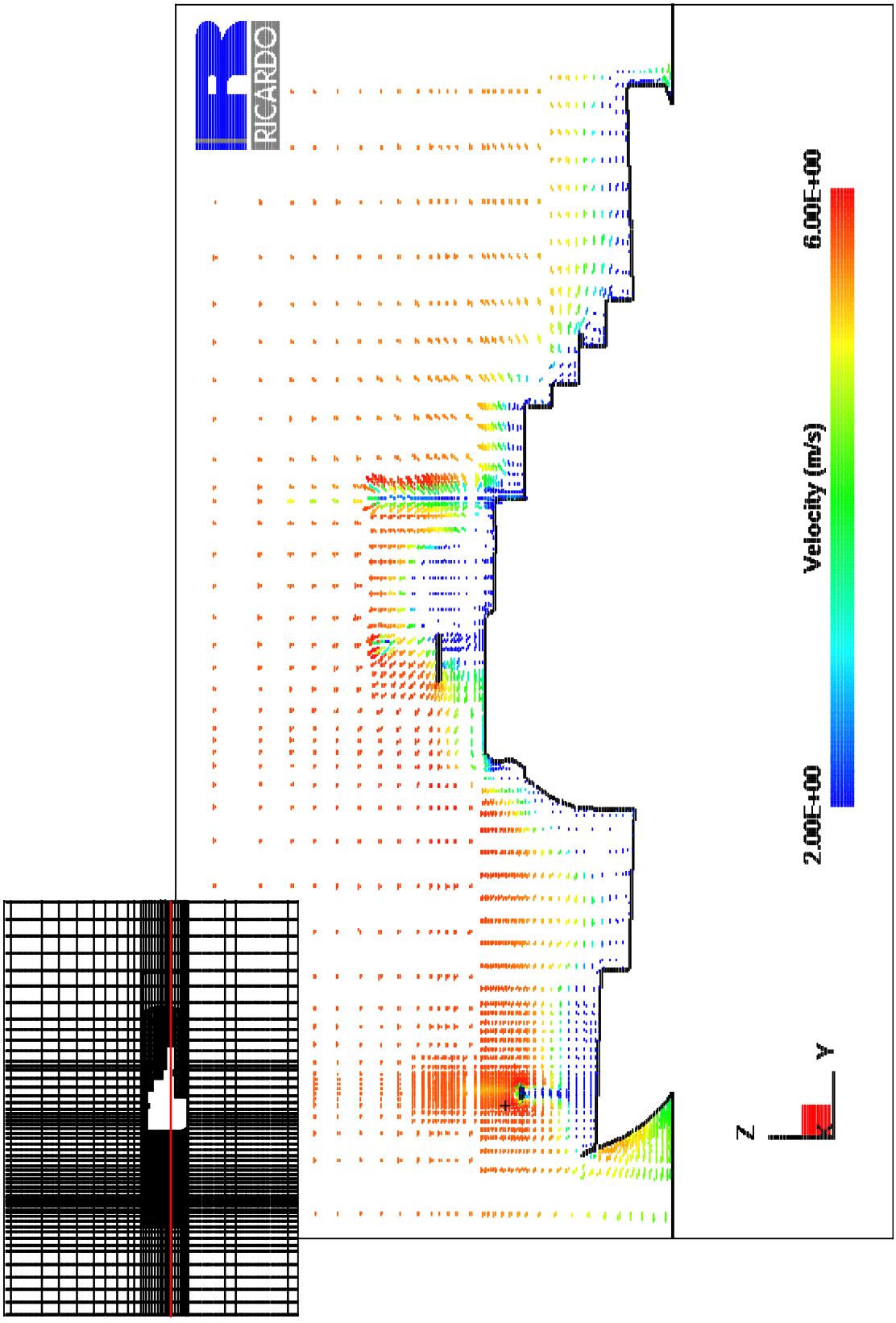

Figure A6

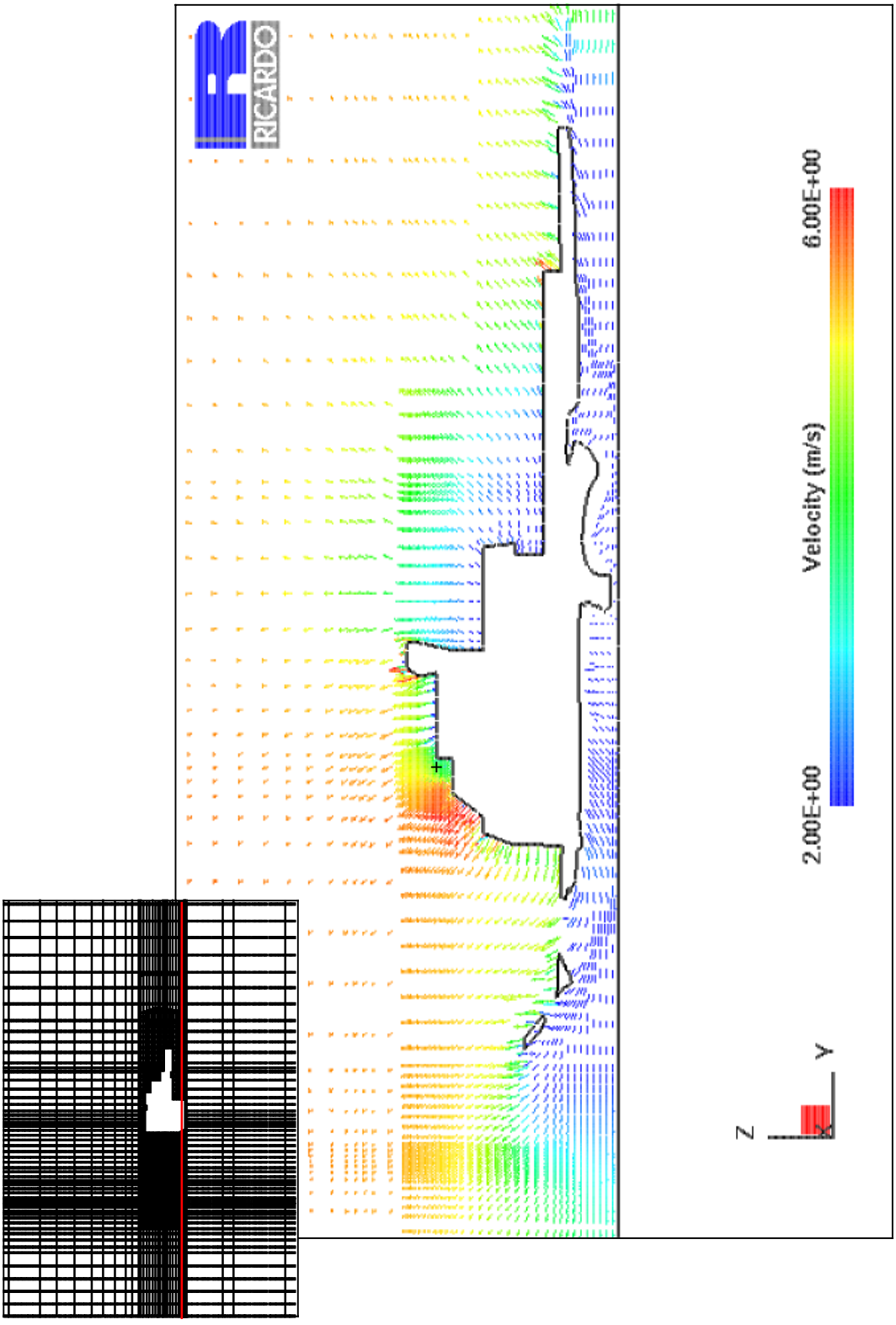

Figure A7

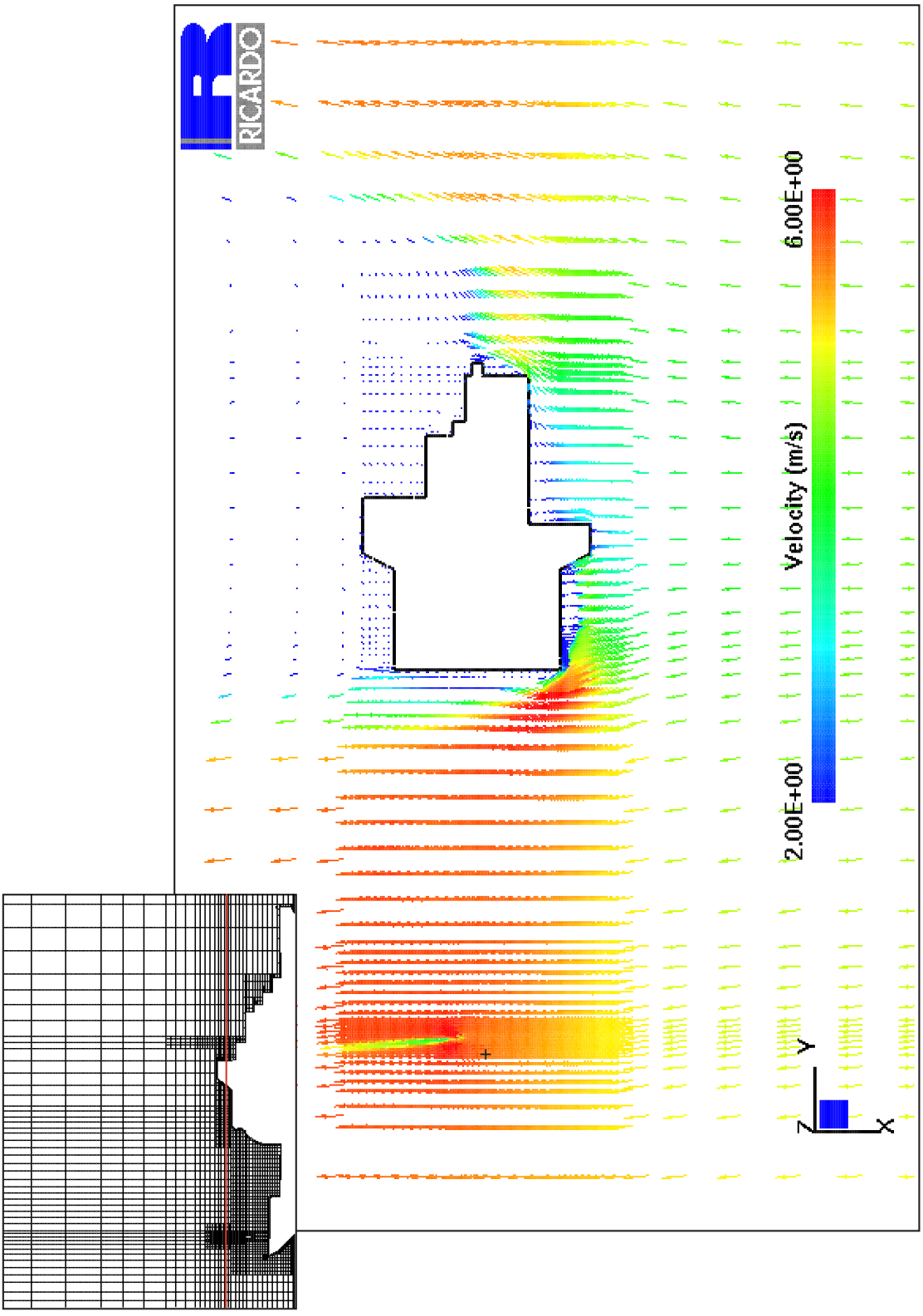

Figure A8

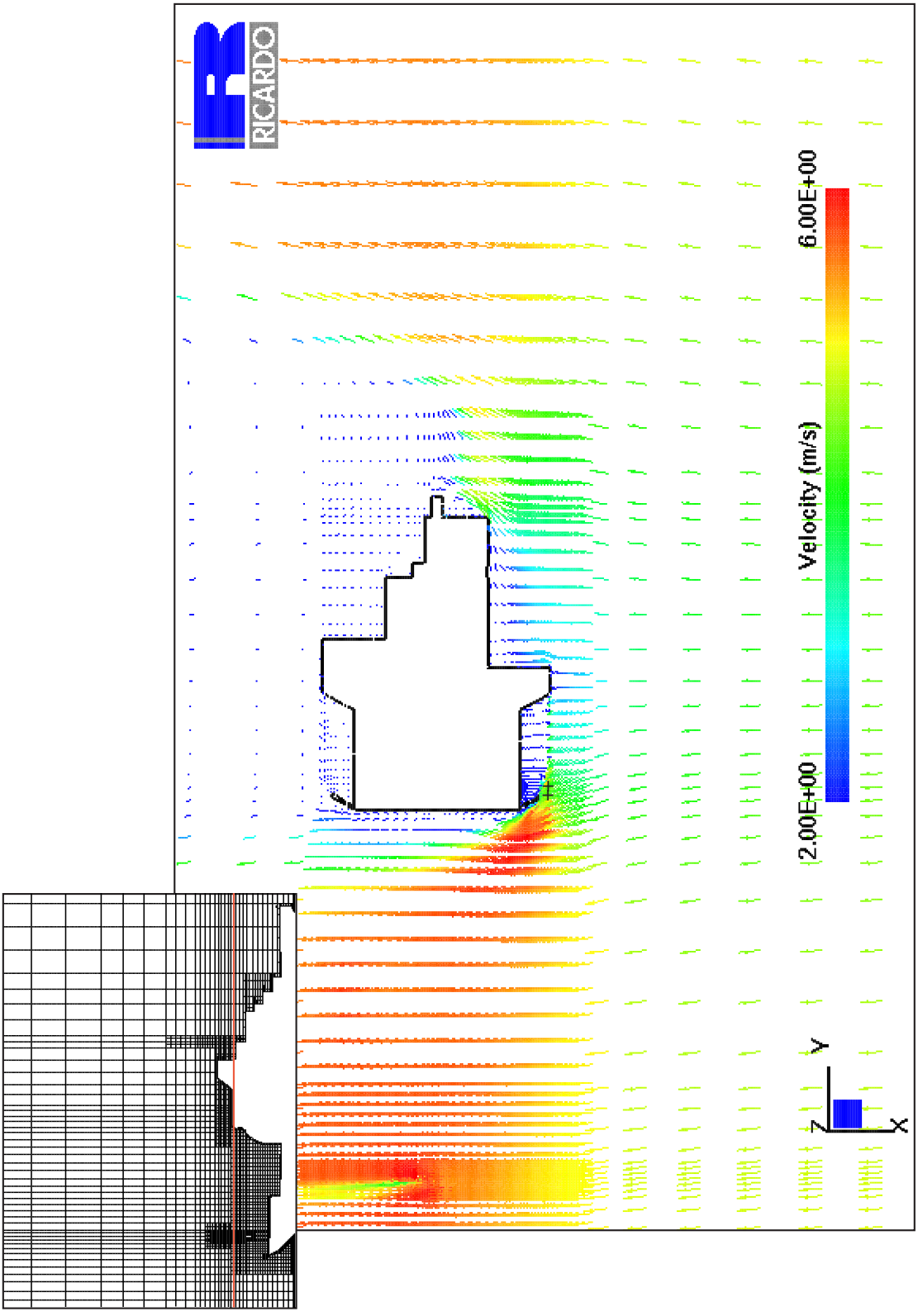

Figure A9

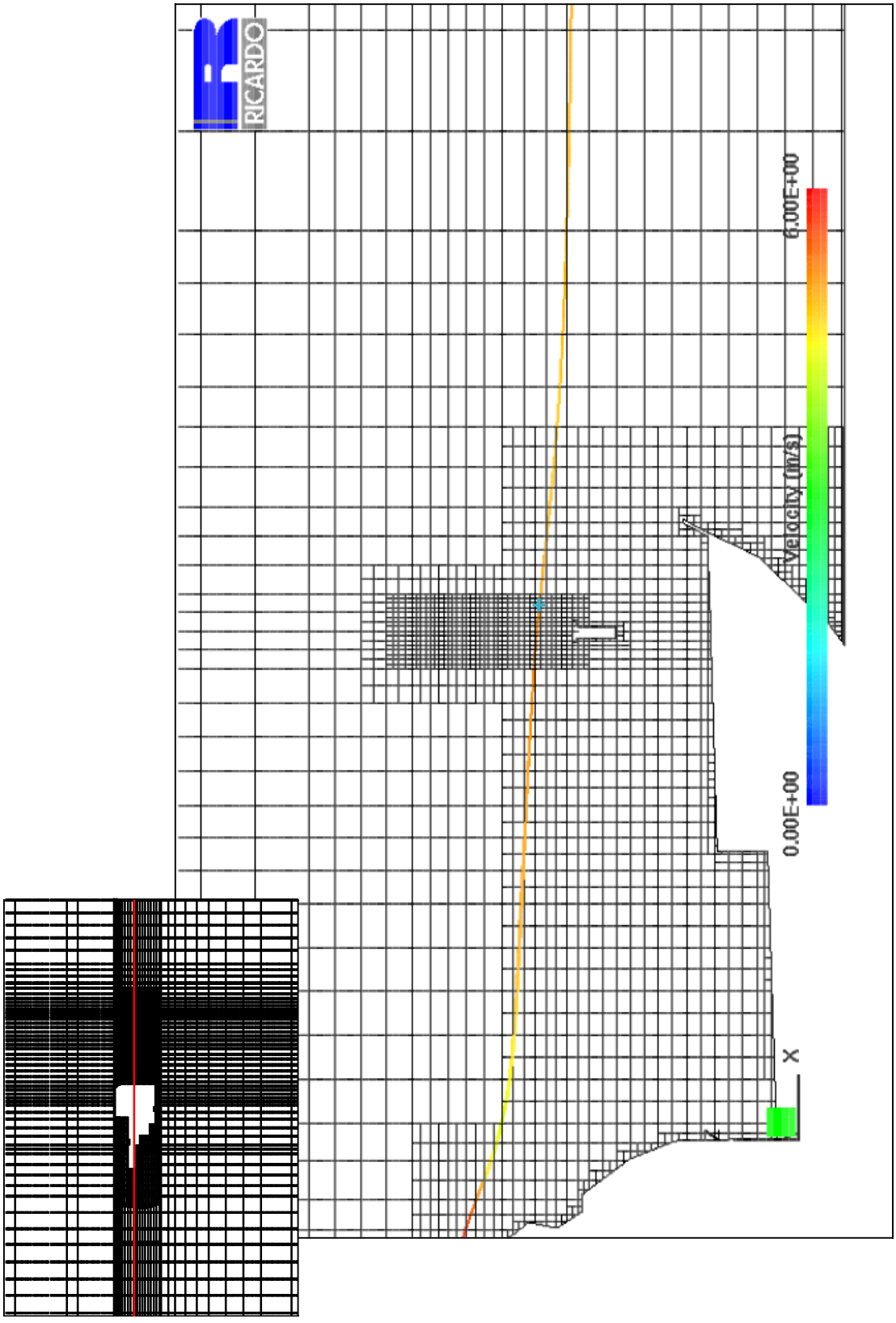

Figure A10

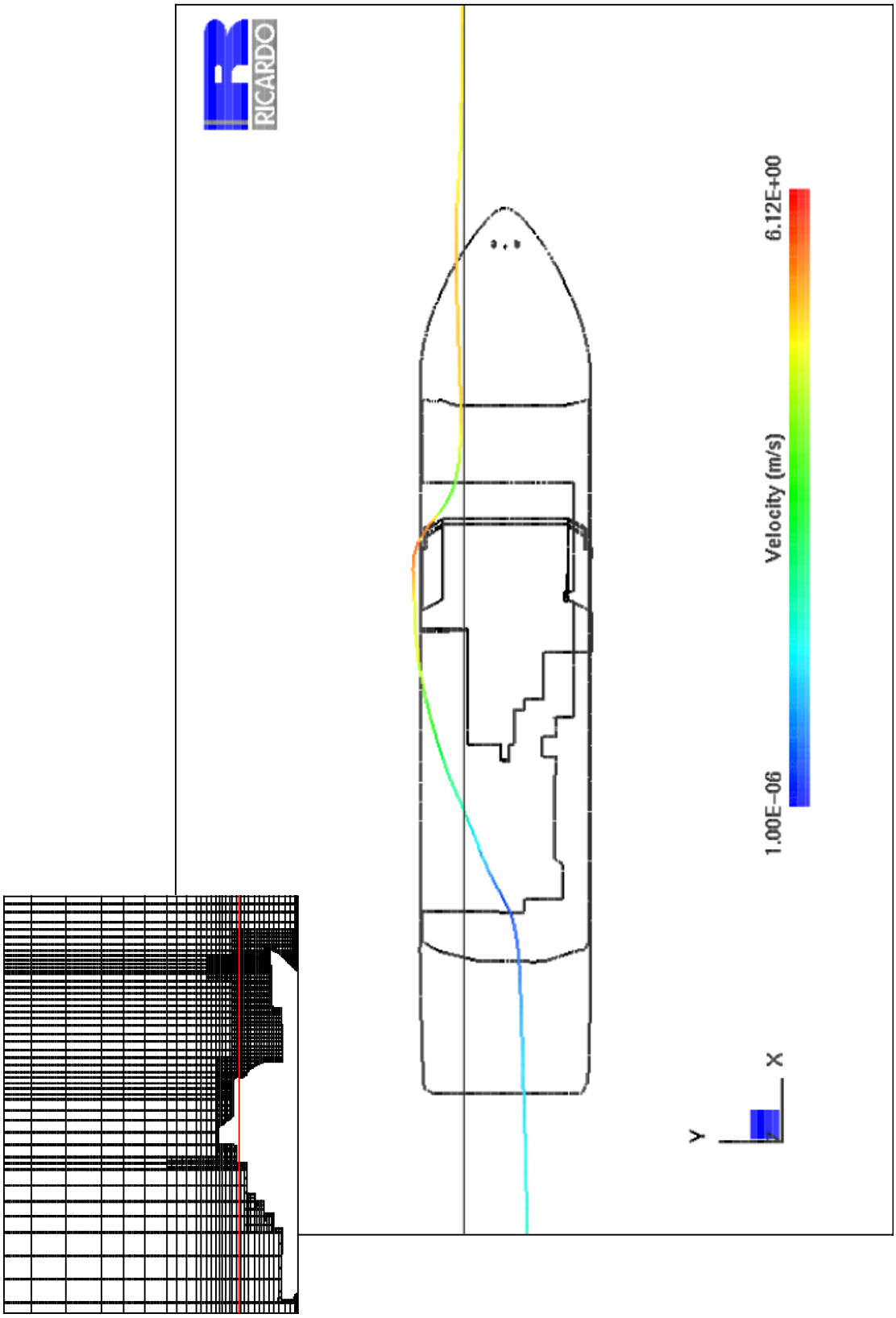

Figure A11

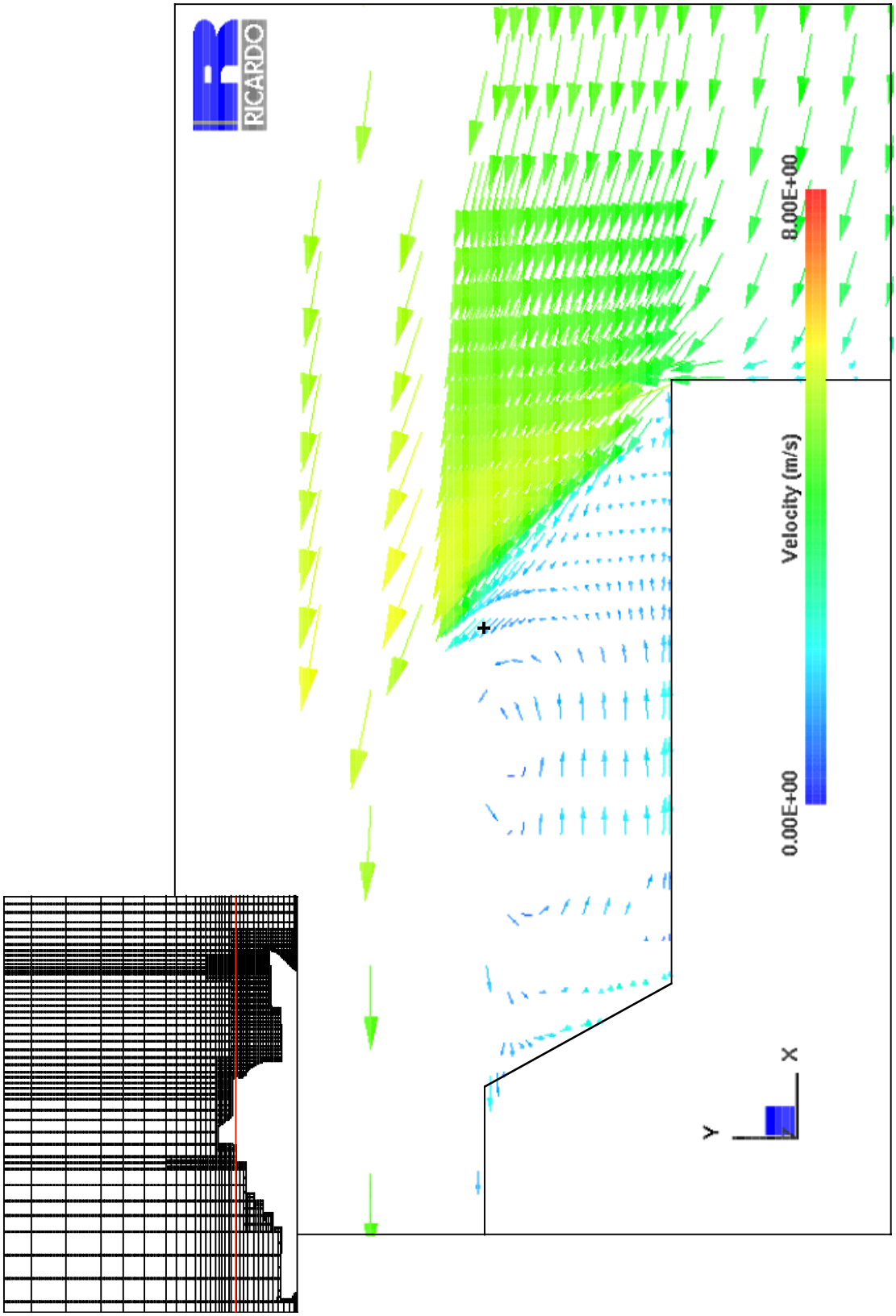

Figure A12